NORTHWESTERN UNIVERSITY

# Multi-Faceted Immunomodulatory and Tissue-Tropic Clinical Bacterial Isolate Potentiates Prostate Cancer Immunotherapy

A DISSERTATION

SUBMITTED TO THE GRADUATE SCHOOL
IN PARTIAL FULLFILLMENT OF THE REQUIREMENTS

for the degree

DOCTOR OF PHILOSOPHY

Field of Driskill Graduate Training Program in Life Sciences

By

Jonathan F. Anker

EVANSTON, ILLINOIS

June 2018

**ABSTRACT**

Immune checkpoint inhibitors have not been effective for immunologically "cold" tumors, such as prostate cancer, which contain scarce tumor infiltrating lymphocytes. We hypothesized that select tissue-specific and immunostimulatory bacteria can potentiate these immunotherapies. Here we show that a patient-derived prostate-specific microbe, CP1, in combination with anti-PD-1 immunotherapy, increased survival and decreased tumor burden in orthotopic *MYC*- and *PTEN*-mutant prostate cancer models. CP1 administered intra-urethrally specifically homed to and colonized tumors without causing any systemic toxicities. CP1 increased immunogenic cell death of cancer cells, T cell cytotoxicity, and tumor infiltration by activated CD8 and Th17 T cells, mature dendritic cells, M1 macrophages, and NK cells. CP1 also decreased intra-tumoral regulatory T cells and VEGF. Mechanistically, blocking CP1-recruited T cells from infiltrating the tumor inhibited its therapeutic efficacy. CP1 is a novel immunotherapeutic tool demonstrating how a tissue-specific microbe can increase tumor immunogenicity and sensitize an otherwise resistant cancer type to immunotherapy.

**ACKNOWLEDGEMENTS**

To my advisors, Dr. Sarki Abdulkadir and Dr. Praveen Thumbikat, thank you both for all of the support over the past few years. I really appreciate you both providing me this opportunity to pursue my interests, and for taking the risk of going outside of your general areas of interest. This type of collaborative project only worked because you both have always been open to exploring new ideas and working together. I appreciate all of our discussions and debates, whether about new scientific ideas, troubleshooting experiments, or analyzing results, and especially your willingness to allow me the freedom and independence to explore different experiments and directions during the course of this project. I truly would not have completed this PhD without both of your continued reassurance and support, thank you.

To everyone in the Thumbikat and Abdulkadir labs, thank you for putting up with me. Rajita, Rose, and Ashlee, it was always helpful have you guys around to commiserate about graduate school struggles. Stephen, Kenny, Larry, Madhu, Ziggy, HuiYing, Vinay, Younga, Sahithi, Meejeon, and Kenji, thank you for being available for questions and for being willing to discuss my project and experiments. Thank you Barbara and Christel for being so nice even when I place an order 10 minutes after you've finished with the others, and thank you Hanlin and Anum for the dozens of hours you've helped with all of the surgeries. To Dr. Anthony Schaeffer, thank you for all of your constructive feedback and encouragement during the entire PhD, I appreciate all of the time you have given me. To my thesis committee, Dr. Bin Zhang, Dr. Derek Wainwright, and Dr. Melissa Brown,

thank you all for your helpful advice and constructive critique. Many of your comments and suggestions had a major impact on the direction of this project and the experimental methodology. To my MSTP classmates, it has been great to have you all to confide in during this process. And thank you to the entire MSTP administration, and especially Jayms, for the ongoing support and care. I would also like to acknowledge the grant I was awarded supporting this work: NCI F30 CA203472.

Finally, thank you to my family. Mom and Dad, this PhD would have never happened if you had not been there for me, driving me to Cold Spring Harbor Laboratories over the weekends and always encouraging all of the other activities I've wanted to pursue. Thank you for always putting your kids first. Alex and Allison, your company has been a very welcome distraction and has helped me during tough times, TT. Anna, I'm glad you were able to get so much joy out of my time in the lab. Your refrigerator full of fuzzy polaroid pictures sums up some of my most enjoyable times. Cane, your loyalty and support knows no bounds, thank you for all of your encouragement. And thank you Grandma Sydell, Poppy, and Grandma Lillie for always making me feel important and capable.

**TABLE OF CONTENTS**

**LIST OF FIGURES AND TABLES**

# CHAPTER 1: INTRODUCTION

## 1.1 Prostate cancer

Prostate cancer (PCa) is one of the most prevalent cancer types, estimated to have an incidence of 164,690 men and cause 29,430 deaths in 2018 (1). Prostate tumors are often initially treated by radical prostatectomy and radiation therapy. In addition, as these tumors are dependent on androgen for their growth and survival, patients with intermediate risk disease and beyond are also treated with androgen deprivation therapy (ADT). Intermediate risk disease is defined as localized prostate cancer occupying at least half of one prostate lobe or bilateral within the tissue, a serum prostate-specific antigen (PSA) ≥10 and <20 ng/ml, or a Gleason score 7 (based on histological quantification of tissue differentiation and glandular organization). ADT successfully induces tumor regression in 80-90% of treated patients. However, ADT is associated with major urological, cardiovascular, and skeletal adverse events and morbidities (2-5), and nearly all regressed tumors recur within 12-33 months as castration-resistant prostate cancer (CRPC) (6-8). CRPC patients have a poor prognosis with a median survival time of 12-37 months after initiation of ADT, or 9-30 months overall (8-10).

In PCa, as with many other cancer types, chronic inflammation is linked to tumor formation and carcinogenesis (11), yet immunosuppression and immune evasion are hallmarks of the tumor microenvironment (12). While some cancer types display a T cell

inflamed phenotype with a high level of tumor infiltrating lymphocytes (TILs), many others do not, with decreased TILs and, often, poor response to immunotherapy (13). Therefore, it is crucial to understand both the level and type of inflammation and immunosuppression found within the prostate tumor microenvironment in order to optimize clinical responses to immunotherapies.

## 1.2 Prostate tumor immunology and microenvironment

### *1.2.1 Tumor infiltrating lymphocytes*

TILs are critical players in driving an anti-tumor immune response and for immunotherapy efficacy in many cancer types (14). Comprehensive review of multiple cancers determined that TILs are linked to a better prognosis in colorectal cancer, hepatocellular carcinoma, gallbladder carcinoma, pancreatic carcinoma, esophageal carcinoma, ovarian cancer, endometrial cancer, cervical cancer, transitional cell bladder cancer, urothelial cancer, lung cancer, breast cancer, and head and neck cancer (15). However, in PCa, TILs are scarce in comparison to those observed in normal prostate tissue and benign prostatic hyperplasia (BPH, a non-cancerous enlargement of the prostate) (16), with another study reporting T cell infiltration remaining constant over the course of disease progression, from benign glandular hyperplasia to prostatic intraepithelial neoplasia (PIN, a potential PCa precursor state) to malignancy (17). In

addition, lymphocytic aggregates and clusters, reported as both predominantly CD8 and CD4 T cells, are only present in normal and pre-invasive epithelial areas, but not within malignant cancerous lesions (18), and these PCa TILs express decreased levels of the important cytotoxicity cytokines perforin and IFNγ in comparison to T cells from healthy prostate tissue (19). However, despite these findings, others have reported increased CD4 and CD8 T cells in PCa tissue in comparison to benign prostatic tissue (20), with CD3 T cells present in 69% of 16 CRPC specimens (21) and 72% of 25 high-grade prostatectomy/biopsy specimens (22). These inconsistencies may represent the heterogeneity both between and within prostate tumors, as well as between different stages of the disease.

Analysis of the clinical consequences of these TILs has also yielded conflicting results in PCa. Low level of PCa TILs was associated with a higher risk of tumor progression and cancer-related death (23), and a large scale study of 3,261 prostatectomy samples reported that both very low and very high CD3 T cell densities were associated with shorter PSA recurrence-free survival (RFS) (24). Further, high CD4 TILs was linked with decreased PCa survival (25), high CD8 TILs with shorter time to biochemical failure (disease recurrence determined by rising serum PSA) (26), and high overall TILs with tumor invasion and as an independent predictor of shortened PSA RFS (27). These conflicting findings highlight the complexity of PCa TILs and the need to better understand not only the overall quantity of infiltrating CD3 T cells, but also the specific phenotypes of these cells.

Within PCa, TILs are mostly Th1 T cells (CD4 T cells expressing IFNγ), and also display strong Th17 (CD4 T cells expressing IL-17) skewing relative to peripheral blood T cells, with Th17 TILs correlating with a lower Gleason score (28). In support of this finding, the efficacy of PCa vaccines was linked to the level of pre-treatment circulating Th17 T cells (29) and the ability of the treatment to induce a Th17-driven immune response (30).

Additional studies have analyzed the T cell receptor (TCR) of PCa TILs to determine the degree of antigen-specific T cells and any clonal T cell expansion within the tumor microenvironment. TCR clonality analyses have demonstrated that PCa TILs display both oligoclonal expansion, as determined by restricted TCR Vβ gene usage (31), and a broad TCR repertoire, indicating a lack of antigen-specific T cell expansion (19). While the degree of antigen-specific T cell clonality is still unclear in PCa, a pre-clinical murine model identified the presence of a CD8 T cell response specific for a histone H4 peptide only found in prostate tumor-bearing mice, signifying that the broad repertoire of PCa TILs may include ubiquitous self antigens exposed upon cancer formation (32).

Prostatic TILs also express high levels of immune checkpoint inhibitory molecules. These molecules normally serve an immune-regulatory role under benign conditions, but in the context of cancer, they are utilized by the tumor to evade the immune response. Specifically, PD-1 is expressed on activated and exhausted T cells after persistent antigen stimulation, and its interaction with its PD-L1 or PD-L2 ligands on antigen-presenting immune cells or tumor cells leads to T cell inhibition via SHP-2 phosphatase-mediated inhibition of downstream phosphatidylinositol-3 kinase (PI3K)

signaling, as well as inhibition of IFNγ, TNFα, and IL-2 production, among other mechanisms (33). The majority of prostate tumors contain PD-1-positive lymphocytic clusters, with as high as 90% of the CD8 TILs expressing PD-1 (31), and most prostate tumors are PD-L1 positive (34). In addition, PSA-specific T cells from PCa patients display higher expression of the Tim-3 exhaustion marker, as well as the CD38 activation marker (35). Tim-3 is specifically involved in regulating the activity of Th1 T cells and CD8 T cells through its interaction with its ligand galectin-9 (36).

Prostate tumor cells also demonstrate decreased expression MHC class I genes, another common mechanism by which tumors circumvent the host CD8 T cell-mediated immune response. 81% of Gleason 7-8 tumors display >50% HLA class I gene downregulation (37), and 50% of prostate tumors have been reported as HLA class I negative with only 22% as homogeneously class I positive, in comparison to 96% positivity in BPH samples (38). By immunohistochemistry (IHC), 88% of prostate tumors contain at least one type of HLA alteration and 50% were HLA class I negative, the latter of which was associated with tumor relapse, perineural invasion, and decreased expression of antigen presenting machinery genes (39). Prostate tumors also seemingly impact the TCR, as circulating CD8 and CD4 T cells from PCa patients display decreased TCRζ chain expression and decreased activation and proliferation in comparison T cells from healthy controls (40).

### *1.2.2 Regulatory T cells*

Regulatory T cells (Tregs) normally function to modulate inflammation and promote self-tolerance. However, in the context of cancer, Tregs infiltrate the tumor,

suppress the anti-tumor immune response through IL-2 deprivation, expression of the immune inhibitory molecule CTLA-4, and secretion of IL-10 and TGF-β, and they are associated with poor prognosis in many cancer types (41). In PCa, multiple studies have confirmed higher levels of infiltrating Tregs in prostate tumors in comparison to adjacent benign tissue and healthy controls (20, 28, 34, 42). A large scale IHC analysis identified $FOXP3^+$ (the Treg lineage-specific transcription factor) cells in 88.8% of 2,002 PCa samples (43). Interestingly, among benign prostatic zones, Tregs are least frequently found in the central zone, the region with the lowest incidence of PCa (20), suggesting a role for Treg-mediated immunosuppression in PCa tumorigenesis. Tregs are also increased in the peripheral blood of PCa patients in comparison to healthy controls (42, 44), and they express the immune inhibitory molecules *CTLA-4*, *GITR*, and *LAG3* (28).

These increased Tregs appear to have functional consequences in PCa. Increased tumor infiltrating Tregs correlated with decreased PSA RFS, advanced tumor stage, and increased Ki67 proliferative staining (43). In a phase II trial of metastatic CRPC (mCRPC) patients treated with an immunotherapeutic vaccine, authors identified a potential link between decreased Tregs and prolonged overall survival (OS) after treatment (45). However, in another vaccine trial, pre-treatment level of Tregs did not correlate with time to disease progression (TTP, defined by rising PSA) (29).

Many of the above clinical findings have been validated in pre-clinical PCa models that also offer evidence for the ability to specifically target these cells. In a transgenic murine model of prostate cancer dysplasia and PIN, immunosuppressive Tregs increased both within the tumor and in the tumor-draining lymph nodes (dLNs) during

the course of disease progression. Importantly, treatment with an anti-CD25 neutralizing antibody inhibited tumor growth (46). In a PSA-expressing TRAMP model of murine PCa, anti-CD25 antibody treatment was able to break CD8 immune tolerance, and, in combination with the otherwise ineffective anti-CTLA-4 antibody, delayed tumor growth (47).

### *1.2.3 γδ T cells*

γδ T cells are a T cell subset containing a TCR composed of a γ and δ chain, as opposed to an α and β chain. These cells display both pro- and anti-tumorigenic properties in cancer, as they may recruit immunosuppressive myeloid-derived suppressor cells (MDSCs) and macrophages and promote tumor angiogenesis, yet they can also directly eliminate tumor cells, produce IFNγ, upregulate tumor expression of MHC class I genes, and enhance CD8 T cell, Th1 T cell, and NK cell anti-tumor activity (48). However, research on γδ T cells has been minimal in prostate cancer. *Ex vivo* expanded human γδ T cells, specifically Vγ9Vδ2 T cells, display perforin- and granzyme-dependent *in vitro* cytolytic activity against the DU-145 and PC-3 CRPC cell lines, but not against the LNCaP androgen-dependent PCa cell line (49). One phase I clinical trial evaluated mCRPC patients treated with the γδ T cell agonist zoledronate plus IL-2. γδ T cells from treated patients displayed an effector memory-like T cell phenotype with IFNγ and perforin production, and increasing numbers of these cells correlated with decreasing PSA and partial remission and stable disease in some patients (50). A further study validated that zoledronate combined with IL-2 activated and increased γδ T cells, which was associated with reduced PSA and PSA velocity (51). The functions and impact of γδ

T cells in the prostate tumor microenvironment must be better understood in order to therapeutically target these cells in PCa.

### *1.2.4 Myeloid-derived suppressor cells*

MDSCs are an immature myeloid cell type that, like Tregs, constitutes a major source of immunosuppression in the tumor microenvironment. MDSCs inhibit T cell function through the production of reactive nitrogen and oxygen species (via iNOS, which leads to nitration of the TCR and inhibition of downstream signaling), deprivation of nutritional molecules (via arginase-1), IL-10 and TGF-β secretion, and Treg induction (52).

MDSCs can be subtyped as monocytic (M-MDSCs) or granulocytic (G-MDSCs), the former of which is considered the more potent immunosuppressor. Multiple studies have identified higher levels of circulating $CD14^{+}HLA\text{-}DR^{lo/-}$ M-MDSCs in the peripheral blood of PCa patients relative to healthy controls (44, 53, 54). These M-MDSCs express high levels of iNOS (44), suppress T cell activity (44, 53), and directly correlate with multiple negative PCa prognostic markers (increased lactate dehydrogenase, PSA, alkaline phosphatase, anemia) (44). Interestingly, after prostatectomy, these high M-MDSC levels normalize and CD8 T cell IFNγ production increases, suggesting that post-prostatectomy may be an optimal time to administer immunotherapies (54).

Circulating $Lin^{-}CD15^{Hi}CD33^{lo}$ G-MDSCs are also high in PCa patients, increasing during disease progression from localized to metastatic cancer. These G-

MDSCs express activated STAT3 and inhibit autologous CD8 T cell proliferation and IFNγ and granzyme B production (55).

Further, both M-MDSCs ($CD14^+$) and G-MDSCs ($CD14^-$) were identified in the positive pelvic lymph nodes (PPLNs) in a report of 10 PCa patients. The CD8 T cells in these lymph nodes expressed decreased Ki67 in comparison to autologous circulating CD8 T cells, and the G-MDSCs expressed higher phosphorylated-STAT3 (important for arginase-1 production), PD-L1, and PD-L2, indicating that salvage pelvic lymph node dissection may also play a role in decreasing immunosuppression (56).

As with Tregs, many of the clinical MDSC findings have been validated in murine PCa models. In a prostate-specific PTEN knockout (KO) mouse model, arginase-1- and iNOS-expressing MDSCs increased within the prostate immediately after *PTEN* deletion, and inhibiting the CSF-1 receptor (via GW2580) decreased both MDSC infiltration and immunosuppression (57). Also in this model, the tumor infiltrating MDSCs antagonized tumor senescence through the secretion of IL-1 receptor antagonist (IL-1RA), and a CXCR2 antagonist decreased tumor infiltrating MDSCs and enhanced the efficacy and senescence induction of docetaxel treatment (58). In another murine PCa model with loss of both *PTEN* and *SMAD4,* tumor-derived CXCL5 (via hyperactivated Hippo-YAP signaling) recruited CXCR2-expressing MDSCs, and CXCR2 inhibition again decreased tumor progression (59). In addition, $TLR9^+$ murine prostate cancer cells were able to recruit $STAT3^+$ G-MSDCs via the LIF cytokine. Importantly, LIF levels are increased in PCa patient blood and its receptor is increased on PCa patient circulating G-MDSCs (60). Finally, in a novel mCRPC murine model, MDSC inhibition with the

multikinase inhibitors cabozantinib and BEZ235 synergized with the combination of anti-CTLA-4 and anti-PD-1 immune checkpoint blockade. Interestingly, in contrast to one of the above findings, the efficacy of these treatments in inhibiting MDSCs was dependent on their ability to increase IL-1RA (61).

### *1.2.5 Tumor-associated macrophages*

Macrophages are commonly observed infiltrating various tumor types, and most often display an M2-polarized phenotype active in promoting immunosuppression, tumor proliferation, and angiogenesis, in contrast to M1-polarized macrophages promote anti-tumor immunity (62). In an analysis of 332 prostatectomy samples, the quantity of $CD68^+$ tumor-associated macrophages (TAMs) was higher in malignant tissue than in PIN or benign tissue, and was associated with higher Gleason score. While this study did not find a link between TAMs and biochemical recurrence (BCR) after prostatectomy (63), others have associated increased TAMs with an increased risk of BCR after both prostatectomy (64) and ADT (65). TAMs have also been associated with decreased survival and increased metastases, tumor grade, stage, and tumor cell proliferation (26, 66). In a study of 71 PCa biopsies after ADT, low level of TAMs was associated with an increased RFS, while high level of TAMs was associated with high PSA, Gleason score, T stage, and PSA failure. Further, TAM count was identified as a significant prognostic factor upon multivariate analysis (67). On the contrary, one study reported that decreased macrophage density within the tumor and stroma was associated with increased clinical stage, Gleason score, and positive lymph nodes, and identified TAMs as a predictive marker of disease-free survival (DFS) after prostatectomy (68).

Further analysis of the phenotype of these TAMs reported M2 macrophages present in 63.4% of PCa specimens. M2 TAMs were primarily observed in extra-capsular extension disease, while M1 TAMs were found in organ confined disease (64). Interestingly, another study on 100 prostatectomy samples reported higher $CD68^+$ total macrophages in benign glands in comparison to malignant glands, yet higher $CD204^+$ M2 macrophages within the malignant glands (17). This M2 polarization appears to be due to prostate tumor-derived factors, as monocytes from healthy controls incubated *ex vivo* with PC-3-conditioned culture medium took on an M2 phenotype, expressing the M2 marker CD164, secreting high IL-10 and low IL-1β and IL-12, and promoting angiogenesis and PC-3 proliferation, mobility, and invasiveness. These M2-like macrophages were dependent on upregulation on the microRNA let-7b for their pro-tumorigenic properties (69). Finally, in both subcutaneous and orthotopic PCa mouse models, TAMs were important for PCa recurrence after ADT. CSF1R inhibition combined with ADT decreased both TAM recruitment and tumor progression (70).

### *1.2.6 Dendritic cells*

Dendritic cells (DCs) are critical for an adaptive anti-tumor immune response, as they can present tumor antigen to T cells. However, tumor infiltrating DCs are often immature and unable to induce strong T cell responses. In PCa, an initial categorization of 15 specimens identified significantly decreased DCs within the tumor in comparison to within benign adjacent tissue (71). The decrease in DCs increased with tumor progression, as circulating levels of plasmacytoid DCs (pDCs) and myeloid DCs (mDCs) were further decreased in mPCa patients than in those with localized disease (72).

Interestingly, this decrease in DCs may be due to a tumor-secreted factor, as incubation with PCa patient serum inhibited monocyte differentiation into DCs, the ability of DCs to stimulate T cell proliferation, and the expression of the CD83, CD86, and CD40 activation and maturation molecules, the latter of which correlated with higher PSA levels (73). In a study of 151 prostatectomy samples, low $CD1a^+$ DCs was association with high Gleason score and tumor stage as well as low CD8 and CD4 TILs (74). In addition, in a transgenic murine model of prostate cancer dysplasia and PIN, tumor infiltrating DCs expressed decreased CD86 and MHC class II (46). Overall, systemic and tumor infiltrating DCs are decreased in both quantity and quality in PCa.

#### *1.2.7 B cells*

Like γδ T cells, B cell have contrasting roles in cancer. B cells can promote anti-tumor immunity through both antibody-mediated mechanisms and by acting as antigen presenting cells (APCs), yet they can also promote angiogenesis, recruit immunosuppressive cells, and the regulatory B cell subset (Bregs) can secrete IL-10 and TGF-β (75). Accordingly, studies on B cells in PCa have yielded conflicting results. One study on 53 prostatectomy specimens reported increased tumor infiltrating B cells in malignant tissue in comparison to adjacent benign tissue (76), yet another analysis of 100 prostatectomy samples reported decreased B cells infiltrating malignant glands relative to benign glands (17). In analyses of patient outcomes, B cell infiltration was increased in high-risk PCa and in patients that later recurred or demonstrated disease progression (76), yet a large scale study of 3,261 samples concluded that the level of B cell infiltration did not correlate with any clinical or histopathological PCa parameters (24). Despite this

negative finding, one case report demonstrated a biochemical response in an advanced $CD20^{+}CCR7^{+}$ PCa patient after treatment with the anti-CD20 antibody rituximab. However, it is unclear to what degree, if any, this efficacy was due to B cell inhibition (77). An early phase I trial (NCT01804712) evaluating rituximab as a neoadjuvant agent prior to PCa prostatectomy may shed light on this association.

In contrast to the conflicting human data, pre-clinical mouse data have suggested a pre-dominantly immunosuppressive role for B cells in PCa progression. In a subcutaneous syngeneic murine PCa model, lymphotoxin-expressing B cells were important in disease progression to CRPC (78). Further, a B cell subset of immunosuppressive $IgA^{+}$ IL-$10^{+}$ PD-$L1^{+}$ plasmocytes were identified in mice that decreased oxaliplatin-induced immunogenic cell death (ICD) and CD8 T cell activation. This B cell subtype is also found in prostate tumors from therapy-resistant patients (79).

### *1.2.8 NK cells*

NK cells are important in bridging the innate and adaptive immune systems. In cancer, NK cells play critical roles in promoting anti-tumor immunity through the production of cytokines, such as IFNγ, TNF, and GM-CSF, directly killing cancer cells, including those with MHC class I downregulation, augmenting APC and CD8 T cell activity, and in controlling metastasis (80). In PCa, NK cells have been observed within the lymphoid aggregates surrounding prostate tumors (18), yet they only account for approximately 3.6% of the total lymphocytic infiltration. NK cells in prostate tumors display an immature phenotype with low cytotoxic potential, in part due to immunosuppressive TGF-β1 within the tumor microenvironment and the inhibitor

receptor ILT2/LILRB1 on tumor cells. (81). Additional studies have confirmed decreased activity and cytotoxic ability of circulating NK cells during PCa progression, with minimal NK cell activity in advanced and metastatic PCa, but not in localized PCa, patients in remission, and healthy controls (81-87), suggesting a role for the immunosuppression of NK cells in PCa progression and metastasis. Differential NK cell activity has also been observed between PCa responders and non-responders to hormonal therapy (86). In addition, NK cell activity may also have diagnostic utility. PCa was diagnosed by IFNγ levels after stimulation with a patented stimulatory cytokine Promoca® with a sensitivity of 72% and specificity of 74% (87) and, more recently, a with sensitivity of 57%, specificity of 91%, positivity predictive value of 86%, negative predictive value of 69%, and an odds ratio of 13.33 by Promoca® in combination with an *in vitro* diagnostic device (IVDD) (88).

### *1.2.9 Mast cells*

As with other cell types, mast cells also display great complexity in the tumor microenvironment, promoting tumorigenesis through increased angiogenesis, extracellular matrix degradation, and MDSC activity, while also displaying anti-tumorigenic properties (89). In one PCa study, mast cells were reported as less numerous than T cells in the tumor microenvironment (18), while another study of 2,300 hormone-naïve prostatectomy specimens reported mast cells present in 95.9% of samples, as assessed by c-kit IHC (90). Interestingly, mast cells are located both surrounding and infiltrating prostate tumors (18, 91), and this geographic distinction is important in elucidating the function of these cells. Intra-tumoral mast cells display anti-tumorigenic

properties, decreasing angiogenesis and tumor growth, while peri-tumoral mast cells are pro-tumorigenic, increasing angiogenesis (via FGF-2) and tumor growth. The peri-tumoral mast cells increased during tumor progression to CRPC in a pre-clinical rat model (92).

Analyzing mast cells also has prognostic value, as high levels of infiltrating mast cells is a significant independent prognostic marker of PCa-specific survival, while low mast cell infiltration is associated with increasing stage, metastases, and tumor cell proliferation (92). In line with these findings, intra-tumoral, but not peri-tumoral mast cells, correlated with low Gleason score (91), and others have reported an association between high mast cell densities and low PSA, Gleason score, and tumor stage, and increasing PSA RFS (90). However, on the contrary, high prostate tumor infiltrating mast cell count has also been associated with increasing stage, Gleason score, and PSA failure, as well as a shortened progression free survival (PFS) in patients treated with prostatectomy, irradiation therapy, or ADT (93). Finally, when classifying tumor regions by differentiation status, mast cell infiltration and degranulation was only observed in well differentiated, but not poorly differentiated, PCa specimens. In mice, mast cells promoted growth of only well differentiated tumors via production of matrix metalloprotease-9, yet they were also protective against the formation of aggressive neuroendocrine tumors (94). The conflicting functional and correlative outcome data highlight both the complexity and potential importance of mast cells in PCa progression.

### *1.2.10 Neutrophils*

Neutrophils have been associated with poor prognosis in multiple cancer types, yet have also displayed both pro- and anti-tumorigenic characteristics (95). Circulating neutrophil levels have been studied specifically in PCa with respect to patient outcomes. In a study of 386 African-American PCa patients, neutropenia before prostatectomy was a significant predictor of high tumor grade (96), validated in a study of 323 Japanese PCa patients reporting low circulating neutrophil count as a predictive marker of a positive tumor biopsy (97). Other studies have utilized the neutrophil:lymphocyte ratio (NLR) relative to clinical outcomes, with opposing results. In 897 PCa patients from the Glasgow Inflammation Outcome Study, high NLR was associated with decreased OS (98). High NLR was also linked to high PSA levels post-docetaxel and -prednisone treatment (99) as well as poor prognosis and survival in in mCRPC patients pre- (100) and post-docetaxel therapy (101, 102). The lack of studies on neutrophils in the prostate tumor microenvironment and the lack of functional analyses of these neutrophils make it difficult to conclude the exact role of neutrophils in PCa development, progression, or response to therapies.

### *1.2.11 Cytokines, chemokines, and inhibitory molecules*

As discussed, the prostate tumor microenvironment is not conducive to an anti-tumor immune response, containing scarce quantity and activation of TILs and other important immune cell types, but an abundance of immunosuppressive immune cells. One cause of this inhibitory microenvironment may be the cytokine and chemokine profile of these tumors. In a study of 14 treatment-naïve PCa specimens, tumors

contained low levels of CCL5, CXCL9, and CXCL10, important for recruiting CD8 and Th1 T cells and NK cells, but high levels of CCL2, CCL22, and CXCL12, important for recruiting MDSCs and Tregs. As expected, these cytokine levels also corresponded with the degree of infiltration of these cell types. However, treatment with poly-I:C, IFNα, and celecoxib reversed many of these chemokine levels, leading to decreased Treg recruitment and increased granzyme B-expressing CD8 T cell recruitment (103). In addition, in murine PCa models, tumor-derived CXCL5 was implicated in recruiting CXCR2-expressing MDSCs into tumors (59), and surgical castration induced upregulation of CXCL13 to recruit pro-tumorigenic B cells (78). TGF-β1 levels are also high in the prostate tumor microenvironment, and are able to suppress NK cell activity (81) and increase extracellular matrix degeneration, angiogenesis, and the epithelial-to-mesenchymal transition to induce tumor metastasis. Potential therapies targeting the TGF-β signaling pathway including neutralizing antibodies, small molecule kinase inhibitors, and antisense oligonucleotides (104). In addition, the IL-6 cytokine is a significant prognostic factor for BCR and decreased prostate cancer survival (105). iNOS is also highly expressed in 68% of specimens from both prostate tumor cells and the immune infiltrate, in comparison to lower levels in benign adjacent tissue, and high iNOS was associated with poor survival, metastasis, and high Gleason score, PSA, and cancer cell proliferation, but not TILs (106, 107). Finally, high cyclooxygenase-2 levels were reported in 40 of 43 PCa specimens, and correlated with high Gleason score, TILs, macrophage density, and microvessel density (108).

## 1.3 Prostate cancer immunotherapy

Despite the immunologically cold and immunosuppressive nature of the prostate tumor microenvironment, PCa remains a viable target for immunotherapy for multiple reasons. Serial analysis of gene expression (SAGE) analysis estimated the prostate transcriptome at approximately 37,000, revealing 156 differentially expressed genes in malignant tissue (109). Further analysis comparing the prostate to other tissues has revealed that there are multiple overexpressed and immunogenic tissue-specific tumor-associated antigens (TAAs), such as PSA, PAP, PSCA, and PSMA (110). TAAs are important for driving an antigen-specific immune response that differentiates malignant from benign tissue. The prostate is also an accessory organ that is not vital for survival, fertility, or urinary function, thereby permitting immunotherapies to induce local inflammation and the possibility of bystander tissue damage with minimal consequences. Finally, the >1 year prognosis of both early stage androgen-dependent PCa and CRPC allows adequate time for immunotherapies to generate and maintain a long-term durable immune response. As a result, multiple immunotherapies have been tested in both the pre-clinical and clinical setting, with mixed results.

### *1.3.1 Androgen deprivation therapy*

ADT was designed to deplete and inhibit androgen function to cause prostate tumor cell death, yet this therapy also has multiple underappreciated immunomodulatory implications. With respect to T cells, firstly, ADT increases T cell infiltration into patient prostate tumors, which has been reported as both predominantly CD8 T cells (65) and

predominantly CD4 T cells (111), and these T cells display restricted TCR Vβ gene usage, suggesting oligoclonal antigen-specific expansion (111). Murine experiments confirmed increased levels of activated and antigen-specific T cells in lymphoid tissues after castration (112). Secondly, ADT abrogates the tolerance of CD4 T cells to prostate cancer antigens, which otherwise inhibits their effector function (113). Thirdly, a recent study demonstrated that after ADT, both *AR* expression and the presence of cytolytic AR-specific T cells increased. Consequently, combining ADT with a DNA vaccine encoding *AR* decreased tumor volume and delayed CRPC development (114).

ADT also increases the level of PCa TAMs, which was associated with an increased risk of BCR (65). In murine PCa models, androgen blockade again increased TAM recruitment (via tumor-derived M-CSF1 and CSF1), and ADT combined with CSF1R inhibition both blocked this recruitment and inhibited tumor progression (70). While B cell and Treg levels were trending, but not significantly increased after ADT in patients, murine castration increased tumor infiltration by lymphotoxin-expressing and CRPC-promoting B cells (via CXCL13) (78) and by Tregs, which exhibited increased inhibitory effects on CD8 T cell effector function after castration (115).

Interestingly, there are differential immunomodulatory effects between surgical orchiectomy and medical ADT, and even between specific medical forms of ADT. In mice, surgical orchiectomy synergized with immunotherapy, while medical ADT suppressed the adaptive immune response by inhibiting initial T cell priming and activation. This immunosuppressive quality of medical ADT was specific for the AR

antagonists flutamide and enzalutamide, but not the gonadotropin inhibitor leuprolide and the androgen synthesis inhibitor abiraterone (116).

### *1.3.2 Sipuleucel-T*

Sipuleucel-T became the first FDA approved cancer vaccine after demonstrating improved OS for patients with mCRPC (117). With this immunotherapy, patients undergo leukapheresis, their peripheral blood mononuclear cells (PBMCs) are exposed *ex vivo* to a fusion peptide (PA2024) of the PAP TAA and the cytokine GM-CSF, and these autologous cells are infused back into the patients to stimulate a PAP-specific immune response. GM-CSF is important in optimizing APC function, and, thus, has also been utilized with many other PCa immunotherapies. As a monotherapy, GM-CSF has reached phase II clinical trial (118, 119) and increased PSA doubling time (119), with a more recent phase I trial of neoadjuvant GM-CSF before prostatectomy demonstrating that the cytokine increased levels of circulating mature DCs, proliferating CD8 and CD4 T cells, and, to a lesser degree, Tregs and CD8 TILs, but not tumor infiltrating APCs (120).

After initial phase I/II Sipuleucel-T clinical trials demonstrated preliminary clinical responses and the successful generation of PAP-specific T cells in PCa patients (121-124), a phase III trial was designed to investigate the efficacy of Sipuleucel-T for mCRPC. While Sipuleucel-T did not significantly improve TTP, it did significantly prolonged median survival time from 21.4 to 25.9 months and increased patient T cell responses (125). In 2010, a phase III trial with 512 mCRPC patients concluded that Sipuleucel-T treatment significantly increased the median survival time by 4.1 months (from 21.7 to 25.8 months), with an increased 36-month survival probability from 23.0%

to 31.7%, yet, again, did not improve TTP (117). In these patients, low pre-treatment PSA level (126), the generation of antigen-specific T cells (detectable in 78.8% of patients) (127), and positive IgG responses specific for PSA and LGALS3 (indicating antigen spreading) (128) were associated with increased OS. Additional integrated analysis of the 2 phase III trials concluded that Sipuleucel-T conferred a 33% reduced risk of death (129).

Further studies have investigated the impact of Sipuleucel-T in the neoadjuvant setting and in combination with other therapies. In a phase II trial of PCa patients treated with Sipuleucel-T prior to prostatectomy, the immunotherapy increased CD8 and CD4 TILs, which were highly PD-$1^{+}$ and Ki-$67^{+}$ (130). Next-generation sequencing (NGS) of TCRs from these patients revealed that Sipuleucel-T treatment increased TCR sequence diversity and broadened the TCR repertoire (131). When combined with enzalutamide, Sipuleucel-T resulted in a durable complete PSA response in one mCRPC case report (132), and a phase II trial of Sipuleucel-T combined with abiraterone reported similar immune responses as seen in the Sipuleucel-T phase III trials (133). In addition, another phase II trial concluded that Sipuleucel-T prior to ADT induced greater immune responses than the reverse treatment order (134). Further, a recent phase I clinical trial (NCT01832870) combining Sipuleucel-T with the anti-CTLA-4 immune checkpoint inhibitor, ipilimumab, in 9 mCRPC patients reported that the combination was well tolerated and resulted in increased serum immunoglobulin specific for PA2024 and PAP, with 1 of the 6 surviving patients demonstrating undetectable PSA levels (135). Current ongoing PCa clinical trials include combining Sipuleucel-T with immediate or delayed

CTLA-4 blockade (phase II NCT01804465), the anti-PD-L1 immune checkpoint inhibitory antibody atezolizumab (phase I NCT03024216), the anti-angiogenic and immunomodulatory agent tasquinimod (phase II NCT02159950), a pTVG-HP DNA booster vaccine for PAP (phase II NCT01706458), radiation therapy (phase II NCT01833208, phase II NCT02232230), docetaxel (phase II NCT02793219, phase II NCT02793765), glycosylated recombinant IL-7 (CYT107) (phase II NCT01881867), the anti-VEGF antibody bevacizumab (phase II NCT00027599), and with indoximod, a small molecule inhibitor of the immunosuppressive indoleamine 2,3-dioxygenase (IDO). Preliminary reports on Sipuleucel-T combined with indoximod have demonstrated significant improvements in radiographic and clinical progression (phase II NCT01560923) (136).

### *1.3.3 Additional autologous APC-based vaccines*

In a similar approach as Sipuleucel-T, the autologous DCVAC/PCa vaccine involves patient leukapheresis followed by *ex vivo* pulsing of mature DCs with killed PCa LNCaP cells. A Phase I/II trial of DCVAC/PCa with cyclophosphamide for mCRPC resulted in an OS of 19 months (predicted at 11.8-13 months with no treatment), decreased circulating Tregs, and the generation of PSA-specific T cells (137). More recently, a phase I/II DCVAC/PCa trial reported significantly increased PSA doubling times in patients with PSA recurrence after prostatectomy or salvage radiotherapy (138), and a phase II trial of DCVAC/PCa combined with docetaxel induced TAA- or vaccine-specific immune responses, but no changes in PFS and disease-specific survival (DSS) (139). There is currently an ongoing phase III trial looking at the efficacy of

DCVAC/PCa combined with the standard of care docetaxel and prednisone for mCRPC (NCT02111577).

Additional APC-based experimental vaccines includes an earlier phase II trial of autologous DCs pulsed with two HLA-specific PSMA peptides, which demonstrated preliminary clinical responses (140). In addition, phase II trial of Dendritophage-rPSA, a vaccine of autologous DCs pulsed with recombinant PSA, resulted in PSA-specific immune responses and clinical responses in some patients (141). More recently, the BDCA-1 BDC-01 vaccine, in which PCa patient blood-derived $CD1c^+$ DCs were pulsed *ex vivo* with patient HLA-restricted peptides (PSA, PAP, PSMA, and a control influenza peptide), was reportedly safe and well tolerated in phase I trial (142). MUC1, a glycoprotein overexpressed and hypoglycosylated in malignant ductal epithelial cells, was also tested as a TAA vaccine. In a phase I/II clinical trial with 17 CRPC patients, autologous DCs were loaded with MUC1 bearing truncated carbohydrate Tn antigen (Tn-MUC1). The vaccine induced Tn-MUC1 specific T cell responses in rhesus macaques as well as MUC-1 specific T cell responses and improved PSA doubling time in patients (143). Finally, a recent phase I trial was conducted investigating BPX101 for mCRPC. For this *in vivo* activated vaccine, autologous patient APCs were transduced with the adenoviral vector Ad5f35f encoding rimiducid-inducible co-stimulatory molecule CD40 and were exposed to PA001 (extracellular domain of PSMA). The vaccine induced immune stimulation, PSA decline, and objective tumor regressions after *in vivo* induced activation (144).

### *1.3.4 GVAX*

GVAX involves the intra-dermal injection of inactivated allogeneic LNCaP and PC-3 cell lines engineered to secrete GM-CSF, as first described in the B16 melanoma murine model (145). In comparison to Sipuleucel-T, DCVAC/PCa, and BDCA-1, GVAX does not require patient leukapheresis or *ex vivo* conditioning, and involves multiple TAAs. An initial phase I GVAX trial demonstrated the induction of prostate cancer-specific T cells and B cells (146). In a phase I/II trial with hormone-naïve PCa patients with PSA relapse after prostatectomy, GVAX treatment led to intradermal infiltration of $CD1a^+$ DCs and $CD68^+$ macrophages at the injection site, the generation of multiple LNCaP and PC-3 antigen-specific antibodies, and a significantly decreased PSA velocity (147). Additionally, high dose GVAX increased the mean survival from 26.2 months (radiologic group) or 24.0 months (low dose GVAX) to 34.9 months (high dose GVAX) in metastatic and rising PSA PCa patients (148). An additional phase I/II trial validated this increased median survival time, reporting an increase from 23.1 months with low dose GVAX to 35 months with high dose GVAX (149). However, 2 larger scale phase III GVAX trials have both been terminated. The VITAL-1 trial was terminated after interim futility analysis concluded that the study would not meet its primary endpoint of improved OS (20.7 months with GVAX vs. 21.7 months with docetaxel and prednisone), and the VITAL-2 trial was terminated due to patient mortality.

Despite the failure of these phase III trials, continuing GVAX research has focused on combining the vaccine with additional immune-modulating therapies. GVAX followed by ipilimumab demonstrated enhanced anti-tumor immunity and efficacy in a

pre-clinical PCa model (150), and, in a phase I clinical trial for mCRPC, GVAX combined with ipilimumab resulted in >50% PSA decline in 25% of treated patients (151). Recent retrospective analysis of the trial identified that increasing OS was associated with the ability of the combination therapy to induce activation of circulating DCs, and OS was inversely correlated with pre-treatment levels of M-MDSCs (152). In addition, a high $CD8^{+}ICOS^{+}$ T cell/Treg ratio and a high plasmacytoid DC/MDSC ratio correlated with increased PFS after additional mitoxantrone treatment (153). GVAX is also being tested in combination with cyclophosphamide and androgen ablation (phase I NCT01696877), and has demonstrated enhanced efficacy in a transgenic murine model when combined with ionizing radiation (154).

### *1.3.5 Additional irradiated cell line vaccines*

Like GVAX, another vaccine approach tested irradiated allogeneic prostate cell lines LNCaP, OnyCap23, and P4E6. Treatment resulted in Th1 immune skewing, decreased PSA velocity in 11 of 26 CRPC patients, and a 58 week median TTP (compared to a 28 week historical control TTP) (155). More recently, in mice, a Streptavidin-GM-CSF surface-modified vaccine with the prostate cancer cell line RM-1 increased CD8 and CD4 T cells, DCs, and, when combined with $ICOS^{+}$ Treg depletion, enhanced therapeutic efficacy (156). This vaccine also increased PD-1 on T cells and PD-L1 on tumor cells, and, consequently, combination with PD-1/PD-L1 blockade increased anti-tumor T cell activity and induced tumor rejection (157).

### *1.3.6 ProstVac-VF*

ProstVac-VF/PSA-TRICOM is a poxvirus-based PCa immunotherapy involving the administration of a recombinant vaccinia virus for initial T cell priming followed by a booster recombinant fowlpox virus to maintain anti-tumor immunity (158), with both viral vectors delivering the transgenes for PSA and the 3 costimulatory molecules, LFA-3, ICAM-1, B7.1 (159). After initial phase I studies demonstrated that ProstVac-VF induced PSA-specific immune response, clinical responses, and was well tolerated in PCa patients (160-163), subsequent phase II trials reported 78.1% of patients with clinical PFS, 45.3% without PSA progression at 19.1 months, (164), and increased 3-year OS (17% in controls vs. 30% in treated) and median survival time (16.6 months in controls vs. 25.1 months in treated), but no improvement in PFS (165). This efficacy was partly attributed to the decreased Treg immunosuppressive function observed in post-vaccination patient PBMCs (45), and, in mice, with the ability of the vaccine to increase immune activation markers, cytokine production, cytotoxic ability of PSA-specific CD8 and CD4 T cells, and intra-tumoral activated effector T cell:Treg ratios. Interestingly, the vaccine also induced antigen-spreading and the subsequent rejection of challenge with PSA-negative tumors in mice (166). However, as with GVAX, the phase III clinical trial PROSPECT (NCT01322490) (167) of mCRPC patients receiving ProstVac-VF with or without GM-CSF was recently terminated after interim analysis concluded that the treatment would not improve OS.

As with the other PCa vaccines, subsequent approaches for ProstVac-VF involve combining the vaccine with additional immune-stimulating agents. A phase I trial

(NCT00113984) of ProstVac-VF combined with ipilimumab conferred a median OS of 31.3 months at all doses and 37.2 months at high ipilimumab dose, while the predicted median OS from ProstVac-VF alone was 18.5 months (168, 169). PBMC analysis revealed associations between increased OS and lower pre-treatment PD-$1^{+}$Tim-$3^{-}$ effector memory CD4 T cells, higher pre-treatment PD-$1^{-}$Tim-$3^{+}$ CD8 T cells, higher pre-treatment CTLA-$4^{-}$ Tregs, and increasing Tim-$3^{+}$ NK cells post-treatment (170). ProstVac-VF is also currently in ongoing clinical trials in combination with ipilimumab (phase II NCT02506114), the anti-PD-1 antibody nivolumab (phase I/II NCT02933255), CV301 (immunotherapeutic targeting the TAAs CEA and MUC-1) and M7824/MSB0011359C (fusion protein of the PD-L1 antibody and the soluble extracellular domain of the TGF-β receptor II) (phase II NCT03315871), docetaxel (phase II NCT02649855, phase II NCT00045227), flutamide (phase II NCT00450463), GM-CSF (phase II NCT00108732, with IL-2 phase II NCT00020254), enzalutamide (phase II NCT01875250, phase II NCT01867333), radiotherapy (phase II NCT00005916), and a phase II trial with the osteoblastic radiopharmaceutical Sm-153-EDTMP (Quadramet®) (171).

### *1.3.7 Additional viral-based PCa vaccines*

Further research has investigated the efficacy of additional viral-based PCa immunotherapies. In mice, a modified vaccinia Ankara vector containing the TRICOM genes as well as the Twist transgene induced Twist-specific CD8 and CD4 T cell responses and increased survival in combination with enzalutamide in the transgenic TRAMP model (172), an alphavirus-based virus-like particle vector encoding PSA

(VLPV-PSA) induced PSA-specific immune response to overcome tolerance and delay tumor growth (173), a CMV vaccine expressing PSA induced antigen-specific CD8 T cells responses and pre-clinical anti-tumor efficacy (174), and a simian adenovirus (ChAdOx1) and modified vaccinia Ankara virus (MVA) encoding the TAA STEAP1, a cell surface TAA specifically and highly expressed in PCa (175), increased survival when combined with PD-1 blockade (176). In PCa patients, a PSA adenovirus vaccine induced PSA-specific T cell responses and resulted in longer than predicted survival in a phase I mCRPC trial (177), and a phase II poxviral PSA vaccine combined with external beam radiation therapy induced antigen spreading, yet the development of autoantibodies was linked to a trending decreased biochemical-free survival (178). There is also currently an ongoing phase III trial for localized PCa treated with radiation therapy combined with ProstAtak® (NCT01436968), an adenovirus encoding the herpes simplex virus thymidine kinase to sensitize tumors to valcyclovir. ProstAtak increased CD8 TILs (179) and induced clinical responses in combination with radiotherapy in phase I/II trials (180). More recently, an adenoviral bivalent vaccine for PSA and PSCA (Ad5-PSA+PSCA) decreased tumor burden and induced PSA-specific T cell responses in mice when used with surgifoam to sustain durable immunity (181).

### *1.3.8 Additional PCa vaccines*

Multiple additional vaccines have been tested in the pre-clinical and clinical setting targeting various TAAs utilizing multiple delivery methods. hTERT, the reverse transcriptase subunit of telomerase, is both upregulated in cancer and is an immunogenic peptide. Therefore, a phase I/IIa trial tested a second generation hTERT vaccine (UV1)

combined with GM-CSF for mPCa. 85.7% of patients had detectable antigen-specific immune responses, 64% displayed PSA decline to <0.5ng/ml, and 45% of treated patients displayed no evidence of persisting disease, resulting in 77% of patients with stable disease at 9 months (182). In addition, a chaperone complex vaccine containing GRP170 and PSCA also inhibited tumor growth in a pre-clinical murine study (183).

Multiple cytokines, in addition to GM-CSF, have also been tested as immunotherapeutic tools for treating PCa. IL-12 has been utilized with PCa vaccines for its immune-promoting anti-tumor effects. A vaccine of apoptotic murine TRAMP-C2 cells infected with an adenovirus containing the IL-12 gene improved survival of prostate tumor-bearing mice (184), and a DC-based vaccine expressing IL-12 and exposed to RM-9 PCa cell line antigens displayed similar efficacy in preclinical murine PCa models (185). In addition, intra-prostatic injection of TNFα in CRPC patients induced tumor necrosis and decreased tumor volumes, with long-term reductions in patient serum PSA levels (186).

Finally, personalized peptide vaccines (PPVs) have also been investigated for PCa. A phase II trial with CRPC patients administered a PPV containing up to 31 pooled immunogenic peptides demonstrated initial clinical responses, and high serum pre-treatment levels of IL-6 was associated with decreased OS after treatment (187). In a subsequent CRPC phase II trial, a PPV of 24 HLA-A02, -A24, or -A03 restricted peptides with lose-dose dexamethasone increased OS and PSA PFS in comparison to dexamethasone alone (188). However, combining the PPV with low-dose

cyclophosphamide did not alter the positive immune responses, PFS, or OS, but did decrease Tregs and increase MDSCs to a greater degree than PPV alone (189).

DNA-based vaccines have also been extensively studied in PCa. A plasmid DNA vaccine encoding PAP induced PAP-specific T cell responses after multiple immunizations, correlating with prolonged PSA doubling time in phase I and I/IIa trials (190, 191). This vaccine also elicited a Th1 T cell phenotype in 75% of patients, but additional real-time immune monitoring-based treatment regimens did not enhance the anti-tumor immune response (192). A current clinical trial (phase II NCT00849121) is investigating the optimal treatment schedule of this vaccine (pTVG-HP) combined with GM-CSF. An additional DNA PSA vaccine (pVAX/PSA) with GM-CSF and IL-2 has also reached clinical trial (193). More recent immunotherapies include a DNA plasmid encoding a human monoclonal antibody specific for PSMA that increased mouse survival and controlled tumor growth, likely via NK cell antibody-dependent cellular cytotoxicity (ADCC) (194), and PSCA plasmid vaccines that have demonstrated pre-clinical efficacy as a monotherapy (195), combined with an alphavirus (196), fused with HSP70 (protein vaccine) (197), and as a fusion plasmid of the *PSCA* and *CTLA-4* genes, which increased PSCA-specific immune responses and decreased tumor growth to a greater degree than a PSCA-only plasmid vaccine (198).

### *1.3.9 Anti-angiogenic immunomodulators*

VEGF inhibitors and tasquinimod are both anti-angiogenic therapies that also display multiple immunomodulatory characteristics. Interestingly, outside of PCa, VEGF has demonstrated roles in promoting Treg, MDSC, and immunosuppressive TAM

differentiation and function, while also inhibiting the maturation of DCs and decreasing T cell trafficking into the tumor and subsequent effector functions (199). Prostate tumors express increased levels of VEGF (200), and plasma VEGF levels inversely correlated with survival in CRPC patients (201). In a phase III clinical trial, the anti-VEGF antibody bevacizumab combined with docetaxel and prednisone improved PFS and objective responses for mCRPC patients, but did not improve OS (202), and a more recent phase II trial combining bevacizumab with ADT demonstrated improved RFS compared to ADT alone (203). Further, the multi-kinase inhibitors sorafenib, sunitinib, and cediranib, which inhibit VEGF receptors, also demonstrated limited efficacy in PCa trials (204, 205), and a phase III trial of the VEGF inhibitor aflibercept also did not improve OS for mCRPC (206). However, in the above trials, the immunomodulatory effects of these VEGF inhibitors were not analyzed.

Like VEGF inhibitors, tasquinimod is an anti-angiogenic agent with additional immunomodulatory roles. Tasquinimod binds the calcium-binding protein S100A9, which promotes inflammation (207) and is upregulated in PCa (208). Interestingly, S100A9 is also expressed on MDSCs, TAMs, DCs, and endothelial cells, and its activity drives MDSC accumulation and inhibits DC differentiation (209, 210). In prostate tumor-bearing mice, tasquinimod enhanced the efficacy of a vaccine immunotherapy, inhibited the immunosuppressive function and levels of MDSCs and M2-polarized TAMs, and increased CD8 TILs and effector functions (211). In PCa patients, tasquinimod demonstrated safety and initial efficacy in a phase I trial (212), and increased PFS (213), demonstrated benefit for patients with skeletal metastases (214), and delayed objective

radiographic bone scan progression (215) in phase II trial. However, a phase III trial for mCRPC with bone lesions was discontinued after tasquinimod did not improve OS, despite prolonging radiographic PFS (216). Current studies are combining tasquinimod with Sipuleucel-T (phase II NCT02159950) and with cabazitaxel and prednisone, which resulted in 63% of treated men having a >30% PSA decline and 48% with stable disease (217).

### *1.3.10 Adoptive and chimeric antigen receptor T cell immunotherapies*

Chimeric antigen receptor (CAR) T cells, comprised of patient T cells engineered to express an antigen-specific antibody single-chain variable fragment fused to an intracellular signaling domain (such as CD3ζ), have shown strong promise in treating multiple cancer types (218). In prostate cancer, CARs have been designed with specificity for the TAAs PSMA and PSCA. PSMA-specific engineered patient derived T cells were first described in 1999 with the ability to lyse PSMA-expressing cancer cells and release multiple cytokines (219). PSMA-specific designer T cells also suppressed tumor growth *in vivo* (220), and, with the addition of a CD28 signaling domain, demonstrated increasing cytokine production, proliferation, *in vitro* cytotoxicity, and *in vivo* tumor suppression (221, 222). Additional studies have demonstrated the ability of PSMA CARs to eliminate murine prostate tumors (223, 224), with increased efficacy in combination with PD-1 blockade (225). Interestingly, as PSMA is also found on the tumor-associated neo-vasculature, third generation PSMA CARs containing CD28 and CD137/4-1BB signaling domains demonstrated enhanced efficacy in mediating vascular disruption and decreasing tumor burden in a pre-clinical ovarian cancer model (226). In

addition, the recent development of PSMA (and PSCA) "UniCARs" allow the use of target modules to retarget CARs *in vivo* in an effort to prevent CAR-induced side effects (227). Phase I clinical trials (NCT01140373 and NCT00664196) with second-generation (CD28/CD3ζ) and designer T cell PSMA CARs demonstrated safety and preliminary clinical responses in mCRPC (228-230). However, activated T cell engraftment also reportedly depleted the administered IL-2 and limited therapeutic efficacy (231).

PSCA-specific CARs have also been developed for PCa, demonstrating cytotoxicity against PSCA-expressing cancer cells (232), with further efficacy in a third generation PSCA CAR containing CD28, OX-40, and CD3ζ signaling domains (233). Interestingly, in a humanized murine pancreatic cancer model, second-generation PSCA CARs displayed greater efficacy than third-generation CARs with an additional 4-1BB domain (234). In addition, T cells transduced with a CAR and a chimeric costimulatory receptor (CCR) that recognized both PSMA and PSCA demonstrated efficacy only against tumors expressing both antigens (235).

Patient-derived T cells have also been engineered with chimeric receptors with specificity for the overexpressed TAA erbB2, demonstrating efficacy in locally advanced PCa, recurrent PCa (236), and PCa with bone metastases (237), as well as for the prostate antigen TARP, which was cytotoxic *in vitro* against PCa and breast cancer cells (238). Further, CARs targeting EPCAM and EMP2, found on circulating tumor cells (CTCs), successfully prevented lung metastasis in a preclinical PCa model (239).

### *1.3.11 Bispecific diabodies, BiTEs*

Similar to CARs activating and targeting patient T cells to specific TAAs, bispecific antibodies, or diabodies, commonly known as bispecific T cell engagers (BiTEs), have been generated to cross-link T cells (via CD3) with target surface cancer antigens. Bispecific diabodies for PCa have been generated with specificity for both PSMA (240-246), PSCA (245, 247-249), and Her2/neu, demonstrating engagement of both CD4 and CD8 T cells, *in vitro* cytotoxic killing, and *in vivo* tumor control (250-252) in pre-clinical xenograft models. In addition, in a phase I trial, 3 of 7 CRPC patients treated with activated T cells with the anti-CD3 x anti-Her2 bispecific antibody displayed decreased PSA levels (253). PSMA and EpCAM BiTEs are currently being evaluated in ongoing phase I clinical trials for CRPC (NCT01723475, NCT02262910, and NCT00635596).

### *1.3.12 Immunostimulatory chemotherapy and radiation therapy*

Interestingly, chemotherapies and radiation therapy demonstrate previously underappreciated immunostimulatory properties, primarily through their ability to stimulate immunogenic cell death. In ICD, dying tumor cells release and expose specific damage-associated molecular patterns (DAMPs), including HMGB1, ATP, and calreticulin, resulting in APC recruitment, activation, and maturation, and subsequent priming of anti-tumor T cells (254). Of the chemotherapeutic agents using in treating PCa, docetaxel induces calreticulin exposure and increases antigen-specific CD8 killing (255) while mitoxantrone induces all major ICD markers of calreticulin cell surface exposure and ATP and HMGB1 release (256). Outside of ICD, docetaxel also decreased

MDSC quantity and function and increased CD8 T cell activity in a pre-clinical breast cancer model (257), and increased CCL2 chemokine production from prostate cancer cell lines (258). In addition, radiation therapy induces ATP and HMGB1 secretion and calreticulin cell surface exposure in LNCaP cells, increasing antigen presentation and tumor antigen-specific CD8 T cell lysis (259). Further, chemotherapies may enhance immunotherapy for PCa patients with high Tregs (260) or MDSCs (261, 262).

### *1.3.13 CTLA-4 immune checkpoint inhibitors*

Immune checkpoint inhibitors have shown great promise in recent years, with anti-PD-1/PD-L1 and anti-CTLA-4 blocking antibodies gaining approval in multiple cancer types. These antibodies target the normally homeostatic immune regulatory mechanisms that act to promote immune evasion in the context of cancer. Specifically, CTLA-4 is normally upregulated on activated T cells, and outcompetes the T cell co-stimulatory molecule CD28, displaying higher affinity for the B7 ligand on APCs. CTLA-4 activity inhibits T cell function by disrupting phosphorylation of CD3ζ and downstream signaling, increasing T cell motility to disrupt TCR engagement with the APC, and through its constitutive expression on Tregs (263).

Initial pre-clinical studies in PCa reported that an *in vivo* anti-CTLA-4 inhibitory antibody augmented the anti-tumor immune response and decreased tumor growth (264). In a pilot clinical trial, treatment with the anti-CTLA-4 antibody, ipilimumab, was safe and induced PSA decline >50% in 2 of 14 CRPC patients (265). In a subsequent phase I trial, ipilimumab combined with GM-CSF administration resulted in 3 of 6 high dose patients demonstrating a >50% PSA decline, with responders having increased

circulating activated and TAA-specific CD8 T cells (266) and increased antibody responses to antigens both specific for individual tumors and shared between patients (267). Ipilimumab therapy also increased overall TCR diversity through expansion of T cell clonotypes, with responders displaying the least loss of T cell clonotypes (268). A phase I/II trial combining ipilimumab with radiotherapy reported 8 of 50 patients with PSA decline >50%, 1 of 50 with complete response (CR), and 6 of 50 with stable disease, yet there was one treatment-related death and multiple others with immune-related adverse events (irAEs) (269). However, in a larger scale phase III trial with 799 mCRPC patients progressing after docetaxel, ipilimumab after radiotherapy did not significantly increase OS (11.2 months in treated vs. 10.0 months placebo, $P = 0.053$), with 26% of ipilimumab-treated patients experiencing grade 3-4 irAEs. However, ipilimumab treatment did significantly improve PFS, and post-hoc analysis demonstrated that ipilimumab did significantly increase OS in patients with good prognostic features (non-elevated alkaline phosphatase, normal hemoglobin concentration, and no visceral metastasis) (270). As a result, a subsequent phase III trial tested ipilimumab in 399 chemotherapy-naïve CRPC patients without visceral metastases. However, again, ipilimumab did not increase OS but did increase PFS and PSA response rates, with 2% treatment-related deaths and 31% grade 3-4 irAEs (271). However, despite these negative survival results, there have been case reports of a mCRPC patient with sustained CR and disease free for 6 years (272) and of 2 mCRPC patients in long-term complete remission at 64 and 52 months after ipilimumab therapy, one of whom demonstrated high CD8 and Treg TILs (273). Interestingly, there is also an ongoing phase I trial (NCT02113657)

assessing the impact of ipilimumab therapy on T cell responses to tumor-specific neo-antigens in patients with mCRPC.

To optimize efficacy, CTLA-4 blockade has and is currently being tested in combination with other immunotherapies and immunomodulators. CTLA-4 blockade combined with a GM-CSF vaccine decreased tumor incidence and increased immune infiltration in TRAMP mice (274), increased anti-tumor immune efficacy when administered to mice after GVAX (150), and a phase I trial combining ipilimumab with GVAX induced >50% PSA decline in 25% of patients (151). Analysis revealed that increasing OS correlated with high pre-treatment CTLA-$4^+$ CD4 T cells, PD-$1^+$ CD4 T cells, and differentiated CD8 T cells, as well as low pre-treatment M-MDSCs and Tregs, and high post-treatment DC activation and seroreactivity to PSMA and other TAAs (152, 275). High $CD8^+ICOS^+$ T cell/Treg ratio and a high pDC/MDSC ratio were also associated with increased PFS after further mitoxantrone therapy (153). In addition, the CTLA-4 antibodies ipilimumab or tremelimumab are currently in clinical trials combined with Sipuleucel-T (phase II NCT01804465), docetaxel (phase II NCT00050596), the PD-L1 and PD-1 antibodies durvalumab (phase II NCT03204812) and nivolumab (phase II NCT02985957, phase II NCT03061539 in prostate tumors with an immunogenic signature of defective MMR or other DNA repair deficiencies or high inflammatory infiltrate, and phase II NCT02601014 in prostate tumors expressing the AR-V7 splice variant), and with ProstVac-VF (phase I NCT00113984, phase I NCT02506114). Results from trials of CTLA-4 combined with ProstVac-VF demonstrated longer than expected survival times (168, 169), with lower pre-treatment PD-$1^+$Tim-$3^-$ effector memory CD4 T

cells, higher pre-treatment PD-1$^-$Tim-3$^+$ CD8 T cells, higher pre-treatment CTLA-4$^-$ Tregs, and increasing post-treatment Tim-3$^+$ NK cells observed in responding patients (170). CTLA-4 checkpoint inhibitors are also being evaluated in phase I and II trials with abiraterone (NCT01688492) and multiple forms of ADT, including bicalutamide, flutamide, degarelix, leuprolide, and goserelin (phase II NCT01498978, phase II NCT00170157, phase II NCT02020070, phase II NCT01377389) (276, 277), with preliminary results reporting increased ICOS$^+$ and memory T cells (278). In addition, CTLA-4 blockade is being combined with sargramostim (GM-CSF) (phase I NCT00064129), which displayed dose-dependent expansion of both activated effector CD4 T cells and Tregs (279). Finally, while not yet in clinical trial, pre-clinical murine data has demonstrated enhanced anti-tumor immunity and efficacy when combining CTLA-4 blockade with an agonistic antibody specific for the costimulatory molecule OX40 (280).

### *1.3.14 PD-1/PD-L1 immune checkpoint inhibitors*

The PD-1/PD-L1 axis represents another regulatory immune checkpoint pathway utilized as a potent form of immunosuppression by many tumors. PD-1 is upregulated on late-stage exhausted T cells after persistent antigen exposure, and interacts with the PD-L1 and PD-L2 ligands found both on APCs and on many tumor cells. This interaction inhibits T cell activity through SHP-2 phosphatase, decreasing production of IFNγ, TNFα, and IL-2, and decreasing T cell survival (33, 263). Checkpoint blockade targeting the PD-1/PD-L1 axis can recover the effector function of exhausted T cells, and the clinical benefits have resulted in FDA approvals in multiple cancer types in recent years.

Studies in PCa have determined that the majority of prostate tumors express moderate or high PD-L1 levels (21, 281), which was an independent prognostic factor for BCR (281). In addition, over half of prostate tumors contain PD-$1^+$ TILs (21), with up to 90% of TILs being PD-$1^+$ within each specimen (31, 34), yet another study found only 8% of 25 high-grade prostate tumors to contain high PD-1 and PD-L1 expression (22). Consequently, PD-1/PD-L1 inhibitory antibodies have been evaluated in clinical trials for patients with PCa. In initial phase I trials with the anti-PD-1 antibody, nivolumab (BMS-936558/MDX-1106/ONO-4538), no objective responses were observed in the 8 (282) and 17 (283) treated CRPC patients. However, further analysis of a subset of these patients revealed that these prostate tumors were negative for PD-L1 expression (282-284), and overall PD-L1 positivity among all cancer types tested was an important predictor of increased infiltrating immune cells, PD-1 expression on T cells, and objective response to anti-PD-1 treatment (284). Additional phase I (NCT01772004 with avelumab, NCT02458638 with atezolizumab) and phase II (NCT02787005 with pembrolizumab) trials are ongoing evaluating PD-1/PD-L1 blockade in treating mCRPC, with PD-L1 status subtyping. Avelumab is also being tested in neuroendocrine PCa (phase II NCT03179410), and nivolumab in mCRPC with DNA repair defects (phase II NCT03040791) and mCRPC with the AR-V7 splice variant (phase II NCT02601014).

Interestingly, the PD-1/PD-L1 axis appears to be closely linked to enzalutamide treatment. Patients progressing after enzalutamide therapy display increased PD-$L1^+$ and PD-$L2^+$ circulating DCs in comparison to naïve or responding patients. Similar DC results were observed in a pre-clinical model of enzalutamide resistant tumors, which

express higher PD-L1 levels (285). In further support of this association, a phase II trial of mCRPC patients progressing on enzalutamide who were treated with the anti-PD-1 antibody, pembrolizumab, reported 3 of 10 patients with rapid PSA decline and partial response in 2 of the 3 patients with measurable disease before treatment (286). Finally, a recent case report presented a patient with CRPC refractory to enzalutamide and multiple chemotherapies who demonstrated undetectable PSA and decreased tumor mass after nivolumab treatment. Interestingly, the tumor displayed loss of expression of DNA repair genes *MSH2* and *MSH6* (287). Enzalutamide has also proven capable of inhibiting expression of homologous recombination DNA repair genes *BRCA1*, *RAD54L*, and *RMI2* in CRPC (288). As a result, an ongoing phase II trial (NCT02312557) has been designed to evaluate pembrolizumab for mCRPC patients progressing after enzalutamide therapy, as well as a phase I trial (NCT02861573) combining concurrent pembrolizumab with enzalutamide, and a phase III trial (NCT03016312) combining atezolizumab with enzalutamide after failed treatment with an androgen synthesis inhibitor and a taxane regimen.

Additional ongoing anti-PD-1 trials include combining nivolumab with ipilimumab for overall mCRPC (phase II NCT02985957) and specifically in prostate tumors with an immunogenic signature (phase II NCT03061539), pembrolizumab with radium-223 (phase II NCT03093428), pembrolizumab with the pTVG-HP plasmid DNA vaccine (phase I/II NCT02499835), pembrolizumab with the PARP inhibitor, olaparib (phase I NCT02861573), pembrolizumab with docetaxel and prednisone (phase I NCT02861573), and the anti-PD-1 antibody, PDR001, with the anti-TGF-β antibody,

NIS793 (phase I NCT02947165). Ongoing combination trials with PD-L1 antibodies include atezolizumab with Sipuleucel-T (phase I NCT03024216), MEDI4736 with olaparib and/or cediranib (phase I/II NCT02484404), MSB0011359C/M7824 (fusion protein of avelumab and a TGF-β inhibitor) with ProstVac-VF and CV301 (a viral vaccine targeting the TAAs CEA and MUC-1) (phase II NCT03315871), avelumab with talazoparib (phase II NCT03330405), durvalumab with tremelimumab (phase II NCT03204812), and atezolizumab with CPI-444 (adenosine-A2A receptor antagonist) (phase I NCT02655822).

Interestingly, another current phase I CRPC trial (NCT02867345) is evaluating the impact of *ex vivo* CRISPR-Cas9 knockout of PD-1 (*PDCD1)* from peripheral blood patient T cells with IL-2, followed by infusion of the autologous T cells after cyclophosphamide treatment. In addition, a pre-clinical murine study demonstrated increased efficacy of PSMA CAR T cells when combined with PD-1 blockade (225). While PD-1/PD-L1 inhibitors have not proven efficacious in treating prostate cancer as monotherapies, the number of completed trials with published results is minimal, and its true potential remains to be seen in combination with other immunomodulatory therapies.

#### *1.3.15 Other immune checkpoints and stimulatory molecules*

There are additional intriguing targetable immune checkpoint molecules, as well as immune stimulatory molecules, for PCa. Analysis of ipilimumab treated prostate tumors revealed that macrophages expressed increased PD-L1 and VISTA, both immunosuppressive molecules (289). However, a recent phase I trial (NCT02671955) with the anti-VISTA antibody (JNJ-61610588) has been prematurely-terminated. In

addition, in TRAMP mice, the immune inhibitory molecule Lag-3 was increased on CD8 TILs and promoted antigen tolerance, and an anti-Lag-3 antibody increased antigen-specific CD8 T cell activity (290). Similarly, expression of the immune checkpoint Tim-3 was significantly higher on both circulating CD4 and CD8 T cells from PCa patients than BPH patients (291). Tim-3 levels also increased in malignant prostate tissue in comparison to adjacent benign tissue, and were a prognostic predictor of RFS and PFS (292). Finally, B7-H3 and B7-H4 (*VTCN1*) are additional immune-regulatory molecules overexpressed in the tumor microenvironment. B7-H3 and B7-H4 expression were reported in 93% and 99% of 823 prostatectomy samples, respectively (strong intensity in 26% and 15%, respectively) (293), they were reported at significantly higher levels in PCa tissue than in BPH and normal prostate tissue (294-296), and their increased levels correlated with cancer cell proliferation, disease spread, grade, Gleason score, risk of BCR, and cancer-specific death (293-295, 297-299). Further, B7-H3 expression increased in bone metastases after ADT (299). However, despite these associations, pre-clinical TRAMP studies demonstrated that mice lacking B7-H3 developed larger tumors with increased Tregs, while B7-H4 loss did not affect tumor size (300). Further studies are warranted, as loss of B7-H3 or B7-H4 in the murine model even before tumor formation does not address the potential efficacy in inhibiting these molecules in the context of an established immunosuppressive tumor.

In contrast to these inhibitory immune checkpoints, the co-stimulatory receptor OX40 is important in amplifying the T cell response, and a phase I trial with an OX40 agonistic antibody demonstrated preliminary regression and stable disease in 5 PCa

patients (301). An OX40 agonist is currently in a phase I/II clinical trial (NCT01303705) in combination with cyclophosphamide and radiation for mPCa.

### *1.3.16 Bacterial cancer therapies*

Interestingly, bacteria and bacterial products have long been used as direct microbial cancer therapeutics. The observation that an infection could induce tumor regression first led to the utilization of bacteria as an anti-cancer agent with Coley's toxin in the 1890s. Since then, attenuated *Mycobacterium bovis* BCG (bacillus Calmette-Guerin) has gained approval for treating bladder cancer, and other bacteria, mainly *Salmonella typhimurium*, *Listeria monocytogenes*, and *Clostridium novyi* spores, have been tested in various cancer types. Bacterial therapies contain a number of advantages over conventional therapies, including their ability to specifically target tumor tissue, being able to infiltrate into the deeper and more hypoxic tumor regions, containing innate tumor cytotoxicity characteristics, and their potential to be manipulated to either constitutively or inducibly express anti-cancer and imaging agents (302). The obligate anaerobe C. novyi and the facultative anaerobes S. *typhimurium*, *L. monocytogenes,* and *Escherichia coli* preferentially colonize and accumulate in tumor tissue over other benign tissues, either due to chemotactic molecules released from the tumor, the favorable hypoxic environment of the tumor, or as a result of either the inflammatory state of the tumor or the protection from the host immune system provided by the immunosuppressive tumor microenvironment. In addition to surviving in hypoxic tissue, bacterial motility and their ability to sense extrinsic molecules allows for them to spread diffusely throughout a tumor. Subsequently, bacteria have demonstrated an ability to

induce tumor regression, either through the expression of cytotoxic bacterial proteins, nutrient depletion, or through the numerous genetic manipulating strategies that have been employed. Specifically, bacteria have been engineered to express the bacterial toxin Cytolysin A, FAS ligand, TRAIL, the cytokines TNFα, IL-2, IL-18, CCL-21, and LIGHT, as well as multiple TAAs or personalized tumor-specific mutated and immunogenic neo-antigens. Bacteria have also been utilized as expression vectors for genetic material, inducing expression of anti-angiogenic molecules, cytokines, TAAs, or delivering small hairpin RNA (shRNA) or small interfering RNA (siRNA) to silence tumor-promoting genes. Finally, bacteria have been modified to allow for detection by imaging modalities including fluorescence, magnetic resonance imaging (MRI), bioluminescence, and positron emission tomography (PET). Many of these delivered factors have been tested under either constitutive expression or through more controlled expression, to limit systemic toxicity and improve therapeutic efficacy. L-arabinose, γ-irradiation, salicylate, and even environmental hypoxia have all been utilized as triggering agents for genes cloned downstream of their appropriate inducible elements using the *pBAD* promoter, *pRecA* promoter, *Pm* promoter, and fumarate and nitrate reduction (FNR) regulator-containing promoters, respectively (302, 303).

Many of these bacterial therapeutic approaches have been performed utilizing *S. typhimurium*, *L. monocytogenes*, and *C. novyi* spores. The facultative anaerobe *S. typhimurium* can preferentially home to and proliferate within tumors and augment the host immune response through activation of toll-like receptors (TLRs) and NOD-like receptors (NLRs). Multiple attenuated *S. typhimurium* strains have been tested expressing

cytotoxic agents (such as cytolysin A, diphtheria toxin, FasL, and TRAIL), cytokines (such as IL-2, IL-18, and CCL-21), as well as various enzymes, TAAs, and genetic material to induce specific gene expression or silencing. As a result, *S. typhimurium* has reached phase I clinical trials for metastatic melanoma and squamous cell carcinoma (304). *L. monocytogenes* has also been utilized as a bacterial therapeutic, especially to deliver tumor antigen and elicit and tumor antigen-specific host immune response. *L. monocytogenes* can infect host APCs, deliver antigen for presentation through both the MHC I and MHC II pathways, and can also stimulate the innate immune system. Attenuated *L. monocytogenes* strains have been used in vaccine approaches for cervical cancer, breast cancer, melanoma, prostate cancer, and hepatocellular carcinoma, and have also reached clinical trial for multiple cancer types (305). Further, *C. novyi* have also been used as anti-cancer agents, as they form spores that are able to germinate within the central, necrotic, hypoxic regions of the tumor, thereby reaching areas of the tumor resistant to most other therapies (306). Intra-tumoral injection of *C. novyi* spores is currently being tested in phase I clinical trial for solid tumor patients unresponsive to standard therapies (NCT01924689).

Multiple bacterial therapies have been tested in PCa. One leucine-arginine auxotrophic *S. typhimurium* strain, A1-R, delivered intra-venously or intra-tumorally specifically localized to and colonized PC-3 xenograft tumors *in vivo* and induced tumor regression (307, 308). In addition, other *S. typhimurium* strains demonstrated an ability to invade PC-3M prostate cancer cells and induce tumor cell mitochondrial destruction (309). *S. typhimurium* has also been engineered to express the TAAs PSCA (310) and

PSA (311), the *p53* gene and *MDM2* siRNA (combined with cisplatin) (312), and *Stat3* siRNA and Endostatin (313). In addition, an attenuated and immunogenic *L. monocytogenes* modified to express PSA decreased tumor infiltrating Tregs, increased PSA-specific T cells, and induced tumor regression in pre-clinical murine PCa (314, 315). Finally, the *L. monocytogenes* vaccine combined with radiation therapy synergistically decreased tumor growth and increased PSA-specific T cells and IFNγ production in treated mice (316).

#### *1.3.17 Future direction: synergistic combinations*

While immune checkpoint inhibitors, vaccines, and other immunotherapies have displayed strong efficacy as monotherapies in many cancer types, they have not achieved as impressive clinical results in immunologically cold tumors, such as PCa. Therefore, current effort has been placed in determining optimal treatment combinations that synergistically enhance the anti-tumor immune response, and, therefore, clinical outcomes. Across many cancer types, combination therapies have included immune checkpoint inhibitory antibodies, immune stimulatory agonists, chemotherapies, radiotherapies, virotherapies, vaccines, and adoptive T cell therapies. However, choosing which immunomodulatory therapies to combine should be carefully considered to achieve synergy and minimize mechanistic overlap. Hallmarks of an ideal immunotherapy include increasing TILs, driving TAA- and neo-antigen-specific T cell responses, activating T cells while minimizing their inhibition and reversing exhaustion, inducing ICD and recruiting and optimizing APCs, and minimizing immunosuppressive

cell types and molecules (317). As described above, there are multiple currently ongoing immunotherapeutic combinations in pre-clinical and clinical trial for PCa.

In addition, as with ADT and chemotherapies, there are many existing therapies that have previously underappreciated immunomodulatory properties (318). A recent pre-clinical study demonstrated that treatment with histone deacetylase (HDAC) inhibitors (pan-HDAC inhibitor vorinostat and class I HDAC inhibitor entinostat) increased LNCaP sensitivity to T cell antigen-specific lysis, increased levels of antigen processing and tumor immune recognition proteins, and reversed immune escape through activating the unfolded protein response (319). Further, while not in PCa, recent studies have demonstrated that the diabetes drug metformin could prevent CD8 T cell apoptosis and promoted effector function regardless of PD-1 and Tim-3 positivity (320), and also potentiated PD-1 blockade *in vivo* (321).

## 1.4 CP1

In this study, we analyzed the immunomodulatory ability of CP1, an *Escherichia coli* isolated from the prostate-specific secretions of a patient with chronic prostatitis without concurrent cystitis. Prior analysis has demonstrated that intra-urethrally administered CP1 specifically colonizes murine prostates before being cleared by the host after one month. During that time, CP1 induces local, tissue-specific Th1/Th17 T cell infiltration (322, 323). In addition, after administration to pre-cancerous genetically-

susceptible mice, CP1 induces chronic inflammation, and therefore, expectedly, modestly increases the frequency of progression from mouse prostatic intraepithelial neoplasia (mPIN) (324). As increasing research has demonstrated the context-dependent balance between chronic inflammation promoting cancer formation and the anti-tumor immune response combating tumor growth, we hypothesized that, in the setting of a developed immunosuppressive tumor, CP1, with its innate tissue-tropism and local immunostimulatory properties, could be exploited on the other side of the spectrum as a cancer therapeutic. Here we demonstrate in multiple clinically relevant orthotopic models of prostate cancer that CP1 specifically ascends to and colonizes prostate tumors, induces infiltration by multiple anti-tumor immune cell types, increases tumor immunogenicity, and decreases immunosuppressive immune cell types and molecules within the tumor microenvironment, resulting in strong synergistic clinical benefit in combination with PD-1 blockade (325). In addition to treating prostate cancer, these results outline the potential to discover additional unique tissue-specific bacteria to benefit patients with other immunologically “cold” cancers, as microbes, specifically pathogenic bacteria, colonize various tissue niches throughout the human body (326-329).

# CHAPTER 2: MATERIALS AND METHODS

## 2.1 Mice

All FVB/NJ mice (The Jackson Laboratory) used in this study were housed in a pathogen-free animal barrier facility or a containment facility, as appropriate. All experiments involving mice utilized male FVB/NJ mice administered intra-prostatic cancer cells at 6-8 weeks old, with the number of mice indicated in respective figure legends. All experiments and procedures were performed in compliance with ethical regulations and the approval of the Northwestern University Institutional Animal Care and Use Committee (IACUC).

## 2.2 Cells lines and tissue culture

Myc-CaP, LNCaP, and 293T cells lines (ATCC) used in this study were verified to be mycoplasma-free (Biotool), and human cell lines were authenticated by short tandem repeat (STR) loci profiling (ATCC). 293T cells were growth in DMEM (Corning), Myc-CaP and LNCaP in RPMI (Gibco), all supplemented with 10% heat inactivated fetal bovine serum (FBS; Corning) and 1% Penicillin-Streptomycin (10,000 U/ml; Life Technologies). All cell culture was performed in a 37°C 5% $CO_2$ incubator with phosphate buffered saline (PBS; VWR) and 0.25% trypsin-EDTA (Gibco).

## 2.3 Bacterial growth and inoculation

CP1 and MG1655 were grown as previously described (323). Bacteria were grown in Luria Broth (LB) media (Sigma) at 37°C for 24 hours shaking followed by 24 hours static, and were subsequently resuspended in PBS at $2\times10^{10}$ cells/ml. For indicated *in vitro* assays, CP1 was heat killed at 70°C for 45 minutes. For *in vivo* experiments, 10µl of CP1 ($2\times10^{8}$ cells), MG1655 ($2\times10^{8}$ cells), or sterile PBS were administered intra-urethrally by catheterization to isoflurane anesthetized mice (330).

## 2.4 Library construction and whole genome sequencing

Library construction and sequencing were performed at the Northwestern University sequencing core facility. DNA libraries were prepared using a Nextera XT DNA Library Preparation Kit (Illumina) per the manufacturer's instructions, and then sequenced. Briefly, a tagmentation reaction was performed which fragmented the DNA and ligated on appropriate PCR. A limited-cycle PCR reaction was then performed which added barcode and sequencing adapter sequences to the tagmented fragments. Very short fragments were removed from the PCR product using Agencourt AMPure XP beads (Beckman Coulter). The distribution of fragment sizes in the libraries was assessed on an Agilent 2100 Bioanalyzer using a High Sensitivity DNA Assay (Agilent), and the concentrations were measured using a Qubit assay (Fischer Scientific). The resulting libraries were then normalized, pooled, and loaded on to a MiSeq (Illumina), using V3 chemistry, to generate paired-end 300bp reads.

## 2.5 Whole genome assembly and annotation

DNA quality was assessed using FastQC, and the reads were trimmed using Trim Galore. The trimmed reads were then used to generate genome assemblies with SPAdes version 3.11.1 (331) using the default parameters for paired-end reads. The resulting assembly graphs were visualized using Bandage (332). The genome was annotated with Rapid Annotation using Subsystem Technology (RAST) (333) and analyzed and visualized using RAST and Artemis (334). CP1 was stratified into 1 of the 4 major *E. coli* phylogenetic groups (A, B1, B2, or D) using the Clermont method based on *chuA, yjaA,* and the DNA fragment TSPE4.C2 (335), and multi-locus sequence typing (MLST) was performing based on the Warwick Medical School scheme of 7 housekeeping genes: *adk, fumC, gyrB, icd, mdh, purA,* and *recA* (336). The phylogenetic tree was created with concatenated MLST sequences of CP1 and reference *E. coli* strains using the Maximum Likelihood method with MEGA7 (337). This CP1 Whole Genome Shotgun project has been deposited at DDBJ/ENA/GenBank under the accession PZKJ00000000 [https://www.ncbi.nlm.nih.gov/nuccore/PZKJ00000000]. The version described in this paper is version PZKJ01000000.

## 2.6 Gentamicin protection assay

As previously described (323), tumor cells were incubated with CP1 or MG1655 (MOI 1) in antibiotic-free media for 2 hours at 37°C 5% $CO_2$. To quantify bacterial invasion, cells were washed 4 times with PBS, treated with 50μg/ml gentamicin, incubated with 0.05% trypsin/0.1% Triton X-100 for 10mins at 37°C 5% $CO_2$, and cells were harvested, plated on LB agar, and colonies counted after 24 hours. To quantify

bacterial adherence, cells were washed, immediately incubated in trypsin/Triton X-100, collected and plated, and adherence was measured as the difference from invasion colony counts. To quantify intracellular proliferation of bacteria, cells were washed and incubated with 50μg/ml gentamicin for 22 hours at 37°C 5% $CO_2$, followed by cell collection.

### 2.7 ICD and cell death assays

Cell death from CP1 or MG1655 (MOI 1 or 10) and cancer cell co-culture was measure by supernatant lactate dehydrogenase (LDH; Cytotoxic 96 Non-Radioactive Cytotoxicity Assay, Promega). For *in vitro* ICD assays, 1μM mitoxantrone was used as a positive control. Supernatants were collected and cell counts performed after 72 hours for quantifying secreted ATP (Bioluminescent Assay Kit, Sigma) and high mobility group protein B1 (HMGB1; ELISA, Tecan Trading). Also after 24 or 72 hours, cells were incubated with rabbit anti-calreticulin (Abcam ab2907 1:1000) for 60 min, followed by Alexa Fluor 488 anti-rabbit secondary (Invitrogen A11008 1μg/ml) for 30 mins, and analyzed by flow cytometry. For *in vivo* ICD assays, HMGB1 immunofluorescence was quantified as the percentage of $HMGB1^-$ nuclei and calreticulin immunofluorescence was analyzed for cell surface staining. *In vitro*, caspase 3/7 activity was assessed at 6 or 24 hours (Caspase-Glo 3/7 Assay, Promega). Early (Annexin $V^+$ $PI^-$) and late (Annexin $V^+$ $PI^+$) stage apoptosis were analyzed at 24 hours by flow cytometry (Annexin V Apoptosis Detection Kit, eBioscience). Phosphorylated MLKL, MLKL, RIP1, and full length and cleaved PARP were analyzed by Western blot. As indicated, select experiments included the addition of 50μg/ml gentamicin 2 hours after co-culture initiation.

## 2.8 Multiplex cytokine/chemokine array

Tissue lysates were prepared in RIPA buffer (Sigma) supplemented with protease (cOmplete Tablets, Mini, EDTA-free, Roche) and phosphatase (PhosSTOP, Roche) inhibitors. Tissues were homogenized using an electric pestle or a gentleMACS dissociator in M Tubes (MACS Miltenyi Biotec). Protein from tissue (10µg) or *in vitro* supernatant (25µl) was added per well of a 32-plex mouse cytokine/chemokine magnetic bead milliplex plate (EMD Millipore), which was run using a MAGPIX Luminex plate reader (Thermo Fisher Scientific) and analyzed on xPONENT Software Solutions.

## 2.9 293T transfection and lentiviral transduction of tumor cells

Lentivirus was produced by co-transfection of 293T cells with 3µg luciferase expressing vector pLV-mCherry-P2A-luciferase, 2µg Δ8.9 HIV-1 packaging vector, 1µg VSVG envelope glycoprotein vector, and 2.5µl/µg Lipofectamine 2000 (Invitrogen) in Opti-MEM media (Gibco) in 6-well plates at 37°C 5% $CO_2$ for 16 hours. Supernatant virus was collected, 0.45µm filtered, and diluted 1:5 and supplemented with 8µg/ml polybrene (Santa Cruz Biotechnology) before spinfecting Myc-CaP cells for 2 hours at 32°C. At least 48 hours later, mCherry positivity was verified and sorted for top 10% positivity using a FacsAria SORP cell sorter (BD).

## 2.10 Orthotopic surgical tumor model

Intra-prostatic surgical injections were performed as described (338). Mice were administered at least 0.05 mg/kg pre-operative buprenorphine and anesthetized with isoflurane, verified by toe pinch. The abdominal region was shaved and sterilized, and

$1\times10^6$ luciferase-expressing Myc-CaP prostate cancer cells in 30µl (1:1 PBS and matrigel [Basement Membrane Mix, Phenol Red-Free, LDEV-Free, Corning]) was injected (Hamilton syringe and 28-gauge needles) into one anterior prostate lobe (Fig. 1a), leading to the development of orthotopic prostate tumors with a clinically relevant tumor microenvironment and the correct prostate-draining lymph nodes (Fig. 1b). This was performed using micro-dissecting scissors, Graefe forceps, Graefe tissue forceps, a needle holder with suture cutters, and a 50 µL syringe with a 28-gauge needle (Fig. 1c). After performing an approximately 1 cm midline abdominal incision above the preputial glands (Fig. 1d), one seminal vesicle and attached anterior prostate lobe were located and externalized (Fig. 1e) and the PBS/matrigel cell suspension was injected into the prostate (Fig. 1f), as initially verified by the engorgement of the lobe and the lack of leakage (Fig. 1g). The inner abdominal wall was closed with 5-0 absorbable sutures (J493G, eSutures) and the outer skin was closed with 4-0 non-absorbable sutures (699H, eSutures). Approximately 1 mg/kg post-operative meloxicam was administered immediately, 24, and 48 hours post-surgery. Sample size was determined with consideration of the duration of each intra-prostatic surgery and the power needed to allow for adequate statistical analyses with the number of experimental groups. *In vivo* orthotopic tumor growth was non-invasively monitored by *in vivo* bioluminescence (Fig. 2). Intra-prostatic injections resulted in the formation of orthotopic tumors located at the site of the anterior prostate lobe (Fig. 3a), with tumor volumes (Fig. 3b) and weights (Fig. 3c) with relatively small standard error. Immune cell infiltration was observed and analyzed in this syngeneic murine model (Fig. 3d), and survival endpoint was defined in advance as the

appearance of hemorrhagic abdominal ascites (Fig. 3e) (339) and/or decreased grooming, ambulation, or piloerection (340). Tumor volumes were calculated using caliper measurements at $\pi/6 \times L \times W \times H$, where L was length of longest axis of the tumor, and W and H were the perpendicular width and height, respectively.

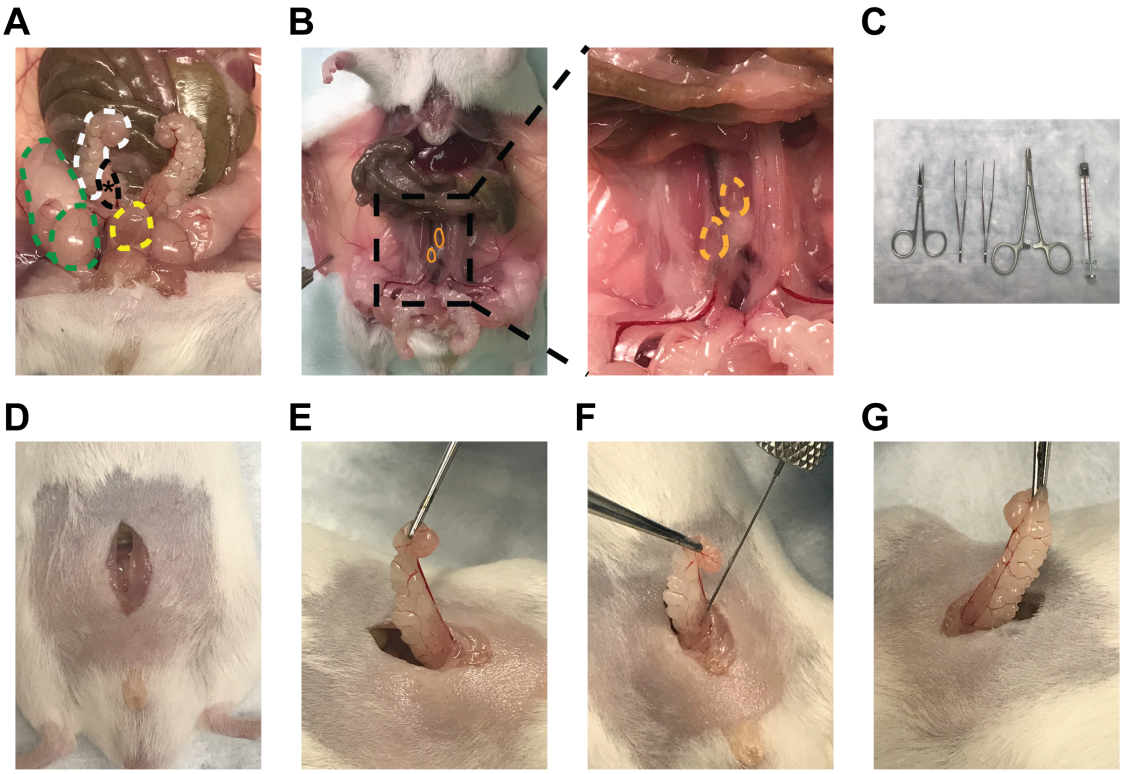


**Figure 1. Anterior prostate lobe, draining lymph nodes, and representative technique for intra-prostatic cell injections**
Images of the **(A)** right anterior prostate lobe (black, *), attached right seminal vesicle (white), right testicle and fat pad (green), and bladder (yellow), **(B)** bilateral prostate-draining para-aortic lymph nodes (orange), **(C)** micro-dissecting scissors, Graefe forceps, Graefe tissue forceps, an needle holder with suture cutters, and 50 µL syringe with 28-gauge needle (left to right), **(D)** midline incisions, **(E)** seminal vesicle and anterior prostate lobe externalization, **(F)**, intra-prostatic injection, and **(G)** engorgement of the anterior prostate lobe.

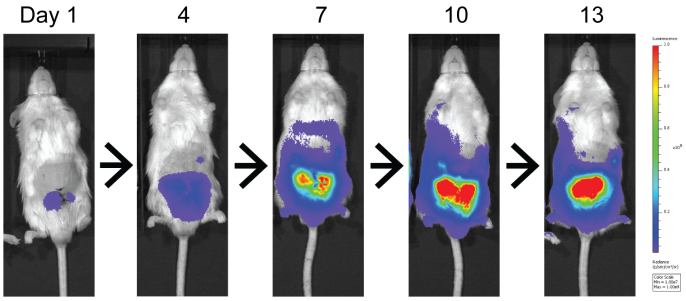


**Figure 2. Representative *in vivo* bioluminescent and fluorescent tumor imaging**
Luciferase-expressing orthotopic Myc-CaP tumors were imaged using an IVIS Spectrum Imaging System.

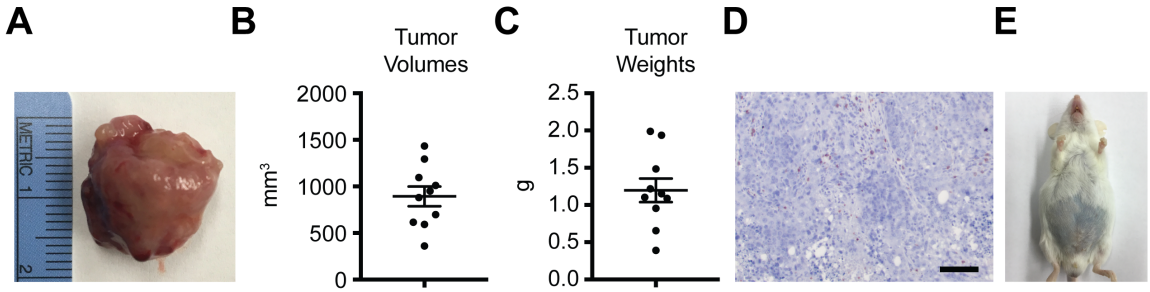


**Figure 3. Orthotopic tumor analyses by tumor volume, weight, histology for immune infiltration, and survival**
Orthotopic tumors were dissected on day 30 after intra-prostatic injection and analyzed by **(A)** gross imaging, **(B)** tumor volume ($\pi/6 \times L \times W \times H$; L=length of the longest axis of the tumor, W=perpendicular width, H=perpendicular height), **(C)** tumor weight, **(D)** CD3 IHC (scale bar=100 μm), and **(E)** survival, with the objective endpoint as the appearance of hemorrhagic abdominal ascites. **(A-B)** Data represented as mean ± standard error of the mean.

Orthotopic tumor modeling ideally allows for tumor development with a clinically representative tumor microenvironment. Prior studies have demonstrated that subcutaneous tumors have an altered tumor vasculature, leading to differential and less clinically accurate responses to anti-angiogenic therapies (341, 342). In addition, multiple studies have observed increased or decreased efficacy of multiple chemotherapeutics in treating the same cell line, depending on whether it was administered subcutaneous or orthotopically, the latter of which best represented what is seen in human cancer (343-345). Further, only in an orthotopic model of colon cancer, but not in the subcutaneous model, did tumors produce the correct degradative enzymes necessary to induce metastasis (346). Finally, as immunotherapies continue to emerge at the forefront of cancer therapy, and especially as they have yet to provide significant benefit for prostate cancer (270, 283), syngeneic pre-clinical models with accurate tumor microenvironment and draining lymph nodes in immunocompetent hosts are critical.

There are many factors responsible for these inconsistent findings based on tumor site. With a different tumor microenvironment, cancer cells are exposed to different tissue-specific endothelium and altered angiogenesis, thereby affecting tumor development (347, 348). Orthotopic tumors with the correct tumor microenvironment allow for clinically relevant drug delivery, hypoxic conditions, and evaluation of anti-angiogenic therapies (349). While genetically engineered models (GEMs) do contain an accurate tumor microenvironment, they require long times for breeding, high cost, and are often based on manipulations of single or few genes knocked out or overexpressed beyond clinically relevant levels. In contrast, the human or murine prostate cancer cell

lines used in orthotopic tumors, like human tumors, are much more genetically complex both within single cells and in displaying heterogeneity between cells (350, 351). Also unlike GEMs, orthotopic cancer cell lines can be engineered to express imaging modalities or increased or decreased levels of other molecules of interest, and *in vitro* and *in vivo* experimental results can be directly compared. Orthotopic tumors can also be formed from primary patient-derived cells.

### 2.11 *In vivo* treatment regimens

CP1 was administered intra-urethrally to tumor-bearing mice on day 8 post-tumor injection. 100μg anti-PD-1 antibody (RMP1-14, BioXCell) or IgG2a isotype control (2A3, BioXCell) were administered intra-peritoneally (i.p.) every other day, as previously performed (352), from day 17-29 for Myc-CaP and from day 13-23 for Myc-CaP PTEN KO experiments. For select experiments, FTY720 (Sigma) was administered 25μg intra-venously (i.v.) 24 hours prior to CP1 administration followed by 5μg i.p. daily until analysis, as previously performed (353). Mice were not randomized, rather pre-treatment tumor imaging was utilized to normalize tumor burden and variance among all experimental groups before CP1 or anti-PD-1 antibody administration (Fig. 15). Blinding during the course of treatment was not possible to prevent cross-contamination between CP1-infected and non-infected mice during handling and the daily (FTY720) and/or every other day (anti-PD-1 or isotype antibody) injections. Investigators were blinded to some outcome analyses.

## 2.12 In vivo bioluminescent imaging

Luciferase-expressing tumor-bearing mice were injected i.p. with 10µl/g body weight of 15mg/ml 0.22µm filtered D-luciferin (sodium salt, Gold Bio). At least 10 minutes after injection, mice were imaged with an IVIS Spectrum Imaging System (PerkinElmer). Images were analyzed and quantified using Living Image software.

## 2.13 In vivo bacterial colonization

Mice tissues were analyzed at day 1 or day 9 after intra-urethral CP1 administration. As previously described (323), tumors, bladders, kidneys, livers, and spleens were aseptically excised, dissected, homogenized by electric pestle, and plated in serial dilutions on eosin methylene blue (EMB) agar and incubated at 37°C for 24 hours.

## 2.14 RNA extraction and qRT-PCR

Excised tissue was immediately placed in RNAlater until homogenization using TissueMiser Homogenizer (Fisher Scientific) or gentleMACS Dissociator in M Tubes (MACS Miltenyi Biotec). RNA was extracted by Trizol (Thermo Fisher Scientific) and subsequent RNAeasy Plus Mini kit (QIAGEN), and complementary DNA (cDNA) was generated using oligo $d(T)_{16}$ primer (Invitrogen) and random hexamer (Promega) at 65°C for 5 mins, followed by the addition of dNTPs (Promega), 1x first strand buffer (Invitrogen), DTT (Invitrogen), SUPERase-In RNase inhibitor (Invitrogen), and M-MLV reverse transcriptase (Invitrogen) at 25°C for 10 mins, 37°C for 50 mins, and 70°C for 15 mins. Quantitative reverse transcription-PCR (qRT-PCR) was performed using a QuantStudio 6 Flex Real-Time PCR System (Applied Biosystems) at 50°C for 2 mins,

95°C for 10 mins, and 40 cycles of 95°C for 15 sec, 60°C for 15 sec, and 72°C for 1 min using SYBR Green master mix (Bio-Rad) and the following primers: *16S* (F: ACTCCTACGGGAGGCAGCAGT, R: TATTACCGCGGCTGCTGGC) or the mouse housekeeping gene *RPLP0* (F: AGATGCAGCAGATCCGCA, R: GTTCTTGCCCATCAGCACC) (Integrated DNA Technologies). Data were analyzed using QuantStudio Real-Time PCR software. In Fig. 8d, *16S* qRT-PCR results from CP1-administered tumors were calibrated to *16S* values of CP1 titrations of known cell counts ($R^2 = 0.98184$), and were subsequently normalized to calibrated PBS-administered tumors, total RNA yield, and the weight of the tumor tissue from which RNA was extracted.

### 2.15 Flow cytometry

Single cell suspensions were generated from tumors using a gentleMACS Dissociator with Heaters with the Tumor Dissociation Kit in C Tubes (MACS Miltenyi Biotec). Tissues were passed through a 70μm filter, resuspended in 30% Percoll (Sigma), and overlayed on top of 70% Percoll, centrifuged without brakes, and the buffy coat layer was isolated and viable cells counted. Tumor-draining para-aortic (Fig. 1b) lymph nodes single cell suspensions were created by passing cells directly through a 70μm filter, followed by red blood cell lysis with ACK buffer (0.15M $NH_4Cl$, 10mM $KHCO_3$, 0.1mM $Na_2$-EDTA; pH 7.2-7.4; 0.2μm filtered). All samples were treated with anti-mouse CD16/CD32 Fc block (2.4G2, BD). For intracellular staining, cells were resuspended in RPMI 10% FBS with 50ng/ml PMA (Sigma), 1μg/ml ionomycin (Cell Signaling), 1μl/ml brefeldin A (GolgiPlug; BD), 2μl/3ml monensin (GolgiStop; BD), and CD107a antibody

when appropriate, for 6 hours at 37°C 5% $CO_2$. Antibodies utilized for flow cytometry are listed in Table 1, and all antibodies were individually titrated to determine optimal staining dilutions. After subsequent extracellular staining, cells were stained with LIVE/DEAD Fixable Blue Dead Cell Stain Kit (Invitrogen). FoxP3 panels were fixed and permeabilized with the FoxP3/Transcription Factor Staining Buffer Set Kit (eBioscience) before antibody incubation. All other panels were fixed in IC fixation buffer (eBioscience) before subsequent permeabilization with the Intracellular Fixation and Permeabilization Buffer Set Kit (eBioscience) and incubation with intracellular antibodies when appropriate. Samples were run on a LSRFortessa 6-Laser (BD). Controls and compensation were performed using anti-rat/hamster Ig, κ/negative control compensation particles set (BD) and appropriate fluorescence minus one and unstained controls. Data were analyzed using FlowJo software. A representative flow cytometry gating strategy is displayed in Fig. 4 (a: tumor, b: dLNs), with initial gating on overall morphology, singlets, live cells, and CD45 positivity before proceeding with all further analyses.

**Table 1. Primary antibodies used in this study for flow cytometry.**

| Antigen (mouse) | Label | Clone | Vendor | Catalog # |
|---|---|---|---|---|
| CD45 | PE | 30-F11 | BD | 553081 |
| CD3ε | V500 | 500A2 | BD | 560771 |
| CD4 | BV786 | RM4-5 | BD | 563727 |
| CD8α | BUV395 | 53-6.7 | BD | 563786 |
| CD25 | BV421 | PC61 | BD | 562606 |
| FoxP3 | eFluor 660 | FJK-16s | eBioscience | 50-5773-80 |
| CD11b | Alexa Fluor 700 | M1/70 | BD | 557960 |
| Gr-1 | BUV395 | RB6-8C5 | BD | 563849 |
| γδ TCR | BV421 | GL3 | BD | 562892 |
| NKp46 | Alexa Fluor 700 | 29A1.4 | BD | 561169 |
| B220 | BV786 | RA3-6B2 | BD | 563894 |
| F4/80 | BV421 | T45-2342 | BD | 565411 |
| CD11c | BV786 | HL3 | BD | 563735 |
| CD80 | FITC | 16-10A1 | BD | 563727 |
| CD107a | BV786 | 1D4B | BD | 564349 |
| IFNγ | Alexa Fluor 488 | XMG1.2 | BioLegend | 505813 |
| TNFα | Alexa Fluor 700 | MP6-XT22 | BD | 558000 |
| IL-17A | BUV395 | TC11-18H10 | BD | 565246 |
| Granzyme B | eFluor 450 | NGZB | eBioscience | 48-8898-80 |
| Perforin | APC | eBioOMAK-D | eBioscience | 17-9392-80 |
| PD-1 | APC | J43 | BD | 562671 |
| PD-L1 | APC | 10F.9G2 | BioLegend | 124312 |
| PD-L2 | BV421 | TY25 | BD | 1564245 |
| CD95 | BV421 | Jo2 | BD | 562633 |
| CD95L | APC | MFL3 | eBioscience | 17-5911-80 |

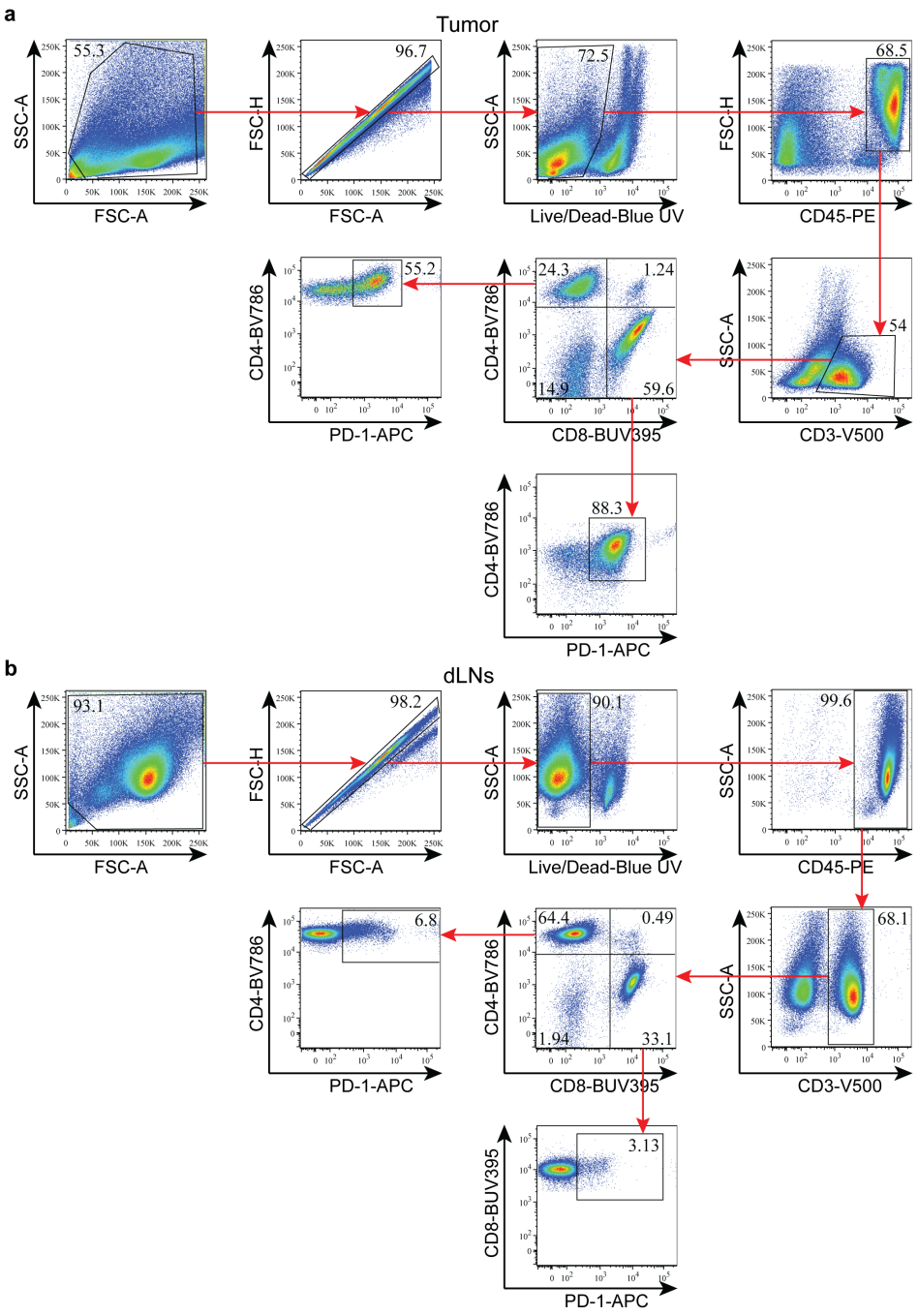


**Figure 4. Representative flow cytometry gating strategy**
For all flow cytometry analyses, initial gating was performed on overall morphology, singlets, live cells, and CD45$^{+}$ cells, followed by antigens of interest, from (**a**) tumors or (**b**) dLNs. SSC-A = Side Scatter-Area, FSC-A = Forward Scatter-Area, FSC-H = Forward Scatter-Height.

## 2.16 Histology

Tissues were fixed in 10% neutral buffered formalin for 24-48 hours at 4°C before paraffin processing at the Northwestern University histology core. For IHC, 5μm sections were deparaffinized and rehydrated, followed by antigen retrieval with citrate buffer pH6 (Dako) or 1mM EDTA pH 8, 3% $H_2O_2$ (Sigma), blocking (BioCare Blocking Reagent BS966M, Dako X0909, or Vector ImmPRESS 2.5% normal horse serum), primary antibody incubation, secondary antibody incubation (Vector biotinylated anti-rat IgG, Dako EnVision+ System HRP, Vector ImmPRESS HRP), streptavidin-HRP (Biocare) when appropriate, 3,3'-Diaminobenzidine chromogenic detection (SIGMA*FAST* tablets, Sigma), hematoxylin counterstain (Vector), tissue dehydration, and slide mounting (Cytoseal-XYL). IHC (Fig. 12) slides were blinded and scored manually over the entire tissue surface area or were quantified using ImageJ with quadruplicate field of views (FOVs) analyzed per sample. For *E. coli* immunofluorescence (IF), as previously described (354), slides were incubated with primary antibody, streptavidin-Alexa Fluor 594 secondary antibody (ThermoFisher Scientific, 1:500), permeabilized with 0.25% Triton-X-100, repeated primary antibody, anti-rabbit IgG (H+L) Alexa Fluor 488 secondary antibody (ThermoFisher Scientific, 1:500), and DAPI (Sigma) counterstain, and mounted with ProLong Gold Antifade Mountant (Molecular Probes), resulting in green intracellular staining and red/yellow (green + red) extracellular staining. HMGB1 and calreticulin immunofluorescence was similarly performed with Alexa Fluor 488 secondary antibody. Primary IHC and IF antibodies are listed in Table 2. Brightfield images were taken with a SPOT RT Color

camera on a Olympus CKX41 inverted microscope and IHC and IF images with CRI Nuance spectral camera on a Zeiss Axioskop upright microscope or a NikonDS-Ri2 microscope.

**Table 2. Primary antibodies used in this study for histology.**

| Antigen (mouse) | Dilution | Protocol | Clone | Vendor | Catalog # |
|---|---|---|---|---|---|
| CD3ε | 1:100 | IHC | CD3-12 | Bio-Rad | MCA1477T |
| CD3ε | Pre-diluted | IHC | 2GV6 | Ventana | 790-4341 |
| Fibrinogen | 1:200 | IHC | ab34269 | Abcam | ab34269 |
| *E. coli* | 1:500 | IF | ab20640 | Abcam | ab20640 |

### 2.17 Chemistry panel and complete blood count

Mouse peripheral blood was collected by cardiac puncture and placed in serum separator or dipotassium-EDTA tubes (BD Microtainer). Frozen serum and whole blood were analyzed, the latter within 24 hours after collection (Charles River Laboratory). Reference value ranges were used from the Charles River Laboratory, (355), the University of Arizona University Animal Care (https://uac.arizona.edu/clinical-pathology), and the University of Minnesota Research Animal Resources (http://www.ahc.umn.edu/rar/refvalues.html).

### 2.18 CRISPR knockout

To stably express CAS9 in Myc-CaP cells, we generated VSVG pseudotyped lentivirus (356, 357) using 293T cells, 2$^{nd}$ generation packaging vectors psPAX2, pMD2.G, and a CAS9 (*Streptococcus pyogenes* CRISPR-Cas) expressing lentiviral vector (Addgene 52962) (358). Lentiviral infection efficacy was >90% and cells were

maintained with 8 μg/ml puromycin. Multiple synthetic guide RNAs (gRNAs) (CRISPR crRNA, Integrated DNA Technologies) were designed using the CRISPR Design Tool (crispr.mit.edu (359)), those with off-target effects were excluded. gRNAs were delivered by transient transfection reagent TransIT-X2 (Mirus Bio). Partial PTEN knockout was confirmed by PTEN and p-AKT western blot and IF. >40 clones were isolated by cloning cylinders and were screened for complete PTEN loss. Two complete PTEN knockout Myc-CaP clones from different gRNAs (AAAGACTTGAAGGTGTATAC [exon 2], TGTGCATATTTATTGCATCG [exon 5]) were selected and analyzed in parallel *in vitro*.

### 2.19 Cancer genomic database analysis

cBioPortal for Cancer Genomics (http://www.cbioportal.org) (360) was utilized to analyze The Cancer Genome Atlas (TCGA) Research Network (http://cancergenome.nih.gov/) (361) and the Stand Up To Cancer/Prostate Cancer Foundation (SU2C/PCF) database (362).

### 2.20 Western blot

Western blotting was carried out as previously described (363), using an anti-rabbit IgG (H+L)-HRP conjugate (Bio-Rad) secondary antibody and imaged using a LAS-3000 imager (Fujifilm). Primary antibodies used are listed in Table 3.

**Table 3. Primary antibodies used in this study for western blot.**

| Antigen (mouse) | Dilution | Clone | Vendor | Catalog # |
|---|---|---|---|---|
| PTEN | 1:1000 | 138G6 | Cell Signaling | 9559 |
| p-AKT | 1:1000 | S473 | Cell Signaling | 4060 |
| pan-AKT | 1:1000 | C67E7 | Cell Signaling | 4691 |
| AR | 1:2000 | N-20 | Santa Cruz Biotechnology | sc-816 |
| c-Myc | 1:1000 | Y69 | Abcam | ab32072 |
| β-actin | 1:3000 | AC-74 | Sigma | A5316 |

### 2.21 Cell proliferation assay

Cell proliferation was assessed by quantification of MTS tetrazolium reduction (Promega). Select experiments were performed with low (1%) or charcoal-stripped (C.S.) FBS.

### 2.22 Organoid culture

Cells were resuspended in Hepatocyte Defined Medium (Corning) supplemented with 10ng/ml epidermal growth factor (Corning), 5% C.S. FBS, 1x Glutamax (Gibco), 5% matrigel (Corning), 10uM ROCK inhibitor (Y-27632, STEMCELL Technologies), 100nM DHT (Sigma), and 1x Gentamicin/Amphotericin (Lonza). Cells were plated in Ultra-Low Attachment Surface plates (Corning).

### 2.23 Statistical analyses

Statistical analyses were performed in GraphPad Prism 7 software. The number of technical replicates, biological replicates, and independent experiments performed are listed in the figure legends. Unpaired two-tailed Student's *t*-test, one-way Analysis of Variance (ANOVA) with post-hoc Tukey, and two-way ANOVA with post-hoc Sidak

were utilized as appropriate. Survival studies were analyzed by Log-rank (Mantel-Cox) test. Correlations were analyzed by Pearson's correlation coefficient (r). Slopes of linear regression trend lines were compared by Analysis of Covariance (ANCOVA). Data are presented as mean ± standard error of the mean (S.E.M.), unless otherwise indicated. All data were included, no outliers were excluded. For all analyses, results were considered statistically significant with $P<0.05$. * $P<0.05$, ** $P<0.01$, *** $P<0.001$, **** $P<0.0001$.

# CHAPTER 3: RESULTS

## 3.1 CP1 is a patient-derived UPEC that homes to prostate tumors

CP1 is a clinically-derived *E. coli* from a patient with chronic prostatitis that has previously been shown able to colonize murine prostates and induce a tissue-specific local inflammatory response (323). To further characterize the bacteria, we performed whole genome sequencing, which revealed that CP1 contains a 5,841,456 base pair genome with 50.9% GC content and 5172 unique coding sequences, 74 unique rRNA sequences, and 95 unique tRNA sequences (Fig. 5a). Further, CP1 is categorized within the B2 phylogenetic group (Fig. 5b) and sequencing type 131 (ST131). Phylogenetic tree analysis grouped CP1 closely with other UPEC isolates, including CFT073, UTI89, 536, J96, and NA114. Interestingly, CP1 is an atypical ST131 *E. coli*, as it lacks multiple consensus virulence genes (each with ≥93% ST131 population prevalence). While CP1 contained identical multi-locus sequence typing (MLST) alleles as the ST131 NA114 strain, only NA114 contained all consensus virulence factor genes (Fig. 5b) (364), indicating that CP1 is potentially less virulent than other similar UPECs.

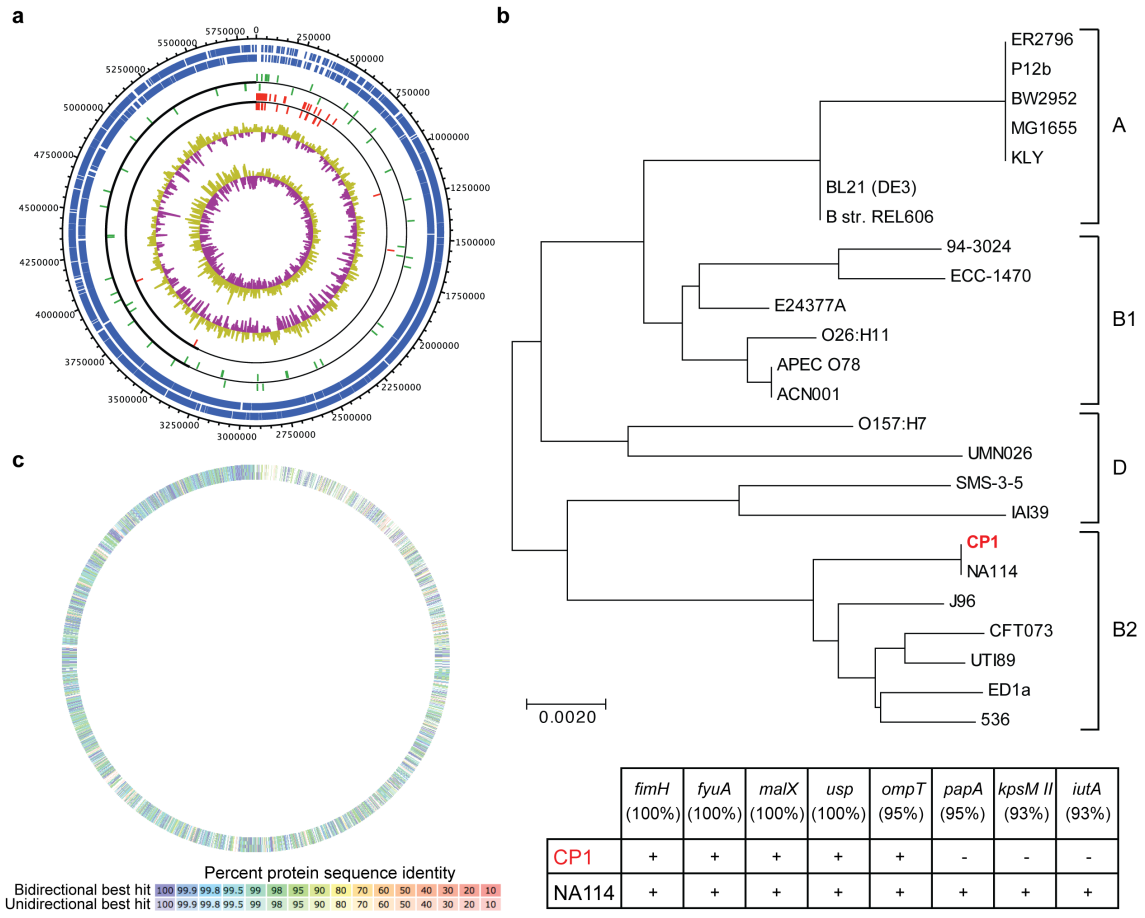


| | *fimH* (100%) | *fyuA* (100%) | *malX* (100%) | *usp* (100%) | *ompT* (95%) | *papA* (95%) | *kpsM II* (93%) | *iutA* (93%) |
|---|---|---|---|---|---|---|---|---|
| CP1 | + | + | + | + | + | - | - | - |
| NA114 | + | + | + | + | + | + | + | + |

**Figure 5. Whole genome sequencing of CP1**
(**a**) The sequenced CP1 genome was visualized with Artemis DNAPlotter. Tracks from outermost to innermost: forward coding sequence (CDS), reverse CDS, forward tRNA, reverse tRNA, forward rRNA, reverse rRNA, GC plot, GC skew. (**b**) Phylogenetic tree of CP1 with reference *E. coli* strains using the Maximum Likelihood method with concatenated MLST sequences, constructed with MEGA7. Branch lengths were measured in the number of substitutions per site. Phylogenetic groups A, B1, D, or B2 are indicated. Table depicts the presence or absence of ST131 consensus virulence factor genes (with overall ST131 population prevalence indicated) in the CP1 or NA114 genomes. (**c**) Sequence comparison of the CP1 genome with the MG1655 genome, performed with RAST.

UPECs are able to colonize the urinary tract and invade and proliferate within host epithelial cells (365), and prior analysis of CP1 demonstrated that it is able to adhere to and invade benign prostate epithelial cell lines (323). To test if CP1 could invade prostate cancer cells, we repeated this *in vitro* gentamicin protection assay with the *MYC*-driven murine prostate cancer cell line, Myc-CaP (366). As a control, we utilized MG1655, the prototypical strain of the patient-derived K-12 *E. coli* isolate that has been maintained with "minimal genetic manipulation" and whose complete genome has been sequenced (367). About 19.7% of the genes in CP1 were not present in the MG1655 genome, and the remaining shared genes contained an average 93.9% identity (Fig. 5c). As with the benign prostate epithelial cell lines, CP1 was able to adhere to, invade, and intracellularly proliferate within Myc-CaP cells, and did so to a greater degree than did MG1655 (Fig. 6).

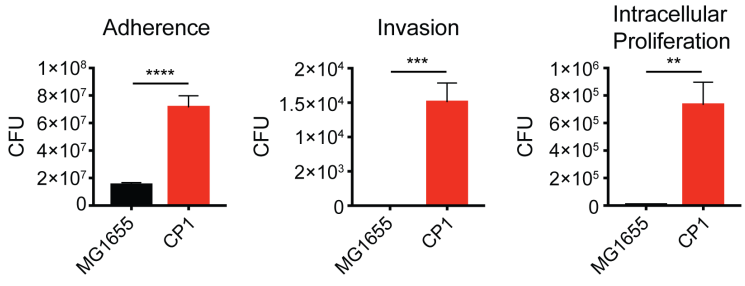


**Figure 6. CP1 adheres to, invades, and intracellularly proliferates within prostate cancer cells**
Gentamicin protection assay with CP1 and MG1655 with Myc-CaP cells *in vitro*, performed in sextuplicates, plated in serial dilutions. Data represented as mean ± S.E.M. Statistical significance was determined by Student's *t*-test. ** $P<0.01$, *** $P<0.001$, **** $P<0.0001$.

A prior study has established that intra-urethral instillation of $2\times10^8$ CP1 in mice leads to bacterial colonization of the benign prostate, and, to a lesser degree, the bladder, thereby recapitulating the common natural ascending pattern of prostatic infection in humans (323). To similarly evaluate CP1 in a clinically relevant *in vivo* model of prostate cancer, we injected Myc-CaP cells intra-prostatically, leading to orthotopic prostate tumor development. 8 days after intra-prostatic injection, mice with established tumors were intra-urethrally administered $2x10^8$ CP1. Tissue analysis 9 days after CP1 administration revealed that CP1 specifically colonized prostate tumor tissue, ascending from the urethra to the bladder to the tumor without progressing to the kidneys or colonizing systemic tissues (Fig. 7a). An average $3.8\times10^6$ total CP1 colony forming units (CFUs) (Fig. 7a), or $3.3\times10^6$ CFU/g tumor (Fig. 7b), were cultured from tumors, representing approximately 1.9% of the initial CP1 inoculation (Fig. 7c). Additional comparison of CP1 tumor colonization on day 1 and day 9 after intra-urethral administration revealed no significant changes in CFUs over time (Fig. 8a-c). We also analyzed bacterial *16S* RNA from tumor tissue as an additional means of tracking intra-tumoral CP1. As expected, *16S* RNA levels were higher in CP1-administered tumors (Fig. 7d). Calibrating *16S* RNA values to CP1 cell counts resulted in similar values as those attained by tumor tissue culture at both timepoints (Fig. 8d), suggesting that viable but non-culturable (VBNC) CP1 were absent or minimal in this model. Finally, immunofluorescent analysis of tumor tissue 9 days after intra-urethral CP1 administration identified the presence of both extracellular (approximately 58.2%) and intracellular (approximately 41.8%) *E. coli* throughout the tumors (Fig. 7e). Importantly, CP1

administration did not cause any systemic toxicities, with no changes in body weight or any serum chemistry laboratory values, and all complete blood count (CBC) values fell within their normal range (Fig. 9), other than low RDW, which is clinically insignificant in the absence of anemia. Thus, intra-urethrally administered CP1 specifically and safely colonized prostate tumor tissue.

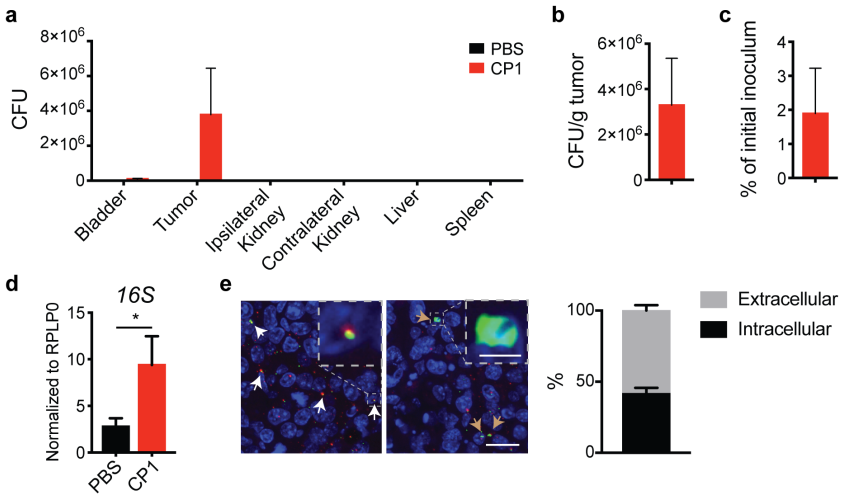


**Figure 7. CP1 specifically homes to and colonizes prostate tumor tissue**
Orthotopic prostate tumor-bearing mice were analyzed 9 days after intra-urethral CP1 administration. (**a**) Bacterial colonization in the bladder, prostate tumor (also represented as (**b**) CFU/g and (**c**) percentage of the initial $2\times10^8$ CP1 intra-urethral inoculum), ipsilateral and contralateral kidneys, liver, and spleen, performed in biological triplicates, plated in serial dilutions. (**d**) *16S* qRT-PCR of tumor RNA, normalized to *RPLP0*, performed in biological quadruplicates, technical duplicates. (**e**) *E. coli* IF of tumor tissue (yellow/red = extracellular, indicated with white arrows; green = intracellular, indicated with brown arrows), (scale bar, 20µm; magnified scale bar, 4µm). Mice $n$ = 4-5/group, performed in 2 independent experiments, *E. coli* IF quantified with quadruplicate FOVs/tumor. Data represented as mean ± S.E.M. Statistical significance was determined by two-tailed Student's *t*-test. * $P<0.05$.

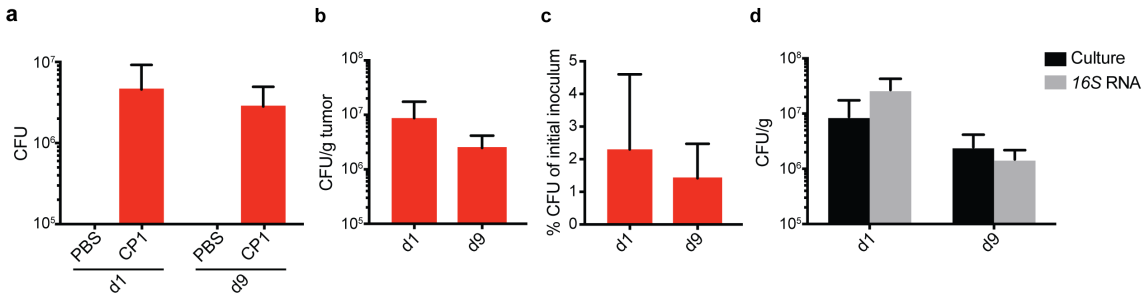


**Figure 8. Intra-tumoral CP1 is culturable and colonization levels remain constant over time**

(**a**) Total bacterial colonization, (**b**) bacterial colonization normalized to tumor weight, and (**c**) bacterial colonization as a percentage of the original $2\times10^8$ CP1 inoculum, performed on day 1 (d1) and day 9 (d9) after intra-urethral PBS or CP1 administration to orthotopic Myc-CaP prostate tumor-bearing mice. (**d**) Bacterial colonization/g tumor as determined by both cultured tumor tissue and *16S* RT-PCR calibrated to CP1 counts on day 1 and day 9 after CP1 administration. Mice $n$ = 4-5/group, tissue cultures plated in serial dilutions, technical duplicates, RT-PCR performed in technical duplicates. Data represented as mean ± S.E.M. Statistical significance was determined by (**a-c**) two-tailed Student's *t*-test, (**d**) two-way ANOVA.

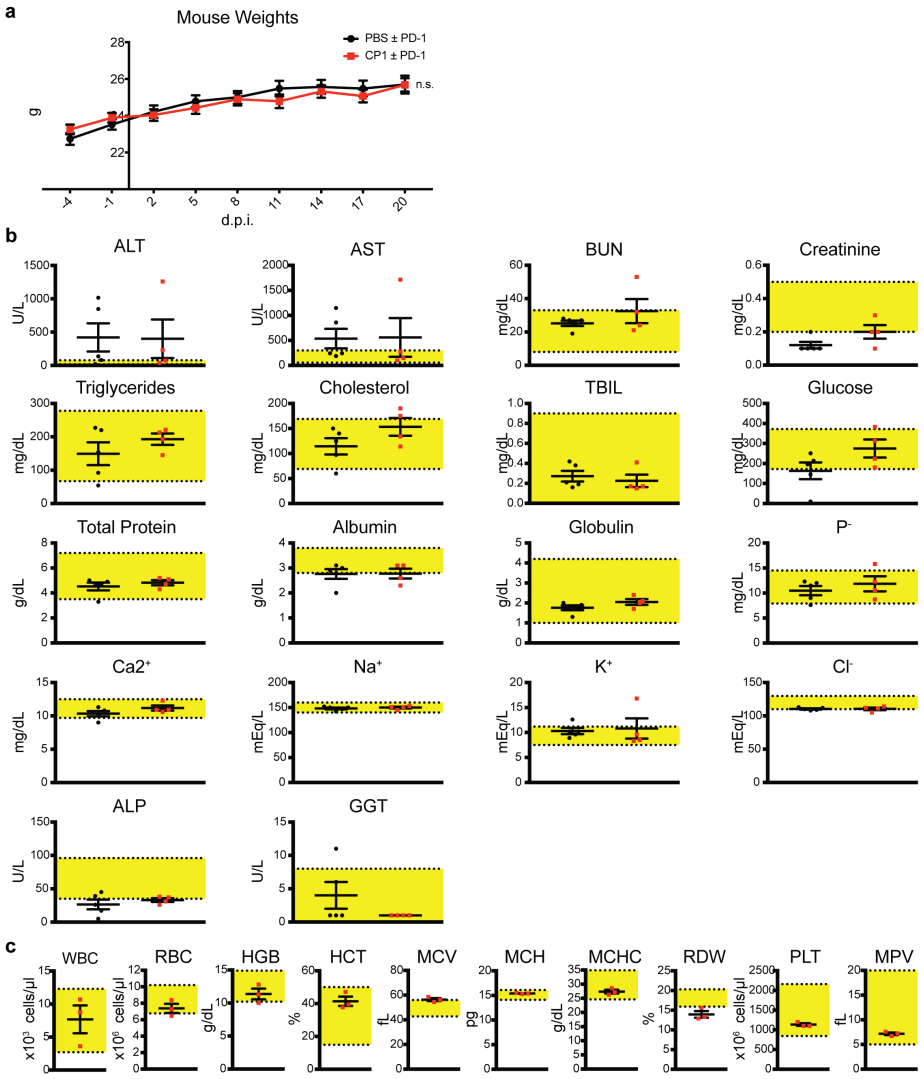


**Figure 9. CP1 does not cause any systemic toxicities**
(**a**) Weights of PBS and CP1 administered mice (± anti-PD-1 antibody), plotted as days post-infection (d.p.i.), n.s. = not significant, *n* = 23-28 mice/experimental group. (**b**) Chemistry laboratory values of PBS and CP1 administered mice, yellow indicating the normal murine range (ALT = alanine aminotransferase, AST = aspartate aminotransferase, BUN = blood urea nitrogen, TBIL = total bilirubin, $P^-$ = phosphorous, $Ca^{2+}$ = calcium, $Na^+$ = sodium, $K^+$ = potassium, $Cl^-$ = chloride, ALP = alkaline phosphatase, GGT = gamma glutamyl transferase), *n* = 4-5 mice/experimental group. (**c**) Complete blood count (CBC) values of CP1 administered mice, yellow indicating the normal murine range (WBC = white blood cell, RBC = red blood cell, HBG = hemoglobin, HCT = hematocrit, MCV = mean corpuscular volume, MCH = mean corpuscular hemoglobin, MCHC = mean corpuscular hemoglobin concentration, RDW = RBC distribution width, PLT = platelet count, MPV = mean platelet volume), *n* = 3 mice. Data represented as mean ± S.E.M.

### 3.2 CP1 induces ICD and pro-inflammatory cytokine production

Interestingly, *in vitro* culture of Myc-CaP cells with CP1 resulted in cancer cell death in a dose-dependent manner (Fig. 10a). Therefore, we analyzed whether this was specifically immunogenic cell death (ICD). All three major ICD damage-associated molecular patterns (DAMPs): HMGB1, ATP, and calreticulin (368), were elevated in the presence of live, but not heat killed, CP1 (Fig. 11a). Similar results were seen with human LNCaP prostate cancer cells (Fig. 11b). CP1 also induced all ICD markers to a significantly higher level than did MG1655 (Fig. 10b, CP1 vs. MG1655: HMGB1 $P = 0.0011$, ATP $P = 0.009$, calreticulin $P = 0.0014$ all by two-tailed Student's *t*-test). To more accurately represent the quantity of CP1 present within the tumor, the *in vitro* ICD assays were repeated with the addition of gentamicin at a multiplicity of infection (MOI) of 1. These conditions resulted in a final average CP1:Myc-CaP ratio of 0.005, with the surviving intracellular CP1 representing approximately 10.9% of the initial bacteria added to the culture (multiple orders of magnitude less bacteria than without gentamicin). In the presence of gentamicin, CP1 still significantly increased the percent of calreticulin$^+$ Myc-CaP cells, but did not induce HMGB1 or ATP secretion (Fig. 10c). However, it is important to note that in addition to decreasing total CP1 count, gentamicin also eliminated any potential importance of extracellular CP1 interacting with tumor cells or CP1 spreading between cells. Finally, we tested for ICD within tumor tissue 9 days after intra-urethral CP1 administration. CP1-administered prostate tumors contained an increased percentage of HMGB1$^-$ nuclei (Fig. 11c), signifying HMGB1 release (369), and areas of increased cell surface calreticulin levels (Fig. 11d).

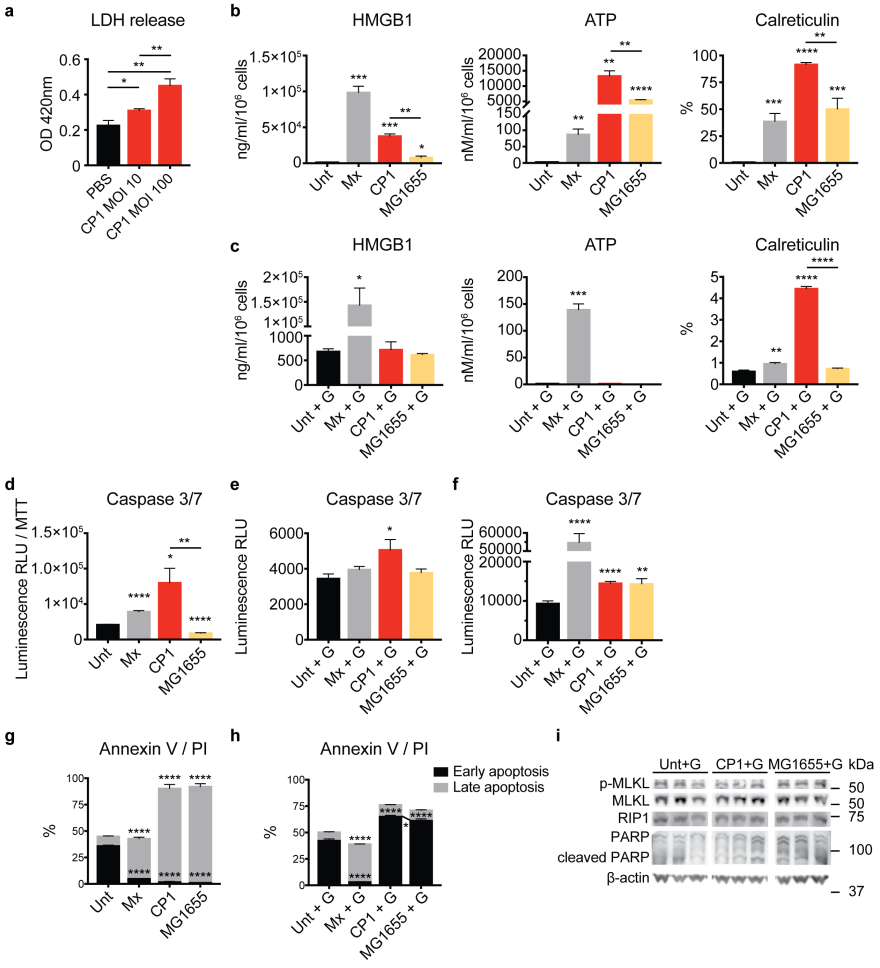


**Figure 10. CP1 induces ICD and select cell death markers, with and without gentamicin, and to a greater degree than MG1655**

(**a**) LDH level, as a measure of cell death, from CP1 and Myc-CaP co-culture, performed in triplicates. (**b-i**) Myc-CaP cells were co-cultured with mitoxantrone (Mx), CP1 (MOI 1), or MG1655 (MOI 1) (**b, d, g**) in normal media or (**c, e, f, h, i**) with gentamicin (+ G) added after 2 hours. (**b, c**) ICD was measured via HMGB1 (ELISA, 72 hours), ATP (luminescence assay, 72 hours), and calreticulin (flow cytometry, 24 or 72 hours), performed in biological triplicates, technical duplicates. (**d-f**) Caspase 3/7 activity (luminescence assay, reported in relative light units [RLU]) was measured at (**d, e**) 6 hours or (**f**) 24 hours, (**d**) normalized to cell count (MTT assay), performed in sextuplicates. (**g, h**) Early stage apoptosis (Annexin $V^+$ $PI^-$) and late stage apoptosis (Annexin $V^+$ $PI^+$) were determined by flow cytometry after 24 hours, performed in triplicates. (**i**) Western blot analysis of phosphorylated and total MLKL, RIP1, full length and cleaved PARP, and β-actin after 24 hours, performed in triplicates. Data represented as mean ± S.E.M. Statistical significance was determined by two-tailed Student's *t*-test (each group compared to Unt, and CP1 compared to MG1655). * $P<0.05$, ** $P<0.01$, *** $P<0.001$, **** $P<0.0001$.

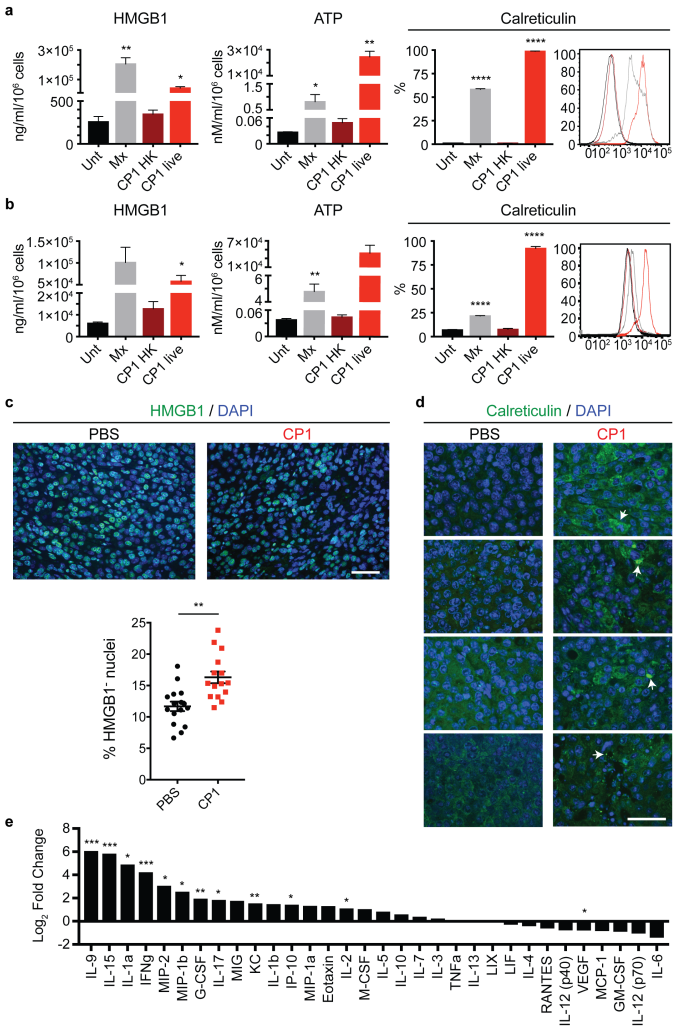


**Figure 11. CP1 induces immunogenic cell death while increasing pro-inflammatory cytokines and chemokines and decreasing VEGF**

ICD was assessed *in vitro* from co-culture of (**a**) Myc-CaP or (**b**) LNCaP cells with untreated (Unt.), mitoxantrone (Mx), heat killed (HK) CP1, or live CP1 via HMGB1 (ELISA), ATP (luminescence assay), and calreticulin (flow cytometry, with representative histogram [Unt = black, Mx = gray, CP1 HK = dark red, CP1 live = red]), performed in biological triplicates, technical duplicates, statistics compared to Unt. ICD was assessed *in vivo* by (**c**) HMGB1 or (**d**) calreticulin IF of prostate tumor tissue 9 days after intra-urethral CP1 administration, with representative images (each calreticulin image representative of a different tumor with white arrows indicating foci of cell surface staining, green = HMGB1 or calreticulin, scale bar, 50μm). Mice $n = 4$/group, HMGB1 quantified with quadruplicate FOVs/tumor. (**e**) Multiplex cytokine and chemokine array from Myc-CaP supernatant, performed in biological triplicates, technical duplicates. Data represented as mean ± S.E.M. or $\log_2$ fold change with and without CP1 exposure. Statistical significance was determined by two-tailed Student's *t*-test (**a, b**, each group compared to Unt.). * $P<0.05$, ** $P<0.01$, *** $P<0.001$, **** $P<0.0001$.

Further analysis of cell death pathways identified that CP1 significantly increased caspase 3/7 activity without gentamicin (Fig. 10d, $P = 0.0103$ by two-tailed Student's *t*-test, CP1 significantly greater than MG1655, $P = 0.0037$ by two-tailed Student's *t*-test) and with gentamicin (Fig. 10e [$P = 0.0286$ by two-tailed Student's *t*-test], f). CP1 exposed Myc-CaP cells also displayed an increased late apoptotic phenotype (Annexin $V^+$ $PI^+$) without gentamicin (Fig. 10g) and an increased early apoptotic phenotype (Annexin $V^+$ $PI^-$) with gentamicin (Fig. 10h, CP1 significantly greater than MG1655, $P = 0.0329$ by two-tailed Student's *t*-test). However, no changes were observed in the phosphorylation of MLKL, RIP1 levels, or PARP cleavage after Myc-CaP culture with either CP1 or MG1655 and gentamicin (Fig. 10i), suggesting that CP1-induced ICD is occurring in a necroptosis-independent manner (369).

Finally, CP1 significantly increased the *in vitro* Myc-CaP production of pro-inflammatory cytokines and chemokines IL-9, IL-15, IL-1α, IFNγ, MIP-2, MIP-1β, G-CSF, IL-17, KC, IL-2, and IP-10 (CXCL10), which is important for ICD, while also decreasing VEGF from cancer cells (Fig. 11e). Overall, CP1 induced ICD, increased pro-inflammatory cytokines and chemokines, and decreased VEGF from cancer cells.

### 3.3 CP1 increases TILs and reprograms the tumor microenvironment

To evaluate CP1's ability to remodel the "cold" prostate tumor microenvironment, we immunophenotyped tumors 9 days after intra-urethral bacterial administration. CP1 increased T cells not only in the tumor stroma and periphery, but also intra-tumorally (Fig. 12a), consisting of both CD8 and CD4 TILs (Fig. 12b). In

contrast, intra-urethral MG1655 administration did not result in increased TILs (Fig. 13). Further analysis revealed that the increased CD8 TILs in CP1-administered tumors expressed increased TNFα (Fig. 12c) and the activation marker PD-1 (Fig. 12d), and a higher percentage expressed IFNγ within the dLNs (Fig. 12e). In addition, intra-tumoral (Fig. 12f) and dLN (Fig. 12g) CD4 T cells were Th17-polarized. CP1 administration also decreased the percentage of regulatory T cell (Treg) TILs, with most tumors containing a >3-fold increased CD8/Treg ratio (Fig. 12h). Notably, despite increasing overall hematopoietic infiltration, CP1 did not increase infiltration of myeloid-derived suppressor cells (MDSCs; $CD11b^{+}Gr\text{-}1^{+}$) (Fig. 12i). Interestingly, CP1 significantly increased both mature dendritic cells (DCs) and M1-polarized macrophages to a much greater degree than either total cell type (Fig. 12j, k), while also increasing infiltration of NK cells (Fig. 12l), γδ T cells (Fig. 12m), and B cells (Fig. 14a). While CP1 did not increase PD-L1 on tumor or hematopoietic cells, the immune compartment was a greater source of PD-L1 within these tumors due to increased overall $CD45^{+}$ infiltration (Fig. 14b-d). IL-5 and TNFα were the most upregulated cytokines in CP1-treated tumors, and, consistent with the *in vitro* cytokine/chemokine array, IFNγ was among the most upregulated and IL-6 and VEGF among the most downregulated cytokines after CP1 administration (Fig. 12n). Overall, intra-tumoral CP1 increased infiltration of multiple anti-tumor immune cell types while decreasing Tregs.

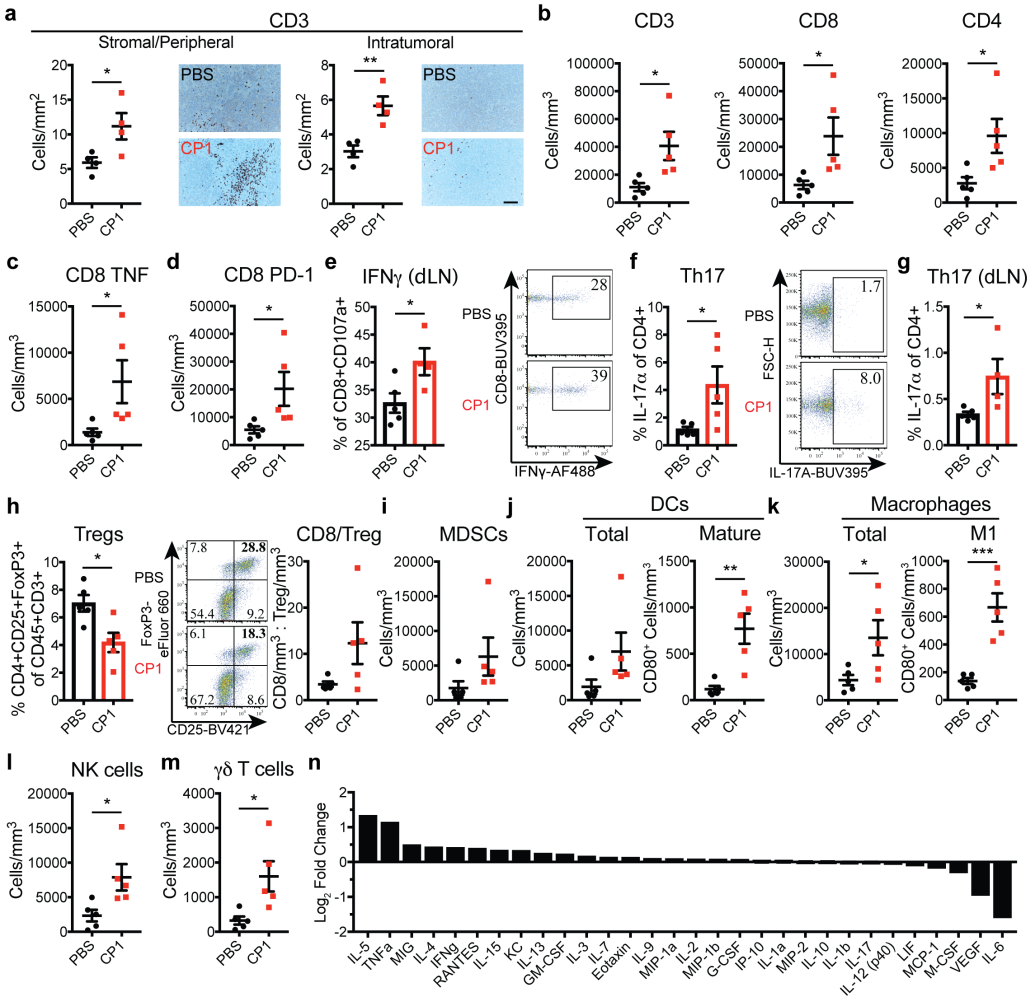


**Figure 12. CP1 increases TILs and tumor immune infiltration while decreasing Tregs**

(**a**) Blinded IHC with representative images (scale bar, 100μm) and (**b-m**) flow cytometry analysis of Myc-CaP tumors or dLNs, as indicated, displayed as cell counts normalized to tumor volume (scatter plots) or percentages of parent gate (scatter boxed plots), with representative flow cytometry plots. MDSCs were defined as $CD11b^{+}Gr\text{-}1^{+}$. (**n**) Multiplex cytokine and chemokine array from Myc-CaP tumors. Mice $n$ = 4-5/group, performed in 2 independent experiments. Data represented as mean ± S.E.M. or $\log_2$ fold change with and without CP1 administration. Statistical significance was determined by two-tailed Student's $t$-test. * $P$<0.05, ** $P$<0.01, *** $P$<0.001.

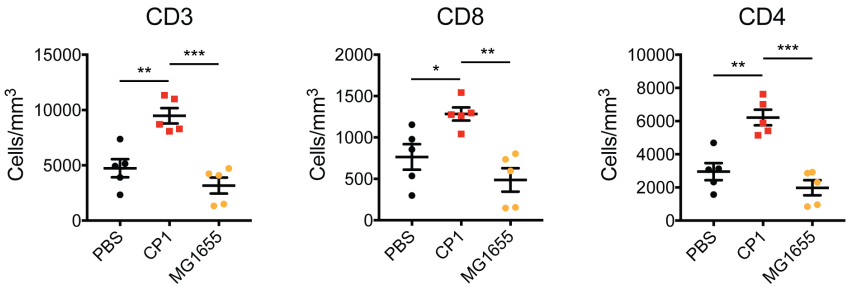


**Figure 13. Intra-urethrally administered MG1655 does not increase prostatic TILs**
Flow cytometry analysis of orthotopic Myc-CaP tumors 9 days after intra-urethral administration of PBS, CP1, or MG1655, displayed as cell counts normalized to tumor volume. Mice $n$ = 5/group. Data represented as mean ± S.E.M. Statistical significance was determined by two-tailed Student's $t$-test. * $P$<0.05, ** $P$<0.01, *** $P$<0.001.

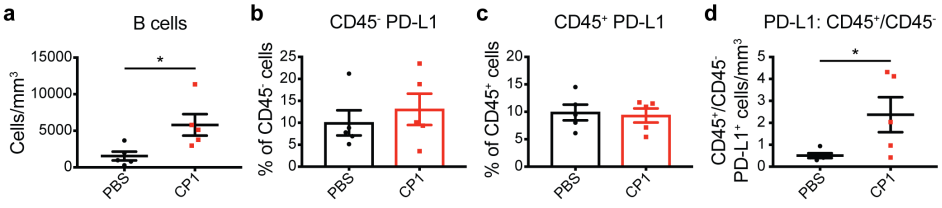


**Figure 14. CP1 increases B cells and does not increase PD-L1 expression**
Flow cytometry analysis of (**a**) B cells, and PD-L1 on (**b**) $CD45^-$ and (**c**) $CD45^+$ intra-tumoral cells, and (**d**) the ratio of $CD45^+PD\text{-}L1^+/CD45^-PD\text{-}L1^+$ cell densities. $n$ = 4-5 mice/experimental group, performed in 2 independent experiments. Data represented as mean ± S.E.M. as cell counts normalized to tumor volume (scatter plots) or percentages of parent gate (scatter boxed plots). Statistical significance was determined by two-tailed Student's $t$-test. * $P$<0.05.

### 3.4 CP1 with PD-1 blockade is efficacious for prostate cancer

To determine the functional implications of this immunomodulation, we treated orthotopic Myc-CaP tumor-bearing mice with intra-peritoneal anti-PD-1 antibody beginning 9 days after intra-urethral CP1 administration. We utilized pre-treatment *in vivo* bioluminescent imaging to normalize tumor burden and variance between experimental groups in this and all subsequent experiments (Fig. 15). To analyze survival, mice were followed after treatment termination with no additional interventions. Combination immunotherapy of CP1 and PD-1 blockade (CP1+PD-1) significantly increased survival ($P = 0.0066$ by Log-rank test), conferring >2-fold increased 50% survival time. In contrast, neither CP1 nor anti-PD-1 monotherapy significantly enhanced survival (Fig. 16a). In mice analyzed immediately after treatment termination, CP1+PD-1 decreased tumor burden, as assessed by *in vivo* bioluminescent imaging, tumor weight, and tumor volume (Fig. 16b-e). In addition, CP1 treated tumors showed evidence of bacterial colonization, as determined by *16S* RNA (Fig. 17a). Interestingly, all long-term surviving mice (>75 days) contained relatively high *16S* RNA ratios (normalized to a mouse housekeeping gene) (Fig. 17b), suggesting that high bacterial load was important for therapeutic efficacy. In addition, as observed previously (Fig. 8), relative bacterial load did not increase over time (Fig. 17b). Further, within CP1 treated tumors, MIP-2 was the most upregulated and VEGF was again the most downregulated cytokine (Fig. 18a).

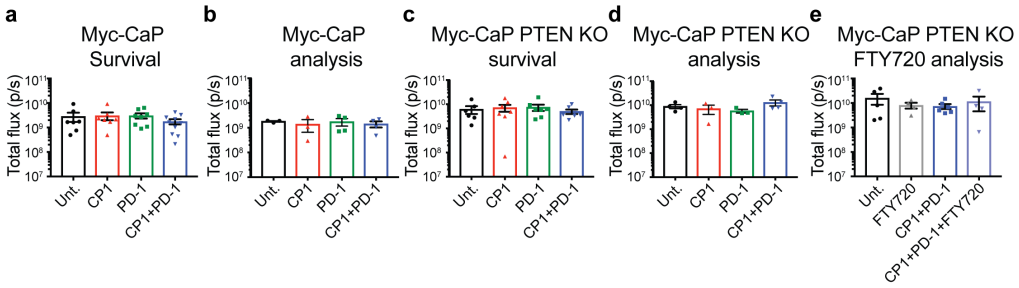


**Figure 15. Normalization of orthotopic pre-treatment tumor burden in all *in vivo* experiments**

Pre-treatment tumor IVIS quantification of Unt., CP1, anti-PD-1 antibody, and combination CP1 and anti-PD-1 antibody treated mice in (**a**) Myc-CaP survival (Fig. 16a,b, 17, 18a), (**b**) Myc-CaP analysis (Fig. 16b-e), (**c**) Myc-CaP PTEN KO survival (Fig. 20e), (**d**) Myc-CaP PTEN KO analysis (Fig. 18b, 20f, 21, 22), and (**e**) of Unt., FTY720, combination CP1 and anti-PD-1 antibody, and combination CP1 and anti-PD-1 antibody and FTY720 treated mice (Fig. 23). Data represented as mean ± S.E.M. Statistical significance was determined by one-way ANOVA.

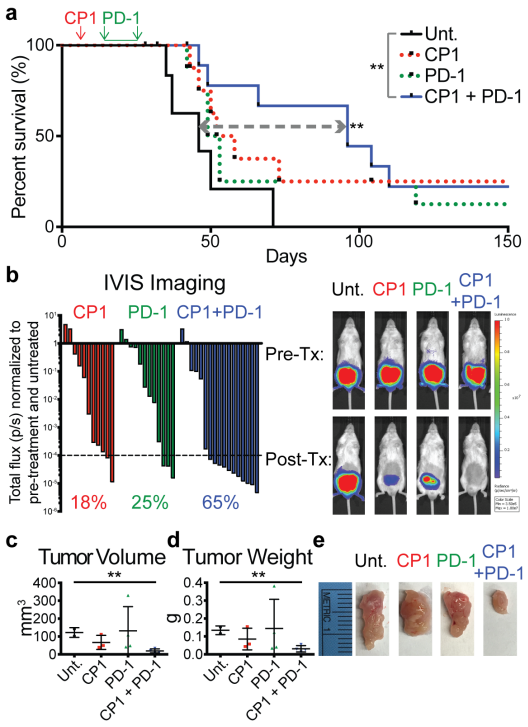


**Figure 16. Combination CP1 and anti-PD-1 immunotherapy is efficacious in treating orthotopic prostate tumors**

(**a**) Kaplan Meier survival curve of Unt., CP1, anti-PD-1 antibody, or combination CP1 and anti-PD-1 antibody treated mice, mice $n$ = 6-12/group, performed in 3 independent experiments. (**b**) Waterfall plot of IVIS imaging quantification, with each bar representing the post-treatment (Tx) total flux of a single tumor normalized to both its own pre-tx total flux and Unt. normalized total flux, with representative images. Percentages indicate the fraction of tumors with values <0.0001. $n$ = 11-17 mice/experimental group, performed in 4 independent experiments. Post-tx tumor (**c**) volumes, (**d**) weights, and (**e**) gross images, mice $n$ = 3-4/group. data represented as mean ± S.E.M. Statistical significance was determined by (**a**) Log-rank test, (**c, d**) two-tailed Student's $t$-test. ** $P$<0.01.

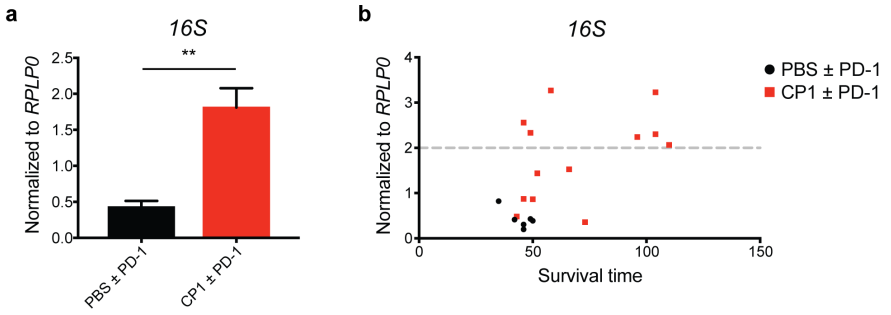


**Figure 17. CP1 load is linked to treatment efficacy**
*16S* qRT-PCR of Myc-CaP survival mice tumors (**a**) at their endpoints and (**b**) plotted over time after tumor injection, dotted line indicates cutoff for high CP1. Data represented as mean ± S.E.M. Statistical significance was determined by two-tailed Student's *t*-test. ** $P<0.01$.

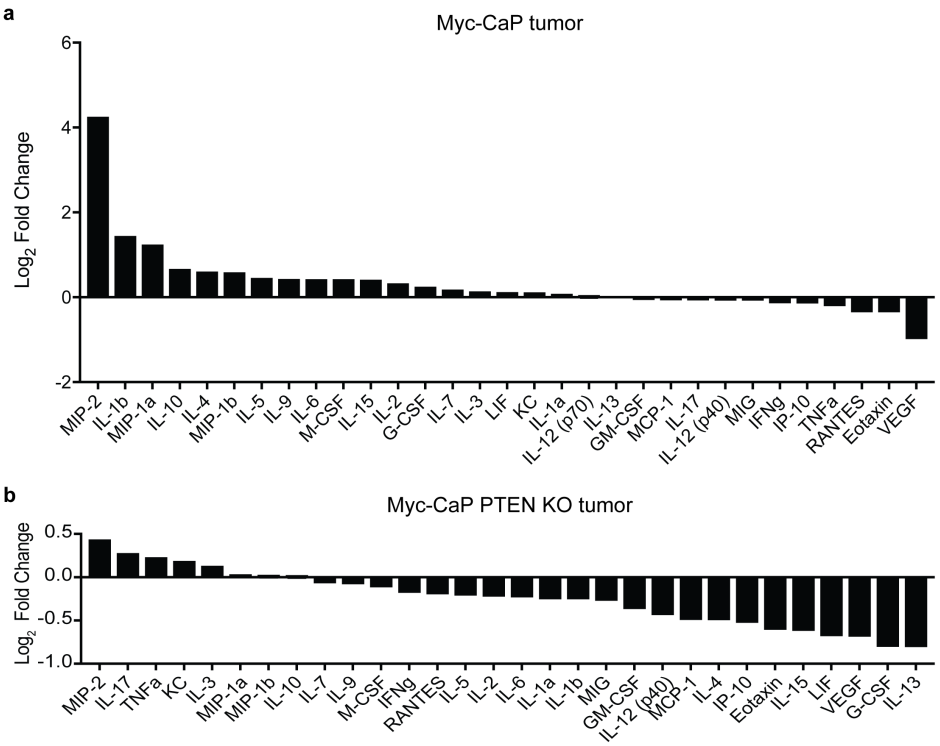


**Figure 18. CP1 decreases intra-tumoral VEGF, increases pro-inflammatory cytokines and chemokines**
Multiplex cytokine and chemokine array from (**a**) Myc-CaP survival tumors, performed with $n$ = 11-12 mice/experimental group, and from (**b**) Myc-CaP PTEN KO tumors, performed with $n$ = 5-6 mice/experimental group and technical duplicates. Data represented as $\log_2$ fold change with and without CP1 administration.

### 3.5 CP1 with PD-1 blockade treats *PTEN*-deficient prostate cancer

To challenge our combination immunotherapy in a second, more aggressive and immunosuppressive model of advanced prostate cancer, we utilized CRISPR-Cas9 to knock out (KO) *PTEN* from the Myc-CaP genome. Loss of PTEN is linked to increased PD-L1 in prostate and breast cancer (370), and decreased TILs and resistance to PD-1 blockade in melanoma (371). Further, concurrent copy number gain of *MYC* and loss of *PTEN* is associated with prostate cancer-specific mortality, reported in 57% of metastatic tumors compared to 9.6% in localized disease (372). Similarly, this combination copy number alteration was present in 24.8% and 11.2% of SU2C/PCF metastatic and TCGA primary prostate tumors, respectively (Fig. 19). Myc-CaP PTEN KO cells contained increased phosphorylated-AKT and androgen receptor (Fig. 20a), and expressed approximately 2-fold higher levels of PD-L1, PD-L2, CD95, and CD95L, all important in tumor immune-evasion (Fig. 20b). These cells proliferated faster, particularly in low and charcoal-stripped serum (Fig. 20c), and more rapidly formed 3-dimensional organoids (Fig. 20d). Thus, we generated a novel PTEN KO Myc-CaP cell line that displayed many characteristics of advanced human prostate cancer.

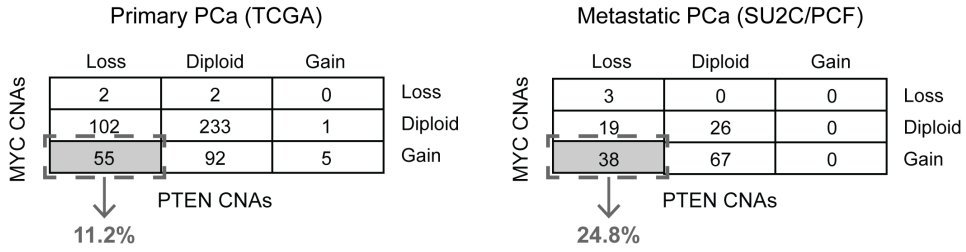


**Figure 19. Concurrent *MYC* copy number gain and *PTEN* copy number loss represents advanced human prostate cancer**
Tables of the number of samples with *MYC* and *PTEN* copy number diploid, loss, or gain in the TCGA and SU2C/PCF databases, with gray numbers indicating the percent of samples with concurrent *MYC* gain and *PTEN* loss.

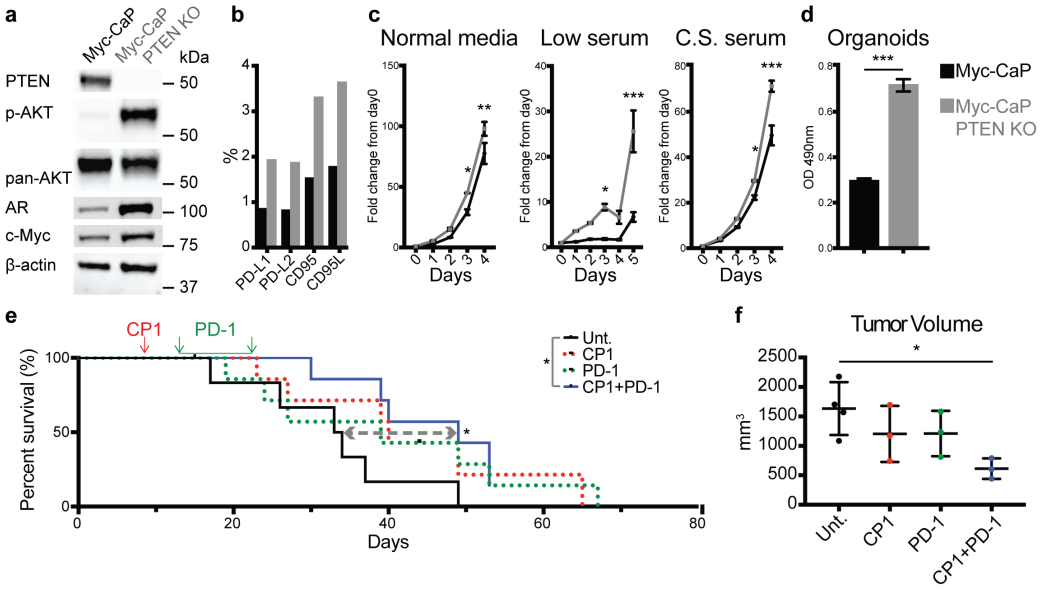


**Figure 20. Combination CP1 and anti-PD-1 immunotherapy is efficacious in treating a novel orthotopic advanced prostate cancer model**
*In vitro* comparison of Myc-CaP and Myc-CaP PTEN KO cell lines by (**a**) western blot (p-AKT = phosphorylated AKT, AR = androgen receptor), (**b**) flow cytometry, (**c**) growth rate by MTS assays in normal media (10%), low serum (1%), and charcoal stripped (C.S.) FBS, performed in triplicates, and as (**d**) 3-dimensional organoids, performed in sextuplicates. Myc-CaP PTEN KO (**e**) Kaplan Meier survival curve, $n = 7$ mice/experimental group, performed in 2 independent experiments, and (**f**) tumor volumes, $n = 3$-6 mice/experimental group. Data represented as mean ± S.E.M. Statistical significance was determined by (**c**) two-way ANOVA, (**d**) two-tailed Student's *t*-test, (**e**) Log-rank test, (**f**) one-way ANOVA. * $P<0.05$, ** $P<0.01$, *** $P<0.001$.

Orthotopic Myc-CaP PTEN KO tumor-bearing mice were again administered intra-urethral CP1 and subsequent anti-PD-1 antibody. As previously observed, neither CP1 nor anti-PD-1 monotherapy significantly increased survival of mice, whereas CP1+PD-1 combination therapy conferred a significant 1.5-fold increased survival ($P$ = 0.0251 by Log-rank test) (Fig. 20e). Upon analysis immediately after treatment termination, combination CP1+PD-1 also significantly decreased tumor size (Fig. 20f, $P$ = 0.0344 by one-way ANOVA). However, while tumor weight did not differ between groups (Fig. 21a), CP1 tumors were significantly denser (Fig. 21b), and contained increased exudate, as measured by fibrinogen (Fig. 21c). Therefore, tumor weight did not accurately assess therapeutic efficacy, consistent with pseudo-progressions observed with clinical immunotherapies (373).

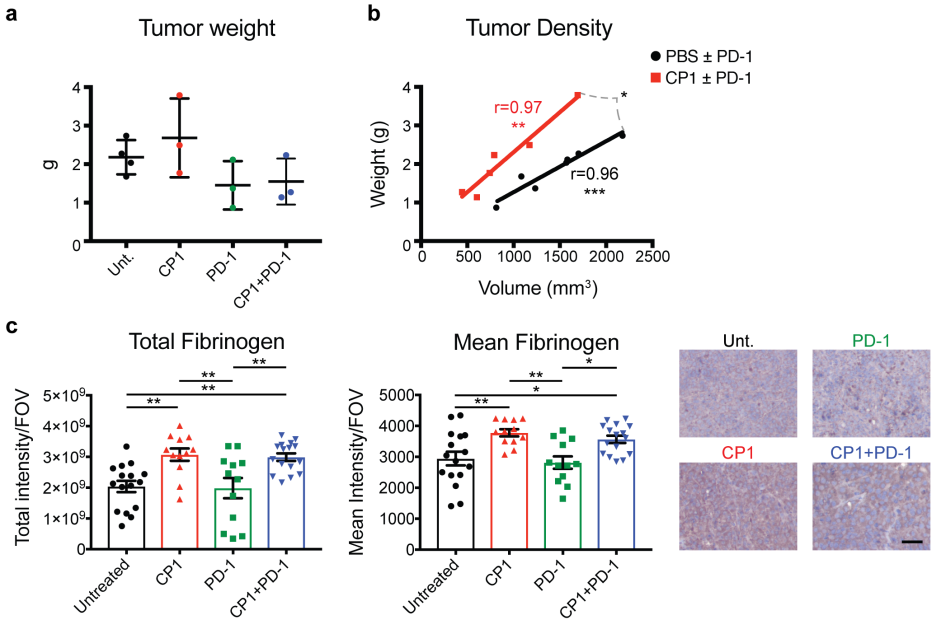


**Figure 21. CP1 increases tumor density via fibrinous exudate**
Myc-CaP PTEN KO tumor (**a**) weights, *n* = 3-4 mice/experimental group and (**b**) densities, *n* = 6-7 mice/experimental group. (**c**) Fibrinogen IHC quantified by total and mean positivity/FOV and representative images, quadruplicate FOVs scored per sample, scale bar: 50µm, *n* = 4-6 mice/experimental group. Data represented as mean ± S.E.M. or linear regression trend lines**.** Statistical significance was determined by (**a**) two-tailed Student's *t*-test, (**b**) Pearson's correlation coefficient (r) an ANCOVA comparing slopes of trend lines, (**c**) one-way ANOVA. * $P<0.05$, ** $P<0.01$, *** $P<0.001$.

### 3.6 CP1 increases activated TILs and decreases Tregs and VEGF

In Myc-CaP PTEN KO tumors, CP1 treatment again increased TILs (Fig. 22a), with degranulated T cells from CP1 and/or CP1+PD-1 treated mice displaying increased cytotoxic functionality via IFNγ (Fig. 22b), granzyme B (Fig. 22c), and perforin (Fig. 22d) expression. Also consistent with its effects in Myc-CaP tumors, CP1 increased PD-1 on CD8 TILs (Fig. 22e), decreased the percentage of Treg TILs (Fig. 22f), and caused decreased VEGF and increased MIP-2, IL-17, and TNFα within the tumor microenvironment (Fig. 18b). Overall, combination CP1 and anti-PD-1 immunotherapy was efficacious in a second, more advanced model of the disease, increasing TILs and cytotoxic T cell function while decreasing Tregs and VEGF.

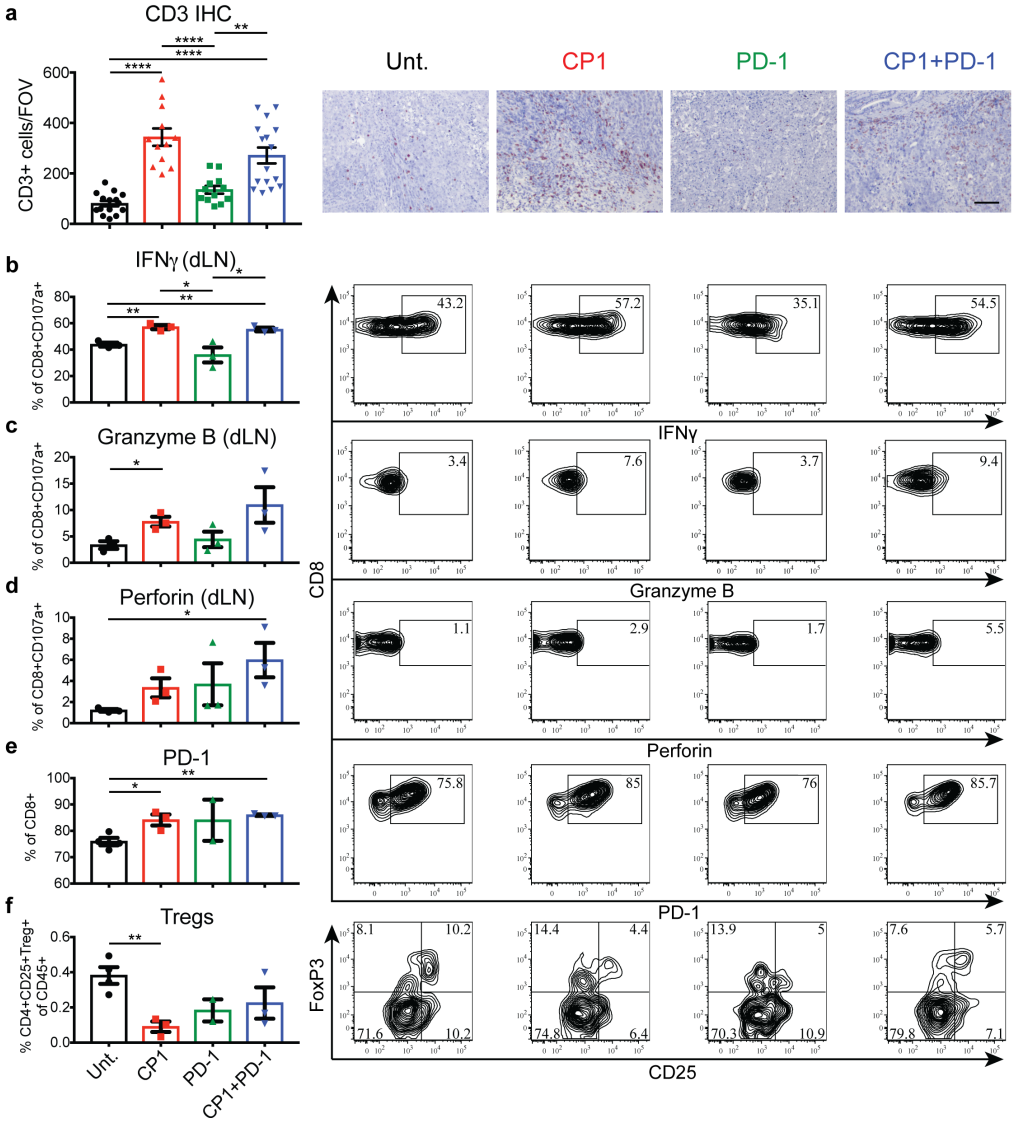


**Figure 22. CP1 increases TILs and T cell cytotoxicity while decreasing Tregs in Myc-CaP PTEN KO tumors**

(**a**) IHC with representative images, quadruplicate FOVs scored per sample (scale bar, 100μm). (**b-f**) Flow cytometry analyses of tumors or dLNs with representative flow cytometry plots. *n* = 3-4 mice/experimental group. Data represented as mean ± S.E.M. Statistical significance was determined by (**a**) one-way ANOVA, (**b-f**) two-tailed Student's *t*-test. * $P<0.05$, ** $P<0.01$, **** $P<0.0001$.

### 3.7 CP1 therapeutic efficacy is dependent on recruitment of TILs

To determine if CP1-recruited TILs were necessary for its efficacy with PD-1 blockade, we utilized fingolimod (FTY720), a sphingosine-1 phosphate mimetic, to block egress of T cells from lymph nodes into peripheral tissues (374). This approach did not inhibit the quantity or functionality of baseline TILs, thereby selectively blocking only those T cells recruited by CP1. FTY720 administration successfully blocked the CP1-dependent increase in both CD8 and CD4 TILs (Fig. 23a-d), and, consequently, reversed the anti-tumor efficacy of CP1+PD-1 combination therapy (Fig. 23e, f). Therefore, TILs specifically recruited by CP1 were necessary to drive the anti-tumor immune response.

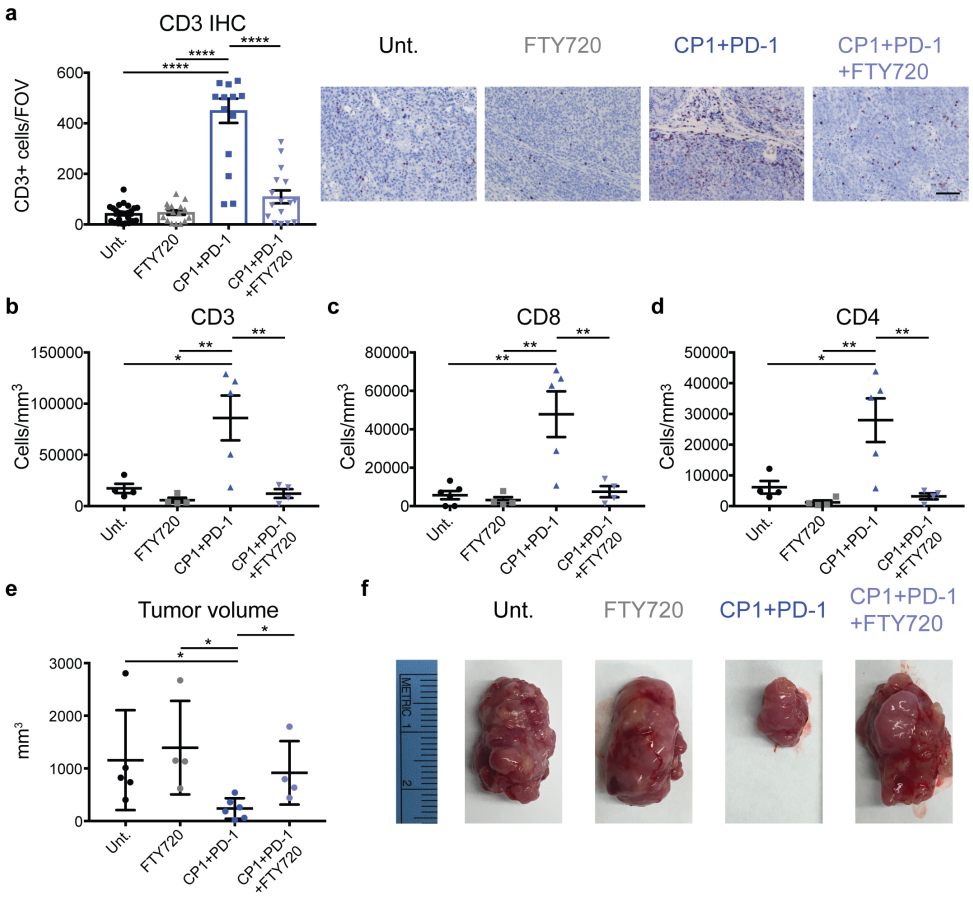


**Figure 23. CP1 therapeutic efficacy is dependent on its recruitment of TILs**
Myc-CaP PTEN KO tumor bearing mice untreated or treated with FTY720, CP1 and anti-PD-1 antibody, or CP1 and anti-PD-1 antibody and FTY720. (**a**) IHC with representative images, quadruplicate FOVs scored per sample (scale bar, 100μm). (**b-d**) Flow cytometry analyses of tumors. Post-tx tumor (**e**) volumes and (**f**) gross images. *n* = 4-6 mice/experimental group. Data represented as mean ± S.E.M. Statistical significance was determined by (**a-d**) one-way ANOVA, (**e**) two-tailed Student's *t*-test. * $P<0.05$, ** $P<0.01$, **** $P<0.0001$.

# CHAPTER 4: DISCUSSION

Immune checkpoint inhibitors have thus far failed to provide significant clinical benefit for prostate cancer (270, 283). Similar to other immunologically "cold" and unresponsive tumor types, prostate tumors display strong PD-L1 positivity (281) and their microenvironment contains scarce (16) but high PD-1-expressing TILs (31, 34), and high levels of Tregs (20, 34) and M2-polarized tumor-associated macrophages (TAMs) (64), all of which are linked to disease progression and death. However, another similarity between these cancers is that they stem from tissues frequently colonized by pathogenic bacteria. This study demonstrates how a unique patient-derived prostate-specific bacteria was isolated and utilized to enhance immunotherapy efficacy in multiple orthotopic models of the disease.

CP1 specifically homed to prostate tumors, ascending from the urethra to the bladder to the tumor without progressing to the kidneys or inducing any systemic toxicities. Further, CP1 induced ICD in both mouse and human prostate cancer cells, as determined by increased HMGB1, ATP, calreticulin, and CXCL10. ICD is important for the recruitment, activation, and optimization of antigen presentation of intra-tumoral DCs (368). Intra-tumoral CP1 increased infiltration by CD8 and CD4 TILs, both of which are linked to response to PD-1 blockade (14), and T cells from these mice expressed increased levels of IFNγ, granzyme B, perforin, and TNFα, all critical for a functional anti-tumor adaptive immune response (375). In addition, CP1 decreased the Treg TIL

phenotype with a corresponding increase in Th17 T cells. Tregs are a major source of immunosuppression in the tumor microenvironment (41), while IL-17 can promote anti-tumor immunity by increasing infiltration of CD8 TILs, NK cells, and APCs, as well as increasing IFNγ production (376). CP1 also increased intra-tumoral levels of mature DCs, M1-polarized macrophages, NK cells, and γδ T cells. Prostate TAMs are typically M2-polarized immunosuppressive cells linked to disease progression (64, 67). However, the $CD80^{+}$ TAMs recruited and polarized by CP1 represent an M1 macrophage proven to inhibit tumor growth and promote cytotoxic T cell activity (377). Additionally, NK cells can directly kill cancer cells, secrete IFNγ, TNF, GM-CSF and other cytokines to promote CD8 T cell and APC activity, while also controlling tumor metastasis and recognizing CD8 T cell-resistant tumors with downregulated MHC I (80, 378). γδ T cells can also directly eliminate cancer cells, produce IFNγ, and enhance CD8 and Th1 T cell and NK cell activity (48). Finally, CP1 consistently increased levels of IFNγ, TNFα, and the innate chemokine MIP-2, possibly secreted by the M1 macrophages (379), and decreased levels of VEGF and IL6 from both cancer cells and within the tumor microenvironment. VEGF is not only important in tumor angiogenesis, but also in actively suppressing the anti-tumor immune response by increasing tumor-infiltrating Tregs, TAMs, and MDSCs, while decreasing APC maturation and T cell infiltration and effector function (199). Likewise, IL-6 can promote tumorigenesis and is linked to prostate cancer progression (380) and MDSC recruitment (381). Thus, through multiple mechanisms, CP1 reprogrammed the prostate tumor microenvironment, thereby sensitizing tumors to anti-PD-1 immunotherapy (Fig. 24).

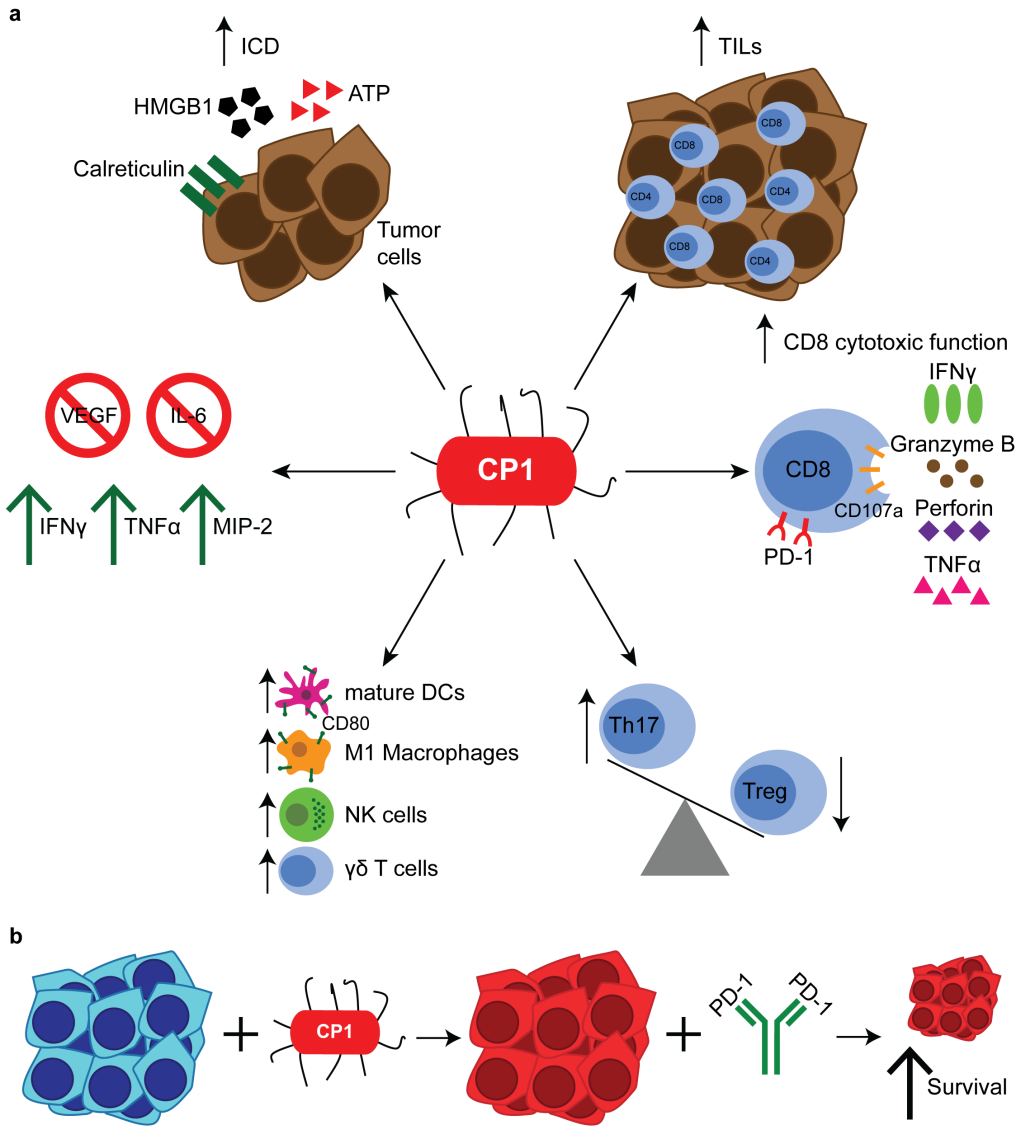


**Figure 24. CP1 is a tissue-specific and multifaceted immunomodulatory tool**
(**a**) Intra-urethrally administered CP1 colonized tumor tissue and increases CD8 and CD4 TILs, T cell cytotoxic function via IFNγ, granzyme B, perforin, and TNFα expression, skews the Th17/Treg axis to increase Th17 cells and decrease Treg TILs, increases tumor infiltration of mature DCs, M1 macrophages, NK cells, and γδ T cells, decreases intra-tumoral VEGF and IL-6 and increases IFNγ, TNFα, and MIP-2, and directly kills cancer cells with induction of immunogenic cell death (ICD). (**b**) CP1 reprograms non-immunogenic "cold" prostate tumor microenvironment and sensitizes tumors to anti-PD-1 blockade, resulting in decreased tumor burden and increased survival.

Multiple microbial cancer therapies have been previously tested in different cancer types. Bacteria in particular have many properties that offer potential advantages over other conventional therapeutic modalities. Bacteria are able to sense the external environment and potentially preferentially home to tumor tissue, and obligate and facultative anaerobes can survive and penetrate deep into the hypoxic core of tumors. Further, these bacteria may then stimulate a host immune response, they often display innate tumor cytotoxic properties, and they can be modified to express various anti-cancer or imaging detection agents (302, 303). These studies have led to the development of the BCG therapy for bladder cancer, TLR agonists (382), and the use of *S. typhimurium*, *L. monocytogenes*, and *C. novyi* spores to deliver various cytokines, cytotoxic agents, and TAAs, even reaching the clinical trial level. Specifically in prostate cancer, attenuated *S. typhimurium* strains demonstrated an ability to localize to prostate xenograft tumors and induce tumor regression when delivered intra-venously or intra-tumorally (307, 308), as well as causing direct tumor cell mitochondrial destruction (309). *S. typhimurium* were also modified to deliver prostate TAAs (310, 311), the *p53* gene and *MDM2* siRNA, and *Stat3* siRNA and Endostatin (313), and demonstrated enhanced anti-tumor efficacy when combined with cisplatin (312). In addition, attenuated *L. monocytogenes* demonstrated efficacy in inducing antigen-specific immune responses against PSA in pre-clinical murine PCa (314, 315), which was enhanced when combined with radiation therapy (316).

CP1 displays multiple similarities and advantages in comparison to these microbial therapies. Unlike BCG and TLR agonists, CP1 is a live bacteria capable of

colonizing tumor tissue to directly induce ICD and continually enforce its multi-faceted immunomodulatory abilities. It is a prostate-tropic bacteria with the motility to ascend from the urethra to the bladder to the prostate tumor, where it survives long-term to augment the host immune response. In addition, in contrast to TLR agonists that activate limited pathways, live CP1 likely interacts with and activates may receptors and signaling pathways in the urogenital tract and the tumor microenvironment. Further, unlike many prior *Salmonella* (383)- and *Listeria* (384)-based therapies, CP1 does not require systemic i.v. instillation or intra-tumoral injection to reach the tumor. Intra-urethral CP1 administration led to bacterial ascension from the urethra to specifically colonize the tumor, and CP1 did not induce any systemic toxicities even without attenuation of the bacteria. Unlike the prior bacterial cancer therapies, CP1 is novel in being a clinical isolate from the prostate of a patient with chronic prostatitis, thereby representing a more endogenous, personalized therapy for prostate cancer, displaying innate tropism for the tissue of interest. CP1 also was able to mobilize and activate an adaptive anti-tumor immune response and an innate response, conferring strong synergistic efficacy with PD-1 blockade, without any major genetic manipulation, in contrast to some bacterial therapies that have been utilized predominantly as an adjuvant for a cancer vaccine. Importantly, CP1 was also able to concurrently decrease immunosuppressive intra-tumoral Tregs and VEGF while increasing important anti-tumor immune cell types and cytokines.

Another strength of this study was in representing multiple clinically relevant genetic backgrounds of prostate cancers. We utilized the androgen-dependent Myc-CaP

cell line (366), driven by *MYC* overexpression, as is seen in 80-90% of human prostate tumors (385). Additionally, we performed a CRISPR-Cas9 knock out of *PTEN* from the Myc-CaP genome, as concurrent *MYC* copy number gain and *PTEN* copy number loss is associated with prostate cancer-specific mortality and is reported in over half of deadly metastatic prostate tumors (372). *PTEN* loss is also linked to increased PD-L1 expression (370), decreased TILs, and resistance to PD-1 blockade (371). Further, both cell lines were surgically instilled into the prostate, allowing for the development of genetically complex and clinically relevant orthotopic tumors within prostatic microenvironments and with endogenous prostate-draining lymph nodes. In both models, a single dose of CP1 consistently augmented the anti-tumor response to significantly increase survival and decrease tumor burden when combined with less than two weeks of anti-PD-1 blockade.

In our murine models, prostate cancer cells were injected into the anterior prostate lobe of mice. The mouse prostate consists of the anterior, ventral, and dorsolateral prostate lobes, and the human prostate consists of a peripheral zone, transitional zone, and central zone within a single lobe (386). While prior studies have anatomically and histologically compared the dorsolateral mouse lobe to the human peripheral zone, the site of the majority of prostate cancers (387), and the anterior mouse lobe to the human central zone (388, 389), more recent and comprehensive analysis has demonstrated that the anterior lobe and dorsolateral lobe display closely related gene expression patterns, as compared to the ventral lobe (390). Further, prostate cancer development has been observed in the anterior lobe of GEMs (386), and, for the intra-prostatic procedure, the

anterior lobe allows for the injection of the necessary volume of cancer cell solution with minimal leakage and variability.

Subcutaneous and transgenic GEM cancer models have multiple flaws and limitations. Subcutaneous tumors grown in an artificial tumor microenvironment have demonstrated differential responses to chemotherapies, in contrast to both orthotopic tumors from the same cell lines and human disease (343-345). This may be due to the altered vasculature of subcutaneous tumors, as exemplified by their differential response to anti-angiogenic therapy (341, 342). On the contrary, orthotopic tumors develop with a proper tumor microenvironment, draining lymph nodes, and vasculature, and can be performed with murine cell lines, thereby also allowing for analysis of tumor immunology and response to immunotherapies.

Transgenic GEMs develop tumors with a proper tumor microenvironment in an immunocompetent host, yet these models typically oversimplify human cancer by developing tumors with single or few genetic alterations (350). An analysis of Myc-CaP and other prostate cancer cell lines revealed that they contained much greater somatic copy number alterations and chromosomal alterations than tumors from the Hi-Myc mice and other GEMs from which they were derived (350). Further, GEMs are limited by the increased cost and time needed for mice breeding to perform experiments of sufficient power. Orthotopic tumor modeling can overcome these limitations. Human and murine prostate cancer cell lines contain many genetic alterations relevant to human disease (350), and, like human cancer, also show great heterogeneity between individual cells (351). Orthotopic murine syngeneic tumors allow for immunological analyses, while

orthotopic human xenogeneic tumors allow for analyses of therapeutics on human cells. Finally, unlike with GEMs, cell lines can be modified *in vitro* before injection, which allowed us to stably express luciferase for *in vivo* bioluminescent imaging to monitor tumor growth and normalize tumor burden among experimental groups, as well as to perform the CRISPR-Cas9 knockout of the tumor suppressor *PTEN*.

Multiple future steps can be taken to overcome limitations and achieve optimal clinical success. While we extensively evaluated the safety of CP1, future studies can attempt to attenuate the bacteria without diminishing the pro-inflammatory qualities important for its anti-tumor efficacy. To increase its therapeutic potency, CP1 can be engineer similar to prior bacterial cancer therapies to deliver cytotoxic agents, cytokines or chemokines, tumor antigen, or genetic material, as described above (302). Specifically, one prior study demonstrated that an oncolytic virus engineered to express a soluble form of PD-1 was more efficacious that the virus combined with anti-PD-1 antibody administration in a preclinical melanoma model (391). The authors suggested that the enhanced efficacy of soluble microbial-delivered PD-1 blockade over antibody injections may have been due to increased affinity of the soluble molecule for its ligands, enhanced diffusion of the smaller molecule throughout the tumor, and the potential for the soluble PD-1 to bind to any additional ligand binding partners (392). Given the synergistic efficacy of combining CP1 with anti-PD-1 antibody, engineering CP1 to produce the soluble inhibitory PD-1 molecule may enhance the anti-tumor benefit. However, this strategy does increase the risk of systemic toxicities, as the degree of PD-1 blockade would be under less control than with anti-PD-1 antibody administration.

Further, as stated above, to optimize immunotherapy efficacy, focus has shifted toward combining immunotherapies with various other immunomodulatory therapeutics, such as adoptive T cell therapies, chemotherapies, and radiation (317). Interestingly, our flow cytometry analysis revealed that CP1 increased tumor infiltrating B cells. While B cells are able to present antigen at comparable levels as mature DCs (393) and are associated with increased survival (394), others have demonstrated tumor-promoting and immunosuppressive properties of B cell subsets in prostate cancer (79). Therefore, CP1 may be optimized in combination with a B cell inhibitor, such as rituximab, which has previously resulted in a biochemical response in a patient with advanced prostate cancer (77).

In addition to optimizing synergistic combination therapies, it will also be important to analyze specific markers that may predict response to CP1. Tumor mutational burden and neo-antigen load, DNA repair defects and MSI (as observed in prostate tumors), the status of various gene signaling pathways, and the presence of select bacterial species in the gut microbiome (or potentially the prostate tumor flora) may serve as either predictive or targetable markers with CP1 administration.

One reason for the scarcity of TILs in the prostate tumor microenvironment may be its weak mutagenicity. Interestingly, in addition to increased TILs, T cell inflamed tumors also contain a higher tumor mutational burden (395). mCRPC tumors, on the contrary, displayed a low mutation rate of approximately 2 mutations/megabase (Mb) (396). Increased mutations increase the likelihood of generating immunogenic and tumor-specific neo-antigens, which amplify tumor immunogenicity to increase both the

endogenous anti-tumor immune response and the response to exogenous immunotherapies. As expected, neo-antigen load directly correlates with overall mutational burden, and prostate tumors also display low levels of neo-antigens (397). Importantly, neo-antigen load, but not overall mutational burden, is significantly associated with increased OS across multiple tumor types (398), and, retrospective stratification of tumors with high neo-antigen load strongly associated with responders to anti-PD-1 therapy in NSCLC (399) and anti-CTLA-4 therapy in metastatic melanoma (400). High tumor mutational burden and neo-antigen load may also prove to be a valuable prognostic marker in selecting PCa patients for immunotherapy or for treatment with CP1.

Mutations in DNA repair genes result in a hypermutable state and are associated with increased tumor neo-antigen load. As a result, pembrolizumab has been approved specifically for mismatch repair (MMR)-deficient or microsatellite instability (MSI)-high solid tumors, after clinical trials demonstrated significantly increased efficacy in treating those tumors in comparison to tumors with wildtype DNA repair function (401-403). In addition to defects in MMR, defects in the homologous recombination (HR) DNA repair pathway have also been linked to response to PD-1 blockade, increased neo-antigens, and increased TILs (399, 404-406). Specifically in PCa, 8% of Gleason 9-10 adenocarcinomas and 5% of small cell carcinomas display loss of MSH2, with CD8 TILs directly correlating with mutational burden in theses tumors (407). In addition, 19% of localized PCa TCGA samples contain aberrations in *BRCA2, BRCA1, CDK12, ATM, FANCD2,* or *RAD51C* (361), 22.7% of 150 mCRPC samples contain mutations in

*BRCA2, ATM, BRCA1, FANCA, RAD51B, RAD51C, MLH1,* or *MLH2* (408), and MMR mutations in *MSH2*, *MLH1*, or *MSH6* are specifically associated with a hypermutable state of approximately 50 mutations/Mb (408, 409). Additional studies on mPCa have reported 12% and 0.7% with biallelic *BRCA2* and *BRCA1* mutations, respectively (410), a 7.3-13% germline DNA repair mutation rate (411-414), and that mCRPC have increased mutation rates in comparison to localized PCa (20-28% vs. 6.2-18%) (396, 415). Patient reports have validated the use of these genes as immunotherapy biomarkers, as one CRPC tumor with loss of *MSH2* and *MSH6* expression and which was refractory to chemotherapies and enzalutamide responded well to nivolumab (287), and MSI was observed in a mCRPC enzalutamide-resistant responder to pembrolizumab (286). Accordingly, nivolumab is being tested in mCRPC with DNA repair defects (as defined by mutations in *BRCA1, BRCA2, ATM, PTEN, CHEK2, RAD51C, RAD51D, PALB2, MLH1, MSH2, MSH6,* or *PMS2*) (phase II NCT03040791) and ipilimumab plus nivolumab is being tested in mCRPC patients with defective MMR/DNA repair or high inflammatory infiltrate (phase II NCT03061539). Similarly, tumor stratification based on DNA repair status may serve as a biomarker to predict response to CP1.

Identifying tumors with specific genetic mutations and signaling pathway activation may also be valuable in selecting PCa immunotherapy and CP1 responders. In pre-clinical murine models, *PTEN* knockout prostate tumors contain high levels of infiltrating immunosuppressive MDSCs (57-59) as well as Tregs after castration (115). Further, *PTEN* loss is linked to increased PD-L1 levels in PCa and breast cancer (370), as well as decreased TILs and resistance to PD-1 inhibition in melanoma (371). In addition,

the *MYC* oncogene directly regulates *PD-L1* expression, while activation of the β-catenin pathway is associated with decreased TILs and resistance to PD-L1 and CTLA-4 blockade (416).

The microbiome may also prove to be a valuable resource for the success of immunotherapies. Initial microbiome categorization of prostate tumor tissue identified bacterial DNA in 87% of tumors and a total of 83 distinct microorganisms, with no single species correlating with the level of tissue inflammation (417). More recent ultradeep pyrosequencing analysis of 16 prostatectomy samples revealed the presence of many bacterial populations both intra- and peri-tumoral. *Propionibacterium* spp. was the most numerous bacterial genera within prostate tumors, while *Staphylococcus* spp. was found more frequently within the tumor and peri-tumoral region in comparison to non-tumor tissue, and *Streptococcus* spp. was more frequent in non-tumor tissue (418). While microbiome dysbiosis may play a role in prostate cancer development and pathogenesis (419), it may also be valuable in predicting treatment efficacy. An intact intestinal microbiome is critical for the maximal efficacy of cyclophosphamide and platinum chemotherapy, proving necessary for these treatments to induce a Th17 and Th1 anti-tumor immune response (420) and to modulate tumor-infiltrating myeloid-derived cells (421), respectively. Regarding immune checkpoint inhibitors, an intact microbiome, specifically one that contains *Bacteroides fragilis*, is associated with maximal efficacy of CTLA-4 blockade in melanoma mice and patients (422). In addition *Bifidobacterium* in the intestinal microbiome augments DC function to synergize with PD-L1 blockade in murine melanoma (423). In another study, *Akkermansia muciniphila* was critical for PD-

1 blockade efficacy in mice and patients with epithelial tumors. Oral supplementation with the bacteria increased IL-12 and recruited $CCR9^{+}CXCR3^{+}$ CD4 T cells into the tumor (424). Finally, analysis of melanoma patients treated with PD-1 blockade revealed that responders contained increased microbiome diversity and *Ruminococcaceae* family bacteria (425). Identifying similar key bacteria, either in the local prostate tumor flora or in the gut microbiome, and any interactions they may have with CP1, may be key to identifying immunotherapy responders or augmenting the response to CP1 administration.

Finally, this model can also be utilized to study the effects of CP1 in CRPC. CRPC confers a poor prognosis with a median survival time of 9-30 months, or 12-37 months after ADT initiation, and is in need of novel treatment options (8-10). After intra-prostatic Myc-CaP cell injection and subsequent orthotopic tumor development, mice were surgically castrated. Within 3 days after castration, strong tumor regression was observed, followed by subsequent tumor recurrence after approximately 30 days, representing CRPC (Fig. 25a), as tumors were now able to grow in an androgen-independent manner. These CRPC tumors can be dissection and analyzed histologically, and do not display any neuroendocrine differentiation, as they maintain high AR levels and are negative for the neuroendocrine marker, synaptophysin (Fig. 25b). Therefore, we are able to model both orthotopic androgen-dependent prostate cancer and androgen-independent CRPC in an immunocompetent host.

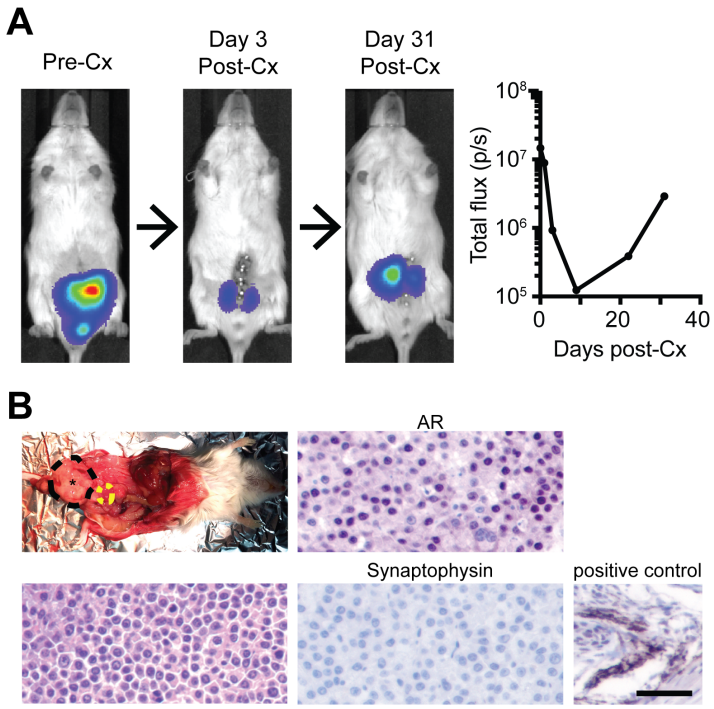


**Figure 25. Intra-prostatic injections with subsequent surgical castration to model both androgen-dependent prostate cancer and CRPC**

**(A)** Mice bearing orthotopic luciferase-expressing tumors were imaged by bioluminescence pre- and post-castration (Cx), and **(B)** recurred CRPC tumors were dissected (black=orthotopic prostate tumor; yellow=bladder) and analyzed by H&E, AR IHC, and synaptophysin IHC (with positive murine control) (scale bar=50 μm).

In summary, CP1 is a novel, single intra-urethral dose, multi-faceted immunomodulatory tool capable of homing to prostate tumor tissue and reprogramming the “cold” microenvironment, thereby sensitizing the otherwise resistant cancer to immune checkpoint inhibition. The combination of CP1 and PD-1 blockade achieved these results in multiple, clinically relevant, orthotopic models of the highly prevalent and deadly disease. More broadly, this study demonstrates how select tissue-specific microbes, as are commonly isolated colonizing the breast (326), pharynx (327), intestines, bladder (328), female genital tract (329), and additional tissues throughout the body, can be screened and evaluated to uncover future CP1-like bacteria to potentiate immunotherapies in other recalcitrant cancers.

**REFERENCES**

1. Siegel RL, Miller KD, Jemal A. Cancer statistics, 2018. CA: a cancer journal for clinicians. 2018;68(1):7-30. doi: 10.3322/caac.21442. PubMed PMID: 29313949.
2. Zhao J, Zhu S, Sun L, Meng F, Zhao L, Zhao Y, Tian H, Li P, Niu Y. Androgen deprivation therapy for prostate cancer is associated with cardiovascular morbidity and mortality: a meta-analysis of population-based observational studies. PloS one. 2014;9(9):e107516. Epub 2014/09/30. doi: 10.1371/journal.pone.0107516. PubMed PMID: 25264674; PMCID: 4180271.
3. Kohutek ZA, Steinberger E, Pei X, Shi W, Zhang Z, Kollmeier MA, Zelefsky MJ. Long-Term Impact of Androgen-Deprivation Therapy on Cardiovascular Morbidity after Radiotherapy for Clinically Localized Prostate Cancer. Urology. 2015. Epub 2015/10/18. doi: 10.1016/j.urology.2015.08.029. PubMed PMID: 26476405.
4. Wilke DR, Parker C, Andonowski A, Tsuji D, Catton C, Gospodarowicz M, Warde P. Testosterone and erectile function recovery after radiotherapy and long-term androgen deprivation with luteinizing hormone-releasing hormone agonists. BJU international. 2006;97(5):963-8. Epub 2006/03/18. doi: 10.1111/j.1464-410X.2006.06066.x. PubMed PMID: 16542340.
5. Shahinian VB, Kuo YF, Freeman JL, Goodwin JS. Risk of fracture after androgen deprivation for prostate cancer. The New England journal of medicine. 2005;352(2):154-64. Epub 2005/01/14. doi: 10.1056/NEJMoa041943. PubMed PMID: 15647578.
6. Djavan B, Eastham J, Gomella L, Tombal B, Taneja S, Dianat SS, Kazzazi A, Shore N, Abrahamsson PA, Cheetham P, Moul J, Lepor H, Crawford ED. Testosterone in prostate cancer: the Bethesda consensus. BJU international. 2012;110(3):344-52. Epub 2011/12/02. doi: 10.1111/j.1464-410X.2011.10719.x. PubMed PMID: 22129242.
7. Huggins C, Hodges CV. Studies on prostatic cancer: I. The effect of castration, of estrogen and of androgen injection on serum phosphatases in metastatic carcinoma of the prostate. 1941. The Journal of urology. 2002;168(1):9-12. Epub 2002/06/07. PubMed PMID: 12050481.
8. Denis L, Murphy GP. Overview of phase III trials on combined androgen treatment in patients with metastatic prostate cancer. Cancer. 1993;72(12 Suppl):3888-95. Epub 1993/12/15. PubMed PMID: 8252511.
9. Hellerstedt BA, Pienta KJ. The current state of hormonal therapy for prostate cancer. CA: a cancer journal for clinicians. 2002;52(3):154-79. Epub 2002/05/23. PubMed PMID: 12018929.
10. Kirby M, Hirst C, Crawford ED. Characterising the castration-resistant prostate cancer population: a systematic review. International journal of clinical practice. 2011;65(11):1180-92. Epub 2011/10/15. doi: 10.1111/j.1742-1241.2011.02799.x. PubMed PMID: 21995694.
11. Gurel B, Lucia MS, Thompson IM, Jr., Goodman PJ, Tangen CM, Kristal AR, Parnes HL, Hoque A, Lippman SM, Sutcliffe S, Peskoe SB, Drake CG, Nelson WG, De

Marzo AM, Platz EA. Chronic inflammation in benign prostate tissue is associated with high-grade prostate cancer in the placebo arm of the prostate cancer prevention trial. Cancer epidemiology, biomarkers & prevention : a publication of the American Association for Cancer Research, cosponsored by the American Society of Preventive Oncology. 2014;23(5):847-56. doi: 10.1158/1055-9965.EPI-13-1126. PubMed PMID: 24748218; PMCID: PMC4012292.
12. Shalapour S, Karin M. Immunity, inflammation, and cancer: an eternal fight between good and evil. J Clin Invest. 2015;125(9):3347-55. doi: 10.1172/JCI80007. PubMed PMID: 26325032; PMCID: PMC4588298.
13. Gajewski TF, Schreiber H, Fu YX. Innate and adaptive immune cells in the tumor microenvironment. Nat Immunol. 2013;14(10):1014-22. doi: 10.1038/ni.2703. PubMed PMID: 24048123; PMCID: PMC4118725.
14. Tumeh PC, Harview CL, Yearley JH, Shintaku IP, Taylor EJ, Robert L, Chmielowski B, Spasic M, Henry G, Ciobanu V, West AN, Carmona M, Kivork C, Seja E, Cherry G, Gutierrez AJ, Grogan TR, Mateus C, Tomasic G, Glaspy JA, Emerson RO, Robins H, Pierce RH, Elashoff DA, Robert C, Ribas A. PD-1 blockade induces responses by inhibiting adaptive immune resistance. Nature. 2014;515(7528):568-71. doi: 10.1038/nature13954. PubMed PMID: 25428505; PMCID: PMC4246418.
15. Jochems C, Schlom J. Tumor-infiltrating immune cells and prognosis: the potential link between conventional cancer therapy and immunity. Exp Biol Med (Maywood). 2011;236(5):567-79. doi: 10.1258/ebm.2011.011007. PubMed PMID: 21486861; PMCID: PMC3229261.
16. Hussein MR, Al-Assiri M, Musalam AO. Phenotypic characterization of the infiltrating immune cells in normal prostate, benign nodular prostatic hyperplasia and prostatic adenocarcinoma. Exp Mol Pathol. 2009;86(2):108-13. doi: 10.1016/j.yexmp.2008.11.010. PubMed PMID: 19111537.
17. Fujii T, Shimada K, Asai O, Tanaka N, Fujimoto K, Hirao K, Konishi N. Immunohistochemical analysis of inflammatory cells in benign and precancerous lesions and carcinoma of the prostate. Pathobiology. 2013;80(3):119-26. doi: 10.1159/000342396. PubMed PMID: 23328608.
18. Yuan H, Hsiao YH, Zhang Y, Wang J, Yin C, Shen R, Su Y. Destructive impact of T-lymphocytes, NK and Mast cells on basal cell layers: implications for tumor invasion. BMC cancer. 2013;13:258. doi: 10.1186/1471-2407-13-258. PubMed PMID: 23705594; PMCID: PMC3722065.
19. Ebelt K, Babaryka G, Figel AM, Pohla H, Buchner A, Stief CG, Eisenmenger W, Kirchner T, Schendel DJ, Noessner E. Dominance of CD4+ lymphocytic infiltrates with disturbed effector cell characteristics in the tumor microenvironment of prostate carcinoma. The Prostate. 2008;68(1):1-10. doi: 10.1002/pros.20661. PubMed PMID: 17948280.
20. Valdman A, Jaraj SJ, Comperat E, Charlotte F, Roupret M, Pisa P, Egevad L. Distribution of Foxp3-, CD4- and CD8-positive lymphocytic cells in benign and malignant prostate tissue. APMIS. 2010;118(5):360-5. doi: 10.1111/j.1600-0463.2010.02604.x. PubMed PMID: 20477811.

21. Massari F, Ciccarese C, Calio A, Munari E, Cima L, Porcaro AB, Novella G, Artibani W, Sava T, Eccher A, Ghimenton C, Bertoldo F, Scarpa A, Sperandio N, Porta C, Bronte V, Chilosi M, Bogina G, Zamboni G, Tortora G, Samaratunga H, Martignoni G, Brunelli M. Magnitude of PD-1, PD-L1 and T Lymphocyte Expression on Tissue from Castration-Resistant Prostate Adenocarcinoma: An Exploratory Analysis. Target Oncol. 2016;11(3):345-51. doi: 10.1007/s11523-015-0396-3. PubMed PMID: 26566945.
22. Baas W, Gershburg S, Dynda D, Delfino K, Robinson K, Nie D, Yearley JH, Alanee S. Immune Characterization of the Programmed Death Receptor Pathway in High Risk Prostate Cancer. Clin Genitourin Cancer. 2017;15(5):577-81. doi: 10.1016/j.clgc.2017.04.002. PubMed PMID: 28461179.
23. Vesalainen S, Lipponen P, Talja M, Syrjanen K. Histological grade, perineural infiltration, tumour-infiltrating lymphocytes and apoptosis as determinants of long-term prognosis in prostatic adenocarcinoma. European journal of cancer. 1994;30A(12):1797-803. PubMed PMID: 7880609.
24. Flammiger A, Bayer F, Cirugeda-Kuhnert A, Huland H, Tennstedt P, Simon R, Minner S, Bokemeyer C, Sauter G, Schlomm T, Trepel M. Intratumoral T but not B lymphocytes are related to clinical outcome in prostate cancer. APMIS. 2012;120(11):901-8. doi: 10.1111/j.1600-0463.2012.02924.x. PubMed PMID: 23009114.
25. McArdle PA, Canna K, McMillan DC, McNicol AM, Campbell R, Underwood MA. The relationship between T-lymphocyte subset infiltration and survival in patients with prostate cancer. British journal of cancer. 2004;91(3):541-3. doi: 10.1038/sj.bjc.6601943. PubMed PMID: 15266325; PMCID: PMC2409839.
26. Zeigler-Johnson C, Morales KH, Lal P, Feldman M. The Relationship between Obesity, Prostate Tumor Infiltrating Lymphocytes and Macrophages, and Biochemical Failure. PloS one. 2016;11(8):e0159109. doi: 10.1371/journal.pone.0159109. PubMed PMID: 27487262; PMCID: PMC4972345.
27. Karja V, Aaltomaa S, Lipponen P, Isotalo T, Talja M, Mokka R. Tumour-infiltrating lymphocytes: A prognostic factor of PSA-free survival in patients with local prostate carcinoma treated by radical prostatectomy. Anticancer research. 2005;25(6C):4435-8. PubMed PMID: 16334122.
28. Sfanos KS, Bruno TC, Maris CH, Xu L, Thoburn CJ, DeMarzo AM, Meeker AK, Isaacs WB, Drake CG. Phenotypic analysis of prostate-infiltrating lymphocytes reveals TH17 and Treg skewing. Clinical cancer research : an official journal of the American Association for Cancer Research. 2008;14(11):3254-61. doi: 10.1158/1078-0432.CCR-07-5164. PubMed PMID: 18519750; PMCID: PMC3082357.
29. Derhovanessian E, Adams V, Hahnel K, Groeger A, Pandha H, Ward S, Pawelec G. Pretreatment frequency of circulating IL-17+ CD4+ T-cells, but not Tregs, correlates with clinical response to whole-cell vaccination in prostate cancer patients. International journal of cancer Journal international du cancer. 2009;125(6):1372-9. doi: 10.1002/ijc.24497. PubMed PMID: 19533748.

30. Kottke T, Sanchez-Perez L, Diaz RM, Thompson J, Chong H, Harrington K, Calderwood SK, Pulido J, Georgopoulos N, Selby P, Melcher A, Vile R. Induction of hsp70-mediated Th17 autoimmunity can be exploited as immunotherapy for metastatic prostate cancer. Cancer research. 2007;67(24):11970-9. doi: 10.1158/0008-5472.CAN-07-2259. PubMed PMID: 18089828.
31. Sfanos KS, Bruno TC, Meeker AK, De Marzo AM, Isaacs WB, Drake CG. Human prostate-infiltrating CD8+ T lymphocytes are oligoclonal and PD-1+. The Prostate. 2009;69(15):1694-703. doi: 10.1002/pros.21020. PubMed PMID: 19670224; PMCID: PMC2782577.
32. Savage PA, Vosseller K, Kang C, Larimore K, Riedel E, Wojnoonski K, Jungbluth AA, Allison JP. Recognition of a ubiquitous self antigen by prostate cancer-infiltrating CD8+ T lymphocytes. Science. 2008;319(5860):215-20. doi: 10.1126/science.1148886. PubMed PMID: 18187659.
33. Okazaki T, Honjo T. PD-1 and PD-1 ligands: from discovery to clinical application. Int Immunol. 2007;19(7):813-24. doi: 10.1093/intimm/dxm057. PubMed PMID: 17606980.
34. Ebelt K, Babaryka G, Frankenberger B, Stief CG, Eisenmenger W, Kirchner T, Schendel DJ, Noessner E. Prostate cancer lesions are surrounded by FOXP3+, PD-1+ and B7-H1+ lymphocyte clusters. European journal of cancer. 2009;45(9):1664-72. doi: 10.1016/j.ejca.2009.02.015. PubMed PMID: 19318244.
35. Japp AS, Kursunel MA, Meier S, Malzer JN, Li X, Rahman NA, Jekabsons W, Krause H, Magheli A, Klopf C, Thiel A, Frentsch M. Dysfunction of PSA-specific CD8+ T cells in prostate cancer patients correlates with CD38 and Tim-3 expression. Cancer immunology, immunotherapy : CII. 2015;64(11):1487-94. doi: 10.1007/s00262-015-1752-y. PubMed PMID: 26289091.
36. Anderson AC. Tim-3: an emerging target in the cancer immunotherapy landscape. Cancer immunology research. 2014;2(5):393-8. doi: 10.1158/2326-6066.CIR-14-0039. PubMed PMID: 24795351.
37. Zhang H, Melamed J, Wei P, Cox K, Frankel W, Bahnson RR, Robinson N, Pyka R, Liu Y, Zheng P. Concordant down-regulation of proto-oncogene PML and major histocompatibility antigen HLA class I expression in high-grade prostate cancer. Cancer Immun. 2003;3:2. PubMed PMID: 12747744.
38. Bander NH, Yao D, Liu H, Chen YT, Steiner M, Zuccaro W, Moy P. MHC class I and II expression in prostate carcinoma and modulation by interferon-alpha and -gamma. The Prostate. 1997;33(4):233-9. PubMed PMID: 9397194.
39. Carretero FJ, Del Campo AB, Flores-Martin JF, Mendez R, Garcia-Lopez C, Cozar JM, Adams V, Ward S, Cabrera T, Ruiz-Cabello F, Garrido F, Aptsiauri N. Frequent HLA class I alterations in human prostate cancer: molecular mechanisms and clinical relevance. Cancer immunology, immunotherapy : CII. 2016;65(1):47-59. doi: 10.1007/s00262-015-1774-5. PubMed PMID: 26611618.
40. Healy CG, Simons JW, Carducci MA, DeWeese TL, Bartkowski M, Tong KP, Bolton WE. Impaired expression and function of signal-transducing zeta chains in

peripheral T cells and natural killer cells in patients with prostate cancer. Cytometry. 1998;32(2):109-19. PubMed PMID: 9627224.
41. Tanaka A, Sakaguchi S. Regulatory T cells in cancer immunotherapy. Cell Res. 2017;27(1):109-18. doi: 10.1038/cr.2016.151. PubMed PMID: 27995907; PMCID: PMC5223231.
42. Miller AM, Lundberg K, Ozenci V, Banham AH, Hellstrom M, Egevad L, Pisa P. CD4+CD25high T cells are enriched in the tumor and peripheral blood of prostate cancer patients. Journal of immunology. 2006;177(10):7398-405. PubMed PMID: 17082659.
43. Flammiger A, Weisbach L, Huland H, Tennstedt P, Simon R, Minner S, Bokemeyer C, Sauter G, Schlomm T, Trepel M. High tissue density of FOXP3+ T cells is associated with clinical outcome in prostate cancer. European journal of cancer. 2013;49(6):1273-9. doi: 10.1016/j.ejca.2012.11.035. PubMed PMID: 23266046.
44. Idorn M, Kollgaard T, Kongsted P, Sengelov L, Thor Straten P. Correlation between frequencies of blood monocytic myeloid-derived suppressor cells, regulatory T cells and negative prognostic markers in patients with castration-resistant metastatic prostate cancer. Cancer immunology, immunotherapy : CII. 2014;63(11):1177-87. doi: 10.1007/s00262-014-1591-2. PubMed PMID: 25085000.
45. Vergati M, Cereda V, Madan RA, Gulley JL, Huen NY, Rogers CJ, Hance KW, Arlen PM, Schlom J, Tsang KY. Analysis of circulating regulatory T cells in patients with metastatic prostate cancer pre- versus post-vaccination. Cancer immunology, immunotherapy : CII. 2011;60(2):197-206. doi: 10.1007/s00262-010-0927-9. PubMed PMID: 20976449; PMCID: PMC3202216.
46. Tien AH, Xu L, Helgason CD. Altered immunity accompanies disease progression in a mouse model of prostate dysplasia. Cancer research. 2005;65(7):2947-55. doi: 10.1158/0008-5472.CAN-04-3271. PubMed PMID: 15805298.
47. Klyushnenkova EN, Riabov VB, Kouiavskaia DV, Wietsma A, Zhan M, Alexander RB. Breaking immune tolerance by targeting CD25+ regulatory T cells is essential for the anti-tumor effect of the CTLA-4 blockade in an HLA-DR transgenic mouse model of prostate cancer. The Prostate. 2014;74(14):1423-32. doi: 10.1002/pros.22858. PubMed PMID: 25111463.
48. Silva-Santos B, Serre K, Norell H. gammadelta T cells in cancer. Nature reviews Immunology. 2015;15(11):683-91. doi: 10.1038/nri3904. PubMed PMID: 26449179.
49. Liu Z, Guo BL, Gehrs BC, Nan L, Lopez RD. Ex vivo expanded human Vgamma9Vdelta2+ gammadelta-T cells mediate innate antitumor activity against human prostate cancer cells in vitro. The Journal of urology. 2005;173(5):1552-6. PubMed PMID: 15821484.
50. Dieli F, Vermijlen D, Fulfaro F, Caccamo N, Meraviglia S, Cicero G, Roberts A, Buccheri S, D'Asaro M, Gebbia N, Salerno A, Eberl M, Hayday AC. Targeting human {gamma}delta} T cells with zoledronate and interleukin-2 for immunotherapy of hormone-refractory prostate cancer. Cancer research. 2007;67(15):7450-7. doi:

10.1158/0008-5472.CAN-07-0199. PubMed PMID: 17671215; PMCID: PMC3915341.
51. Naoe M, Ogawa Y, Takeshita K, Morita J, Shichijo T, Fuji K, Fukagai T, Iwamoto S, Terao S. Zoledronate stimulates gamma delta T cells in prostate cancer patients. Oncology research. 2010;18(10):493-501. PubMed PMID: 20681408.
52. Kumar V, Patel S, Tcyganov E, Gabrilovich DI. The Nature of Myeloid-Derived Suppressor Cells in the Tumor Microenvironment. Trends in immunology. 2016;37(3):208-20. doi: 10.1016/j.it.2016.01.004. PubMed PMID: 26858199; PMCID: PMC4775398.
53. Vuk-Pavlovic S, Bulur PA, Lin Y, Qin R, Szumlanski CL, Zhao X, Dietz AB. Immunosuppressive CD14+HLA-DRlow/- monocytes in prostate cancer. The Prostate. 2010;70(4):443-55. doi: 10.1002/pros.21078. PubMed PMID: 19902470; PMCID: PMC2935631.
54. Brusa D, Simone M, Gontero P, Spadi R, Racca P, Micari J, Degiuli M, Carletto S, Tizzani A, Matera L. Circulating immunosuppressive cells of prostate cancer patients before and after radical prostatectomy: profile comparison. Int J Urol. 2013;20(10):971-8. doi: 10.1111/iju.12086. PubMed PMID: 23421558.
55. Hossain DM, Pal SK, Moreira D, Duttagupta P, Zhang Q, Won H, Jones J, D'Apuzzo M, Forman S, Kortylewski M. TLR9-Targeted STAT3 Silencing Abrogates Immunosuppressive Activity of Myeloid-Derived Suppressor Cells from Prostate Cancer Patients. Clinical cancer research : an official journal of the American Association for Cancer Research. 2015;21(16):3771-82. doi: 10.1158/1078-0432.CCR-14-3145. PubMed PMID: 25967142; PMCID: PMC4537814.
56. Sharma V, Dong H, Kwon E, Karnes RJ. Positive Pelvic Lymph Nodes in Prostate Cancer Harbor Immune Suppressor Cells To Impair Tumor-reactive T Cells. Eur Urol Focus. 2016. doi: 10.1016/j.euf.2016.09.003. PubMed PMID: 28753790.
57. Garcia AJ, Ruscetti M, Arenzana TL, Tran LM, Bianci-Frias D, Sybert E, Priceman SJ, Wu L, Nelson PS, Smale ST, Wu H. Pten null prostate epithelium promotes localized myeloid-derived suppressor cell expansion and immune suppression during tumor initiation and progression. Mol Cell Biol. 2014;34(11):2017-28. doi: 10.1128/MCB.00090-14. PubMed PMID: 24662052; PMCID: PMC4019050.
58. Di Mitri D, Toso A, Chen JJ, Sarti M, Pinton S, Jost TR, D'Antuono R, Montani E, Garcia-Escudero R, Guccini I, Da Silva-Alvarez S, Collado M, Eisenberger M, Zhang Z, Catapano C, Grassi F, Alimonti A. Tumour-infiltrating Gr-1+ myeloid cells antagonize senescence in cancer. Nature. 2014;515(7525):134-7. doi: 10.1038/nature13638. PubMed PMID: 25156255.
59. Wang G, Lu X, Dey P, Deng P, Wu CC, Jiang S, Fang Z, Zhao K, Konaparthi R, Hua S, Zhang J, Li-Ning-Tapia EM, Kapoor A, Wu CJ, Patel NB, Guo Z, Ramamoorthy V, Tieu TN, Heffernan T, Zhao D, Shang X, Khadka S, Hou P, Hu B, Jin EJ, Yao W, Pan X, Ding Z, Shi Y, Li L, Chang Q, Troncoso P, Logothetis CJ, McArthur MJ, Chin L, Wang YA, DePinho RA. Targeting YAP-Dependent MDSC Infiltration Impairs Tumor

Progression. Cancer discovery. 2016;6(1):80-95. doi: 10.1158/2159-8290.CD-15-0224. PubMed PMID: 26701088; PMCID: PMC4707102.
60. Won H, Moreira D, Gao C, Duttagupta P, Zhao X, Manuel E, Diamond D, Yuan YC, Liu Z, Jones J, D'Apuzzo M, Pal S, Kortylewski M. TLR9 expression and secretion of LIF by prostate cancer cells stimulates accumulation and activity of polymorphonuclear MDSCs. Journal of leukocyte biology. 2017;102(2):423-36. doi: 10.1189/jlb.3MA1016-451RR. PubMed PMID: 28533357; PMCID: PMC5505743.
61. Lu X, Horner JW, Paul E, Shang X, Troncoso P, Deng P, Jiang S, Chang Q, Spring DJ, Sharma P, Zebala JA, Maeda DY, Wang YA, DePinho RA. Effective combinatorial immunotherapy for castration-resistant prostate cancer. Nature. 2017;543(7647):728-32. doi: 10.1038/nature21676. PubMed PMID: 28321130; PMCID: PMC5374023.
62. Yang L, Zhang Y. Tumor-associated macrophages: from basic research to clinical application. J Hematol Oncol. 2017;10(1):58. doi: 10.1186/s13045-017-0430-2. PubMed PMID: 28241846; PMCID: PMC5329931.
63. Gollapudi K, Galet C, Grogan T, Zhang H, Said JW, Huang J, Elashoff D, Freedland SJ, Rettig M, Aronson WJ. Association between tumor-associated macrophage infiltration, high grade prostate cancer, and biochemical recurrence after radical prostatectomy. Am J Cancer Res. 2013;3(5):523-9. PubMed PMID: 24224130; PMCID: PMC3816972.
64. Lanciotti M, Masieri L, Raspollini MR, Minervini A, Mari A, Comito G, Giannoni E, Carini M, Chiarugi P, Serni S. The role of M1 and M2 macrophages in prostate cancer in relation to extracapsular tumor extension and biochemical recurrence after radical prostatectomy. Biomed Res Int. 2014;2014:486798. doi: 10.1155/2014/486798. PubMed PMID: 24738060; PMCID: PMC3967497.
65. Gannon PO, Poisson AO, Delvoye N, Lapointe R, Mes-Masson AM, Saad F. Characterization of the intra-prostatic immune cell infiltration in androgen-deprived prostate cancer patients. Journal of immunological methods. 2009;348(1-2):9-17. Epub 2009/06/26. doi: 10.1016/j.jim.2009.06.004. PubMed PMID: 19552894.
66. Lissbrant IF, Stattin P, Wikstrom P, Damber JE, Egevad L, Bergh A. Tumor associated macrophages in human prostate cancer: relation to clinicopathological variables and survival. International journal of oncology. 2000;17(3):445-51. PubMed PMID: 10938382.
67. Nonomura N, Takayama H, Nakayama M, Nakai Y, Kawashima A, Mukai M, Nagahara A, Aozasa K, Tsujimura A. Infiltration of tumour-associated macrophages in prostate biopsy specimens is predictive of disease progression after hormonal therapy for prostate cancer. BJU international. 2011;107(12):1918-22. doi: 10.1111/j.1464-410X.2010.09804.x. PubMed PMID: 21044246.
68. Shimura S, Yang G, Ebara S, Wheeler TM, Frolov A, Thompson TC. Reduced infiltration of tumor-associated macrophages in human prostate cancer: association with cancer progression. Cancer research. 2000;60(20):5857-61. PubMed PMID: 11059783.

69. Wang Z, Xu L, Hu Y, Huang Y, Zhang Y, Zheng X, Wang S, Wang Y, Yu Y, Zhang M, Yuan K, Min W. miRNA let-7b modulates macrophage polarization and enhances tumor-associated macrophages to promote angiogenesis and mobility in prostate cancer. Scientific reports. 2016;6:25602. doi: 10.1038/srep25602. PubMed PMID: 27157642; PMCID: PMC4860600.
70. Escamilla J, Schokrpur S, Liu C, Priceman SJ, Moughon D, Jiang Z, Pouliot F, Magyar C, Sung JL, Xu J, Deng G, West BL, Bollag G, Fradet Y, Lacombe L, Jung ME, Huang J, Wu L. CSF1 receptor targeting in prostate cancer reverses macrophage-mediated resistance to androgen blockade therapy. Cancer research. 2015;75(6):950-62. doi: 10.1158/0008-5472.CAN-14-0992. PubMed PMID: 25736687; PMCID: PMC4359956.
71. Troy A, Davidson P, Atkinson C, Hart D. Phenotypic characterisation of the dendritic cell infiltrate in prostate cancer. The Journal of urology. 1998;160(1):214-9. PubMed PMID: 9628653.
72. Sciarra A, Lichtner M, Autran GA, Mastroianni C, Rossi R, Mengoni F, Cristini C, Gentilucci A, Vullo V, Di Silverio F. Characterization of circulating blood dendritic cell subsets DC123+ (lymphoid) and DC11C+ (myeloid) in prostate adenocarcinoma patients. The Prostate. 2007;67(1):1-7. doi: 10.1002/pros.20431. PubMed PMID: 17075798.
73. Aalamian-Matheis M, Chatta GS, Shurin MR, Huland E, Huland H, Shurin GV. Inhibition of dendritic cell generation and function by serum from prostate cancer patients: correlation with serum-free PSA. Adv Exp Med Biol. 2007;601:173-82. PubMed PMID: 17713004.
74. Liu Y, Saeter T, Vlatkovic L, Servoll E, Waaler G, Axcrona U, Giercksky KE, Nesland JM, Suo ZH, Axcrona K. Dendritic and lymphocytic cell infiltration in prostate carcinoma. Histol Histopathol. 2013;28(12):1621-8. doi: 10.14670/HH-28.1621. PubMed PMID: 23729368.
75. Tsou P, Katayama H, Ostrin EJ, Hanash SM. The Emerging Role of B Cells in Tumor Immunity. Cancer research. 2016;76(19):5597-601. doi: 10.1158/0008-5472.CAN-16-0431. PubMed PMID: 27634765.
76. Woo JR, Liss MA, Muldong MT, Palazzi K, Strasner A, Ammirante M, Varki N, Shabaik A, Howell S, Kane CJ, Karin M, Jamieson CA. Tumor infiltrating B-cells are increased in prostate cancer tissue. J Transl Med. 2014;12:30. doi: 10.1186/1479-5876-12-30. PubMed PMID: 24475900; PMCID: PMC3914187.
77. Dalgleish A, Featherstone P, Vlassov V, Rogosnitzky M. Rituximab for treating CD20+ prostate cancer with generalized lymphadenopathy: a case report and review of the literature. Invest New Drugs. 2014;32(5):1048-52. doi: 10.1007/s10637-014-0063-z. PubMed PMID: 24442368.
78. Ammirante M, Luo JL, Grivennikov S, Nedospasov S, Karin M. B-cell-derived lymphotoxin promotes castration-resistant prostate cancer. Nature. 2010;464(7286):302-5. doi: 10.1038/nature08782. PubMed PMID: 20220849; PMCID: PMC2866639.

79. Shalapour S, Font-Burgada J, Di Caro G, Zhong Z, Sanchez-Lopez E, Dhar D, Willimsky G, Ammirante M, Strasner A, Hansel DE, Jamieson C, Kane CJ, Klatte T, Birner P, Kenner L, Karin M. Immunosuppressive plasma cells impede T-cell-dependent immunogenic chemotherapy. Nature. 2015;521(7550):94-8. doi: 10.1038/nature14395. PubMed PMID: 25924065; PMCID: PMC4501632.
80. Krasnova Y, Putz EM, Smyth MJ, Souza-Fonseca-Guimaraes F. Bench to bedside: NK cells and control of metastasis. Clin Immunol. 2017;177:50-9. doi: 10.1016/j.clim.2015.10.001. PubMed PMID: 26476139.
81. Pasero C, Gravis G, Guerin M, Granjeaud S, Thomassin-Piana J, Rocchi P, Paciencia-Gros M, Poizat F, Bentobji M, Azario-Cheillan F, Walz J, Salem N, Brunelle S, Moretta A, Olive D. Inherent and Tumor-Driven Immune Tolerance in the Prostate Microenvironment Impairs Natural Killer Cell Antitumor Activity. Cancer research. 2016;76(8):2153-65. doi: 10.1158/0008-5472.CAN-15-1965. PubMed PMID: 27197252.
82. Marumo K, Ikeuchi K, Baba S, Ueno M, Tazaki H. Natural killer cell activity and recycling capacity of natural killer cells in patients with carcinoma of the prostate. Keio J Med. 1989;38(1):27-35. PubMed PMID: 2716216.
83. Lahat N, Alexander B, Levin DR, Moskovitz B. The relationship between clinical stage, natural killer activity and related immunological parameters in adenocarcinoma of the prostate. Cancer immunology, immunotherapy : CII. 1989;28(3):208-12. PubMed PMID: 2784355.
84. Kastelan M, Kraljic I, Tarle M. NK cell activity in treated prostate cancer patients as a probe for circulating tumor cells: hormone regulatory effects in vivo. The Prostate. 1992;21(2):111-20. PubMed PMID: 1384013.
85. Tarle M, Kraljic I, Kastelan M. Comparison between NK cell activity and prostate cancer stage and grade in untreated patients: correlation with tumor markers and hormonal serotest data. Urological research. 1993;21(1):17-21. PubMed PMID: 7681242.
86. Kastelan M, Kovacic K, Tarle R, Kraljic I, Tarle M. Analysis of NK cell activity, lymphocyte reactivity to mitogens and serotest PSA and TPS values in patients with primary and disseminated prostate cancer, PIN and BPH. Anticancer research. 1997;17(3B):1671-5. PubMed PMID: 9179216.
87. Koo KC, Shim DH, Yang CM, Lee SB, Kim SM, Shin TY, Kim KH, Yoon HG, Rha KH, Lee JM, Hong SJ. Reduction of the CD16(-)CD56bright NK cell subset precedes NK cell dysfunction in prostate cancer. PloS one. 2013;8(11):e78049. doi: 10.1371/journal.pone.0078049. PubMed PMID: 24223759; PMCID: PMC3817174.
88. Barkin J, Rodriguez-Suarez R, Betito K. Association between natural killer cell activity and prostate cancer: a pilot study. The Canadian journal of urology. 2017;24(2):8708-13. PubMed PMID: 28436356.
89. Maciel TT, Moura IC, Hermine O. The role of mast cells in cancers. F1000Prime Rep. 2015;7:09. doi: 10.12703/P7-09. PubMed PMID: 25705392; PMCID: PMC4311277.

90. Fleischmann A, Schlomm T, Kollermann J, Sekulic N, Huland H, Mirlacher M, Sauter G, Simon R, Erbersdobler A. Immunological microenvironment in prostate cancer: high mast cell densities are associated with favorable tumor characteristics and good prognosis. The Prostate. 2009;69(9):976-81. doi: 10.1002/pros.20948. PubMed PMID: 19274666.
91. Sari A, Serel TA, Candir O, Ozturk A, Kosar A. Mast cell variations in tumour tissue and with histopathological grading in specimens of prostatic adenocarcinoma. BJU international. 1999;84(7):851-3. PubMed PMID: 10532985.
92. Johansson A, Rudolfsson S, Hammarsten P, Halin S, Pietras K, Jones J, Stattin P, Egevad L, Granfors T, Wikstrom P, Bergh A. Mast cells are novel independent prognostic markers in prostate cancer and represent a target for therapy. The American journal of pathology. 2010;177(2):1031-41. doi: 10.2353/ajpath.2010.100070. PubMed PMID: 20616342; PMCID: PMC2913352.
93. Nonomura N, Takayama H, Nishimura K, Oka D, Nakai Y, Shiba M, Tsujimura A, Nakayama M, Aozasa K, Okuyama A. Decreased number of mast cells infiltrating into needle biopsy specimens leads to a better prognosis of prostate cancer. British journal of cancer. 2007;97(7):952-6. doi: 10.1038/sj.bjc.6603962. PubMed PMID: 17848955; PMCID: PMC2360404.
94. Pittoni P, Tripodo C, Piconese S, Mauri G, Parenza M, Rigoni A, Sangaletti S, Colombo MP. Mast cell targeting hampers prostate adenocarcinoma development but promotes the occurrence of highly malignant neuroendocrine cancers. Cancer research. 2011;71(18):5987-97. doi: 10.1158/0008-5472.CAN-11-1637. PubMed PMID: 21896641.
95. Coffelt SB, Wellenstein MD, de Visser KE. Neutrophils in cancer: neutral no more. Nature reviews Cancer. 2016;16(7):431-46. doi: 10.1038/nrc.2016.52. PubMed PMID: 27282249.
96. Sadeghi N, Badalato GM, Hruby G, Grann V, McKiernan JM. Does absolute neutrophil count predict high tumor grade in African-American men with prostate cancer? The Prostate. 2012;72(4):386-91. doi: 10.1002/pros.21440. PubMed PMID: 21681777.
97. Fujita K, Imamura R, Tanigawa G, Nakagawa M, Hayashi T, Kishimoto N, Hosomi M, Yamaguchi S. Low serum neutrophil count predicts a positive prostate biopsy. Prostate Cancer Prostatic Dis. 2012;15(4):386-90. doi: 10.1038/pcan.2012.27. PubMed PMID: 22777394.
98. Shafique K, Proctor MJ, McMillan DC, Qureshi K, Leung H, Morrison DS. Systemic inflammation and survival of patients with prostate cancer: evidence from the Glasgow Inflammation Outcome Study. Prostate Cancer Prostatic Dis. 2012;15(2):195-201. doi: 10.1038/pcan.2011.60. PubMed PMID: 22343838.
99. Sumbul AT, Sezer A, Abali H, Kose F, Gultepe I, Mertsoylu H, Muallaoglu S, Ozyilkan O. Neutrophil-to-lymphocyte ratio predicts PSA response, but not outcomes in patients with castration-resistant prostate cancer treated with docetaxel. Int Urol Nephrol. 2014;46(8):1531-5. doi: 10.1007/s11255-014-0664-7. PubMed PMID: 24526335.

100. Nuhn P, Vaghasia AM, Goyal J, Zhou XC, Carducci MA, Eisenberger MA, Antonarakis ES. Association of pretreatment neutrophil-to-lymphocyte ratio (NLR) and overall survival (OS) in patients with metastatic castration-resistant prostate cancer (mCRPC) treated with first-line docetaxel. BJU international. 2014;114(6b):E11-E7. doi: 10.1111/bju.12531. PubMed PMID: 24529213; PMCID: PMC4004702.
101. Sonpavde G, Pond GR, Armstrong AJ, Clarke SJ, Vardy JL, Templeton AJ, Wang SL, Paolini J, Chen I, Chow-Maneval E, Lechuga M, Smith MR, Michaelson MD. Prognostic impact of the neutrophil-to-lymphocyte ratio in men with metastatic castration-resistant prostate cancer. Clin Genitourin Cancer. 2014;12(5):317-24. doi: 10.1016/j.clgc.2014.03.005. PubMed PMID: 24806399.
102. Templeton AJ, Pezaro C, Omlin A, McNamara MG, Leibowitz-Amit R, Vera-Badillo FE, Attard G, de Bono JS, Tannock IF, Amir E. Simple prognostic score for metastatic castration-resistant prostate cancer with incorporation of neutrophil-to-lymphocyte ratio. Cancer. 2014;120(21):3346-52. doi: 10.1002/cncr.28890. PubMed PMID: 24995769.
103. Muthuswamy R, Corman JM, Dahl K, Chatta GS, Kalinski P. Functional reprogramming of human prostate cancer to promote local attraction of effector CD8(+) T cells. The Prostate. 2016;76(12):1095-105. doi: 10.1002/pros.23194. PubMed PMID: 27199259.
104. Jones E, Pu H, Kyprianou N. Targeting TGF-beta in prostate cancer: therapeutic possibilities during tumor progression. Expert Opin Ther Targets. 2009;13(2):227-34. doi: 10.1517/14728220802705696. PubMed PMID: 19236240.
105. Nakashima J, Tachibana M, Horiguchi Y, Oya M, Ohigashi T, Asakura H, Murai M. Serum interleukin 6 as a prognostic factor in patients with prostate cancer. Clinical cancer research : an official journal of the American Association for Cancer Research. 2000;6(7):2702-6. PubMed PMID: 10914713.
106. Aaltoma SH, Lipponen PK, Kosma VM. Inducible nitric oxide synthase (iNOS) expression and its prognostic value in prostate cancer. Anticancer research. 2001;21(4B):3101-6. PubMed PMID: 11712818.
107. Aaltomaa SH, Lipponen PK, Viitanen J, Kankkunen JP, Ala-Opas MY, Kosma VM. The prognostic value of inducible nitric oxide synthase in local prostate cancer. BJU international. 2000;86(3):234-9. PubMed PMID: 10930922.
108. Wang W, Bergh A, Damber JE. Cyclooxygenase-2 expression correlates with local chronic inflammation and tumor neovascularization in human prostate cancer. Clinical cancer research : an official journal of the American Association for Cancer Research. 2005;11(9):3250-6. doi: 10.1158/1078-0432.CCR-04-2405. PubMed PMID: 15867220.
109. Waghray A, Schober M, Feroze F, Yao F, Virgin J, Chen YQ. Identification of differentially expressed genes by serial analysis of gene expression in human prostate cancer. Cancer research. 2001;61(10):4283-6. PubMed PMID: 11358857.
110. Cunha AC, Weigle B, Kiessling A, Bachmann M, Rieber EP. Tissue-specificity of prostate specific antigens: comparative analysis of transcript levels in prostate and

non-prostatic tissues. Cancer letters. 2006;236(2):229-38. Epub 2005/07/28. doi: 10.1016/j.canlet.2005.05.021. PubMed PMID: 16046056.
111. Mercader M, Bodner BK, Moser MT, Kwon PS, Park ES, Manecke RG, Ellis TM, Wojcik EM, Yang D, Flanigan RC, Waters WB, Kast WM, Kwon ED. T cell infiltration of the prostate induced by androgen withdrawal in patients with prostate cancer. Proceedings of the National Academy of Sciences of the United States of America. 2001;98(25):14565-70. doi: 10.1073/pnas.251140998. PubMed PMID: 11734652; PMCID: PMC64722.
112. Roden AC, Moser MT, Tri SD, Mercader M, Kuntz SM, Dong H, Hurwitz AA, McKean DJ, Celis E, Leibovich BC, Allison JP, Kwon ED. Augmentation of T cell levels and responses induced by androgen deprivation. Journal of immunology. 2004;173(10):6098-108. PubMed PMID: 15528346.
113. Drake CG, Doody AD, Mihalyo MA, Huang CT, Kelleher E, Ravi S, Hipkiss EL, Flies DB, Kennedy EP, Long M, McGary PW, Coryell L, Nelson WG, Pardoll DM, Adler AJ. Androgen ablation mitigates tolerance to a prostate/prostate cancer-restricted antigen. Cancer cell. 2005;7(3):239-49. doi: 10.1016/j.ccr.2005.01.027. PubMed PMID: 15766662; PMCID: PMC2846360.
114. Olson BM, Gamat M, Seliski J, Sawicki T, Jeffery J, Ellis L, Drake CG, Weichert J, McNeel DG. Prostate cancer cells express more androgen receptor (AR) following androgen deprivation, improving recognition by AR-specific T cells. Cancer immunology research. 2017. doi: 10.1158/2326-6066.CIR-16-0390. PubMed PMID: 29051161.
115. Tang S, Moore ML, Grayson JM, Dubey P. Increased CD8+ T-cell function following castration and immunization is countered by parallel expansion of regulatory T cells. Cancer research. 2012;72(8):1975-85. doi: 10.1158/0008-5472.CAN-11-2499. PubMed PMID: 22374980; PMCID: PMC3690568.
116. Pu Y, Xu M, Liang Y, Yang K, Guo Y, Yang X, Fu YX. Androgen receptor antagonists compromise T cell response against prostate cancer leading to early tumor relapse. Sci Transl Med. 2016;8(333):333ra47. doi: 10.1126/scitranslmed.aad5659. PubMed PMID: 27053771.
117. Kantoff PW, Higano CS, Shore ND, Berger ER, Small EJ, Penson DF, Redfern CH, Ferrari AC, Dreicer R, Sims RB, Xu Y, Frohlich MW, Schellhammer PF, Investigators IS. Sipuleucel-T immunotherapy for castration-resistant prostate cancer. The New England journal of medicine. 2010;363(5):411-22. doi: 10.1056/NEJMoa1001294. PubMed PMID: 20818862.
118. Small EJ, Reese DM, Um B, Whisenant S, Dixon SC, Figg WD. Therapy of advanced prostate cancer with granulocyte macrophage colony-stimulating factor. Clinical cancer research : an official journal of the American Association for Cancer Research. 1999;5(7):1738-44. PubMed PMID: 10430077.
119. Rini BI, Weinberg V, Bok R, Small EJ. Prostate-specific antigen kinetics as a measure of the biologic effect of granulocyte-macrophage colony-stimulating factor in patients with serologic progression of prostate cancer. Journal of clinical oncology

: official journal of the American Society of Clinical Oncology. 2003;21(1):99-105. doi: 10.1200/JCO.2003.04.163. PubMed PMID: 12506177.
120. Wei XX, Chan S, Kwek S, Lewis J, Dao V, Zhang L, Cooperberg MR, Ryan CJ, Lin AM, Friedlander TW, Rini B, Kane C, Simko JP, Carroll PR, Small EJ, Fong L. Systemic GM-CSF Recruits Effector T Cells into the Tumor Microenvironment in Localized Prostate Cancer. Cancer immunology research. 2016;4(11):948-58. doi: 10.1158/2326-6066.CIR-16-0042. PubMed PMID: 27688020; PMCID: PMC5115633.
121. Small EJ, Fratesi P, Reese DM, Strang G, Laus R, Peshwa MV, Valone FH. Immunotherapy of hormone-refractory prostate cancer with antigen-loaded dendritic cells. Journal of clinical oncology : official journal of the American Society of Clinical Oncology. 2000;18(23):3894-903. doi: 10.1200/JCO.2000.18.23.3894. PubMed PMID: 11099318.
122. Burch PA, Breen JK, Buckner JC, Gastineau DA, Kaur JA, Laus RL, Padley DJ, Peshwa MV, Pitot HC, Richardson RL, Smits BJ, Sopapan P, Strang G, Valone FH, Vuk-Pavlovic S. Priming tissue-specific cellular immunity in a phase I trial of autologous dendritic cells for prostate cancer. Clinical cancer research : an official journal of the American Association for Cancer Research. 2000;6(6):2175-82. PubMed PMID: 10873066.
123. Burch PA, Croghan GA, Gastineau DA, Jones LA, Kaur JS, Kylstra JW, Richardson RL, Valone FH, Vuk-Pavlovic S. Immunotherapy (APC8015, Provenge) targeting prostatic acid phosphatase can induce durable remission of metastatic androgen-independent prostate cancer: a Phase 2 trial. The Prostate. 2004;60(3):197-204. doi: 10.1002/pros.20040. PubMed PMID: 15176049.
124. Schellhammer PF, Hershberg RM. Immunotherapy with autologous antigen presenting cells for the treatment of androgen independent prostate cancer. World journal of urology. 2005;23(1):47-9. doi: 10.1007/s00345-004-0475-z. PubMed PMID: 15647927.
125. Small EJ, Schellhammer PF, Higano CS, Redfern CH, Nemunaitis JJ, Valone FH, Verjee SS, Jones LA, Hershberg RM. Placebo-controlled phase III trial of immunologic therapy with sipuleucel-T (APC8015) in patients with metastatic, asymptomatic hormone refractory prostate cancer. Journal of clinical oncology : official journal of the American Society of Clinical Oncology. 2006;24(19):3089-94. doi: 10.1200/JCO.2005.04.5252. PubMed PMID: 16809734.
126. Schellhammer PF, Chodak G, Whitmore JB, Sims R, Frohlich MW, Kantoff PW. Lower baseline prostate-specific antigen is associated with a greater overall survival benefit from sipuleucel-T in the Immunotherapy for Prostate Adenocarcinoma Treatment (IMPACT) trial. Urology. 2013;81(6):1297-302. doi: 10.1016/j.urology.2013.01.061. PubMed PMID: 23582482.
127. Sheikh NA, Petrylak D, Kantoff PW, Dela Rosa C, Stewart FP, Kuan LY, Whitmore JB, Trager JB, Poehlein CH, Frohlich MW, Urdal DL. Sipuleucel-T immune parameters correlate with survival: an analysis of the randomized phase 3 clinical trials in men with castration-resistant prostate cancer. Cancer immunology,

immunotherapy : CII. 2013;62(1):137-47. doi: 10.1007/s00262-012-1317-2. PubMed PMID: 22865266; PMCID: PMC3541926.
128. GuhaThakurta D, Sheikh NA, Fan LQ, Kandadi H, Meagher TC, Hall SJ, Kantoff PW, Higano CS, Small EJ, Gardner TA, Bailey K, Vu T, DeVries T, Whitmore JB, Frohlich MW, Trager JB, Drake CG. Humoral Immune Response against Nontargeted Tumor Antigens after Treatment with Sipuleucel-T and Its Association with Improved Clinical Outcome. Clinical cancer research : an official journal of the American Association for Cancer Research. 2015;21(16):3619-30. doi: 10.1158/1078-0432.CCR-14-2334. PubMed PMID: 25649018; PMCID: PMC4868054.
129. Higano CS, Schellhammer PF, Small EJ, Burch PA, Nemunaitis J, Yuh L, Provost N, Frohlich MW. Integrated data from 2 randomized, double-blind, placebo-controlled, phase 3 trials of active cellular immunotherapy with sipuleucel-T in advanced prostate cancer. Cancer. 2009;115(16):3670-9. doi: 10.1002/cncr.24429. PubMed PMID: 19536890.
130. Fong L, Carroll P, Weinberg V, Chan S, Lewis J, Corman J, Amling CL, Stephenson RA, Simko J, Sheikh NA, Sims RB, Frohlich MW, Small EJ. Activated lymphocyte recruitment into the tumor microenvironment following preoperative sipuleucel-T for localized prostate cancer. Journal of the National Cancer Institute. 2014;106(11). doi: 10.1093/jnci/dju268. PubMed PMID: 25255802; PMCID: PMC4241888.
131. Sheikh N, Cham J, Zhang L, DeVries T, Letarte S, Pufnock J, Hamm D, Trager J, Fong L. Clonotypic Diversification of Intratumoral T Cells Following Sipuleucel-T Treatment in Prostate Cancer Subjects. Cancer research. 2016;76(13):3711-8. doi: 10.1158/0008-5472.CAN-15-3173. PubMed PMID: 27216195.
132. Graff JN, Drake CG, Beer TM. Complete biochemical (prostate-specific antigen) response to sipuleucel-T with enzalutamide in castration-resistant prostate cancer: a case report with implications for future research. Urology. 2013;81(2):381-3. doi: 10.1016/j.urology.2012.10.044. PubMed PMID: 23374810; PMCID: PMC4868050.
133. Small EJ, Lance RS, Gardner TA, Karsh LI, Fong L, McCoy C, DeVries T, Sheikh NA, GuhaThakurta D, Chang N, Redfern CH, Shore ND. A Randomized Phase II Trial of Sipuleucel-T with Concurrent versus Sequential Abiraterone Acetate plus Prednisone in Metastatic Castration-Resistant Prostate Cancer. Clinical cancer research : an official journal of the American Association for Cancer Research. 2015;21(17):3862-9. doi: 10.1158/1078-0432.CCR-15-0079. PubMed PMID: 25925891.
134. Antonarakis ES, Kibel AS, Yu EY, Karsh LI, Elfiky A, Shore ND, Vogelzang NJ, Corman JM, Millard FE, Maher JC, Chang NN, DeVries T, Sheikh NA, Drake CG, Investigators S. Sequencing of Sipuleucel-T and Androgen Deprivation Therapy in Men with Hormone-Sensitive Biochemically Recurrent Prostate Cancer: A Phase II Randomized Trial. Clinical cancer research : an official journal of the American

Association for Cancer Research. 2017;23(10):2451-9. doi: 10.1158/1078-0432.CCR-16-1780. PubMed PMID: 27836866.
135. Scholz M, Yep S, Chancey M, Kelly C, Chau K, Turner J, Lam R, Drake CG. Phase I clinical trial of sipuleucel-T combined with escalating doses of ipilimumab in progressive metastatic castrate-resistant prostate cancer. Immunotargets Ther. 2017;6:11-6. doi: 10.2147/ITT.S122497. PubMed PMID: 28361045; PMCID: PMC5365325.
136. Jha GG, Gupta S, Tagawa ST, Koopmeiners JS, Vivek S, Dudek AZ, Cooley SA, Blazar BR, Miller JS. A phase II randomized, double-blind study of sipuleucel-T followed by IDO pathway inhibitor, indoximod, or placebo in the treatment of patients with metastatic castration resistant prostate cancer (mCRPC). Journal of Clinical Oncology. 2017;35(15_suppl):3066-. doi: 10.1200/JCO.2017.35.15_suppl.3066.
137. Podrazil M, Horvath R, Becht E, Rozkova D, Bilkova P, Sochorova K, Hromadkova H, Kayserova J, Vavrova K, Lastovicka J, Vrabcova P, Kubackova K, Gasova Z, Jarolim L, Babjuk M, Spisek R, Bartunkova J, Fucikova J. Phase I/II clinical trial of dendritic-cell based immunotherapy (DCVAC/PCa) combined with chemotherapy in patients with metastatic, castration-resistant prostate cancer. Oncotarget. 2015;6(20):18192-205. doi: 10.18632/oncotarget.4145. PubMed PMID: 26078335; PMCID: PMC4627245.
138. Fucikova J, Podrazil M, Jarolim L, Bilkova P, Hensler M, Becht E, Gasova Z, Klouckova J, Kayserova J, Horvath R, Fialova A, Vavrova K, Sochorova K, Rozkova D, Spisek R, Bartunkova J. Phase I/II trial of dendritic cell-based active cellular immunotherapy with DCVAC/PCa in patients with rising PSA after primary prostatectomy or salvage radiotherapy for the treatment of prostate cancer. Cancer immunology, immunotherapy : CII. 2017. doi: 10.1007/s00262-017-2068-x. PubMed PMID: 28948333.
139. Kongsted P, Borch TH, Ellebaek E, Iversen TZ, Andersen R, Met O, Hansen M, Lindberg H, Sengelov L, Svane IM. Dendritic cell vaccination in combination with docetaxel for patients with metastatic castration-resistant prostate cancer: A randomized phase II study. Cytotherapy. 2017;19(4):500-13. doi: 10.1016/j.jcyt.2017.01.007. PubMed PMID: 28215654.
140. Murphy GP, Tjoa BA, Simmons SJ, Jarisch J, Bowes VA, Ragde H, Rogers M, Elgamal A, Kenny GM, Cobb OE, Ireton RC, Troychak MJ, Salgaller ML, Boynton AL. Infusion of dendritic cells pulsed with HLA-A2-specific prostate-specific membrane antigen peptides: a phase II prostate cancer vaccine trial involving patients with hormone-refractory metastatic disease. The Prostate. 1999;38(1):73-8. PubMed PMID: 9973112.
141. Barrou B, Benoit G, Ouldkaci M, Cussenot O, Salcedo M, Agrawal S, Massicard S, Bercovici N, Ericson ML, Thiounn N. Vaccination of prostatectomized prostate cancer patients in biochemical relapse, with autologous dendritic cells pulsed with recombinant human PSA. Cancer immunology, immunotherapy : CII. 2004;53(5):453-60. doi: 10.1007/s00262-003-0451-2. PubMed PMID: 14760510.

142. Prue RL, Vari F, Radford KJ, Tong H, Hardy MY, D'Rozario R, Waterhouse NJ, Rossetti T, Coleman R, Tracey C, Goossen H, Gounder V, Crosbie G, Hancock S, Diaz-Guilas S, Mainwaring P, Swindle P, Hart DN. A phase I clinical trial of CD1c (BDCA-1)+ dendritic cells pulsed with HLA-A*0201 peptides for immunotherapy of metastatic hormone refractory prostate cancer. Journal of immunotherapy. 2015;38(2):71-6. doi: 10.1097/CJI.0000000000000063. PubMed PMID: 25658616.
143. Scheid E, Major P, Bergeron A, Finn OJ, Salter RD, Eady R, Yassine-Diab B, Favre D, Peretz Y, Landry C, Hotte S, Mukherjee SD, Dekaban GA, Fink C, Foster PJ, Gaudet J, Gariepy J, Sekaly RP, Lacombe L, Fradet Y, Foley R. Tn-MUC1 DC Vaccination of Rhesus Macaques and a Phase I/II Trial in Patients with Nonmetastatic Castrate-Resistant Prostate Cancer. Cancer immunology research. 2016;4(10):881-92. doi: 10.1158/2326-6066.CIR-15-0189. PubMed PMID: 27604597; PMCID: PMC5331878.
144. Sonpavde G, McMannis JD, Bai Y, Seethammagari MR, Bull JMC, Hawkins V, Dancsak TK, Lapteva N, Levitt JM, Moseley A, Spencer DM, Slawin KM. Phase I trial of antigen-targeted autologous dendritic cell-based vaccine with in vivo activation of inducible CD40 for advanced prostate cancer. Cancer immunology, immunotherapy : CII. 2017. doi: 10.1007/s00262-017-2027-6. PubMed PMID: 28608115.
145. Dranoff G, Jaffee E, Lazenby A, Golumbek P, Levitsky H, Brose K, Jackson V, Hamada H, Pardoll D, Mulligan RC. Vaccination with irradiated tumor cells engineered to secrete murine granulocyte-macrophage colony-stimulating factor stimulates potent, specific, and long-lasting anti-tumor immunity. Proceedings of the National Academy of Sciences of the United States of America. 1993;90(8):3539-43. PubMed PMID: 8097319; PMCID: PMC46336.
146. Simons JW, Mikhak B, Chang JF, DeMarzo AM, Carducci MA, Lim M, Weber CE, Baccala AA, Goemann MA, Clift SM, Ando DG, Levitsky HI, Cohen LK, Sanda MG, Mulligan RC, Partin AW, Carter HB, Piantadosi S, Marshall FF, Nelson WG. Induction of immunity to prostate cancer antigens: results of a clinical trial of vaccination with irradiated autologous prostate tumor cells engineered to secrete granulocyte-macrophage colony-stimulating factor using ex vivo gene transfer. Cancer research. 1999;59(20):5160-8. PubMed PMID: 10537292.
147. Simons JW, Carducci MA, Mikhak B, Lim M, Biedrzycki B, Borellini F, Clift SM, Hege KM, Ando DG, Piantadosi S, Mulligan R, Nelson WG. Phase I/II trial of an allogeneic cellular immunotherapy in hormone-naive prostate cancer. Clinical cancer research : an official journal of the American Association for Cancer Research. 2006;12(11 Pt 1):3394-401. doi: 10.1158/1078-0432.CCR-06-0145. PubMed PMID: 16740763.
148. Small EJ, Sacks N, Nemunaitis J, Urba WJ, Dula E, Centeno AS, Nelson WG, Ando D, Howard C, Borellini F, Nguyen M, Hege K, Simons JW. Granulocyte macrophage colony-stimulating factor--secreting allogeneic cellular immunotherapy for hormone-refractory prostate cancer. Clinical cancer research : an official journal of the American Association for Cancer Research. 2007;13(13):3883-91. doi: 10.1158/1078-0432.CCR-06-2937. PubMed PMID: 17606721.

149. Higano CS, Corman JM, Smith DC, Centeno AS, Steidle CP, Gittleman M, Simons JW, Sacks N, Aimi J, Small EJ. Phase 1/2 dose-escalation study of a GM-CSF-secreting, allogeneic, cellular immunotherapy for metastatic hormone-refractory prostate cancer. Cancer. 2008;113(5):975-84. doi: 10.1002/cncr.23669. PubMed PMID: 18646045.
150. Wada S, Jackson CM, Yoshimura K, Yen HR, Getnet D, Harris TJ, Goldberg MV, Bruno TC, Grosso JF, Durham N, Netto GJ, Pardoll DM, Drake CG. Sequencing CTLA-4 blockade with cell-based immunotherapy for prostate cancer. J Transl Med. 2013;11:89. doi: 10.1186/1479-5876-11-89. PubMed PMID: 23557194; PMCID: PMC3666941.
151. van den Eertwegh AJ, Versluis J, van den Berg HP, Santegoets SJ, van Moorselaar RJ, van der Sluis TM, Gall HE, Harding TC, Jooss K, Lowy I, Pinedo HM, Scheper RJ, Stam AG, von Blomberg BM, de Gruijl TD, Hege K, Sacks N, Gerritsen WR. Combined immunotherapy with granulocyte-macrophage colony-stimulating factor-transduced allogeneic prostate cancer cells and ipilimumab in patients with metastatic castration-resistant prostate cancer: a phase 1 dose-escalation trial. The Lancet Oncology. 2012;13(5):509-17. doi: 10.1016/S1470-2045(12)70007-4. PubMed PMID: 22326922.
152. Santegoets SJ, Stam AG, Lougheed SM, Gall H, Jooss K, Sacks N, Hege K, Lowy I, Scheper RJ, Gerritsen WR, van den Eertwegh AJ, de Gruijl TD. Myeloid derived suppressor and dendritic cell subsets are related to clinical outcome in prostate cancer patients treated with prostate GVAX and ipilimumab. Journal for immunotherapy of cancer. 2014;2:31. doi: 10.1186/s40425-014-0031-3. PubMed PMID: 26196012; PMCID: PMC4507359.
153. van Dodewaard-de Jong JM, Santegoets SJ, van de Ven PM, Versluis J, Verheul HM, de Gruijl TD, Gerritsen WR, van den Eertwegh AJ. Improved efficacy of mitoxantrone in patients with castration-resistant prostate cancer after vaccination with GM-CSF-transduced allogeneic prostate cancer cells. Oncoimmunology. 2016;5(4):e1105431. doi: 10.1080/2162402X.2015.1105431. PubMed PMID: 27141390; PMCID: PMC4839338.
154. Wada S, Harris TJ, Tryggestad E, Yoshimura K, Zeng J, Yen HR, Getnet D, Grosso JF, Bruno TC, De Marzo AM, Netto GJ, Pardoll DM, DeWeese TL, Wong J, Drake CG. Combined treatment effects of radiation and immunotherapy: studies in an autochthonous prostate cancer model. International journal of radiation oncology, biology, physics. 2013;87(4):769-76. doi: 10.1016/j.ijrobp.2013.07.015. PubMed PMID: 24064321; PMCID: PMC4417352.
155. Michael A, Ball G, Quatan N, Wushishi F, Russell N, Whelan J, Chakraborty P, Leader D, Whelan M, Pandha H. Delayed disease progression after allogeneic cell vaccination in hormone-resistant prostate cancer and correlation with immunologic variables. Clinical cancer research : an official journal of the American Association for Cancer Research. 2005;11(12):4469-78. doi: 10.1158/1078-0432.CCR-04-2337. PubMed PMID: 15958632.

156. Mo L, Chen Q, Zhang X, Shi X, Wei L, Zheng D, Li H, Gao J, Li J, Hu Z. Depletion of regulatory T cells by anti-ICOS antibody enhances anti-tumor immunity of tumor cell vaccine in prostate cancer. Vaccine. 2017;35(43):5932-8. doi: 10.1016/j.vaccine.2017.08.093. PubMed PMID: 28923424.
157. Shi X, Zhang X, Li J, Zhao H, Mo L, Shi X, Hu Z, Gao J, Tan W. PD-1/PD-L1 blockade enhances the efficacy of SA-GM-CSF surface-modified tumor vaccine in prostate cancer. Cancer letters. 2017;406:27-35. doi: 10.1016/j.canlet.2017.07.029. PubMed PMID: 28797844.
158. Madan RA, Arlen PM, Mohebtash M, Hodge JW, Gulley JL. Prostvac-VF: a vector-based vaccine targeting PSA in prostate cancer. Expert opinion on investigational drugs. 2009;18(7):1001-11. doi: 10.1517/13543780902997928. PubMed PMID: 19548854; PMCID: PMC3449276.
159. Hodge JW, Sabzevari H, Yafal AG, Gritz L, Lorenz MG, Schlom J. A triad of costimulatory molecules synergize to amplify T-cell activation. Cancer research. 1999;59(22):5800-7. PubMed PMID: 10582702.
160. Eder JP, Kantoff PW, Roper K, Xu GX, Bubley GJ, Boyden J, Gritz L, Mazzara G, Oh WK, Arlen P, Tsang KY, Panicali D, Schlom J, Kufe DW. A phase I trial of a recombinant vaccinia virus expressing prostate-specific antigen in advanced prostate cancer. Clinical cancer research : an official journal of the American Association for Cancer Research. 2000;6(5):1632-8. PubMed PMID: 10815880.
161. Sanda MG, Smith DC, Charles LG, Hwang C, Pienta KJ, Schlom J, Milenic D, Panicali D, Montie JE. Recombinant vaccinia-PSA (PROSTVAC) can induce a prostate-specific immune response in androgen-modulated human prostate cancer. Urology. 1999;53(2):260-6. PubMed PMID: 9933036.
162. Gulley J, Chen AP, Dahut W, Arlen PM, Bastian A, Steinberg SM, Tsang K, Panicali D, Poole D, Schlom J, Michael Hamilton J. Phase I study of a vaccine using recombinant vaccinia virus expressing PSA (rV-PSA) in patients with metastatic androgen-independent prostate cancer. The Prostate. 2002;53(2):109-17. doi: 10.1002/pros.10130. PubMed PMID: 12242725.
163. DiPaola RS, Plante M, Kaufman H, Petrylak DP, Israeli R, Lattime E, Manson K, Schuetz T. A phase I trial of pox PSA vaccines (PROSTVAC-VF) with B7-1, ICAM-1, and LFA-3 co-stimulatory molecules (TRICOM) in patients with prostate cancer. J Transl Med. 2006;4:1. doi: 10.1186/1479-5876-4-1. PubMed PMID: 16390546; PMCID: PMC1360095.
164. Kaufman HL, Wang W, Manola J, DiPaola RS, Ko YJ, Sweeney C, Whiteside TL, Schlom J, Wilding G, Weiner LM. Phase II randomized study of vaccine treatment of advanced prostate cancer (E7897): a trial of the Eastern Cooperative Oncology Group. Journal of clinical oncology : official journal of the American Society of Clinical Oncology. 2004;22(11):2122-32. doi: 10.1200/JCO.2004.08.083. PubMed PMID: 15169798.
165. Kantoff PW, Schuetz TJ, Blumenstein BA, Glode LM, Bilhartz DL, Wyand M, Manson K, Panicali DL, Laus R, Schlom J, Dahut WL, Arlen PM, Gulley JL, Godfrey WR. Overall survival analysis of a phase II randomized controlled trial of a Poxviral-

based PSA-targeted immunotherapy in metastatic castration-resistant prostate cancer. Journal of clinical oncology : official journal of the American Society of Clinical Oncology. 2010;28(7):1099-105. doi: 10.1200/JCO.2009.25.0597. PubMed PMID: 20100959; PMCID: PMC2834462.
166. Mandl SJ, Rountree RB, Dela Cruz TB, Foy SP, Cote JJ, Gordon EJ, Trent E, Delcayre A, Franzusoff A. Elucidating immunologic mechanisms of PROSTVAC cancer immunotherapy. Journal for immunotherapy of cancer. 2014;2(1):34. doi: 10.1186/s40425-014-0034-0. PubMed PMID: 25328681; PMCID: PMC4201731.
167. Gulley JL, Giacchino JL, Breitmeyer JB, Franzusoff AJ, Panicali D, Schlom J, Kantoff PW. Prospect: A randomized double-blind phase 3 efficacy study of PROSTVAC-VF immunotherapy in men with asymptomatic/minimally symptomatic metastatic castration-resistant prostate cancer. Journal of Clinical Oncology. 2015;33(15_suppl):TPS5081-TPS. doi: 10.1200/jco.2015.33.15_suppl.tps5081.
168. Madan RA, Mohebtash M, Arlen PM, Vergati M, Rauckhorst M, Steinberg SM, Tsang KY, Poole DJ, Parnes HL, Wright JJ, Dahut WL, Schlom J, Gulley JL. Ipilimumab and a poxviral vaccine targeting prostate-specific antigen in metastatic castration-resistant prostate cancer: a phase 1 dose-escalation trial. The Lancet Oncology. 2012;13(5):501-8. doi: 10.1016/S1470-2045(12)70006-2. PubMed PMID: 22326924.
169. Singh H, Madan RA, Dahut WL, Strauss J, Rauckhorst M, McMahon S, Heery CR, Schlom J, Gulley JL. Combining active immunotherapy and immune checkpoint inhibitors in prostate cancer. Journal of Clinical Oncology. 2015;33(15_suppl):e14008-e. doi: 10.1200/jco.2015.33.15_suppl.e14008.
170. Jochems C, Tucker JA, Tsang KY, Madan RA, Dahut WL, Liewehr DJ, Steinberg SM, Gulley JL, Schlom J. A combination trial of vaccine plus ipilimumab in metastatic castration-resistant prostate cancer patients: immune correlates. Cancer immunology, immunotherapy : CII. 2014;63(4):407-18. doi: 10.1007/s00262-014-1524-0. PubMed PMID: 24514956.
171. Heery CR, Madan RA, Stein MN, Stadler WM, Di Paola RS, Rauckhorst M, Steinberg SM, Marte JL, Chen CC, Grenga I, Donahue RN, Jochems C, Dahut WL, Schlom J, Gulley JL. Samarium-153-EDTMP (Quadramet(R)) with or without vaccine in metastatic castration-resistant prostate cancer: A randomized Phase 2 trial. Oncotarget. 2016;7(42):69014-23. doi: 10.18632/oncotarget.10883. PubMed PMID: 27486817; PMCID: PMC5340090.
172. Kwilas AR, Ardiani A, Dirmeier U, Wottawah C, Schlom J, Hodge JW. A poxviral-based cancer vaccine the transcription factor twist inhibits primary tumor growth and metastases in a model of metastatic breast cancer and improves survival in a spontaneous prostate cancer model. Oncotarget. 2015;6(29):28194-210. doi: 10.18632/oncotarget.4442. PubMed PMID: 26317648; PMCID: PMC4695054.
173. Riabov V, Tretyakova I, Alexander RB, Pushko P, Klyushnenkova EN. Anti-tumor effect of the alphavirus-based virus-like particle vector expressing prostate-specific antigen in a HLA-DR transgenic mouse model of prostate cancer. Vaccine.

2015;33(41):5386-95. doi: 10.1016/j.vaccine.2015.08.062. PubMed PMID: 26319744; PMCID: PMC4581984.
174. Klyushnenkova EN, Kouiavskaia DV, Parkins CJ, Caposio P, Botto S, Alexander RB, Jarvis MA. A cytomegalovirus-based vaccine expressing a single tumor-specific CD8+ T-cell epitope delays tumor growth in a murine model of prostate cancer. Journal of immunotherapy. 2012;35(5):390-9. doi: 10.1097/CJI.0b013e3182585d50. PubMed PMID: 22576344; PMCID: PMC3366429.
175. Hubert RS, Vivanco I, Chen E, Rastegar S, Leong K, Mitchell SC, Madraswala R, Zhou Y, Kuo J, Raitano AB, Jakobovits A, Saffran DC, Afar DE. STEAP: a prostate-specific cell-surface antigen highly expressed in human prostate tumors. Proceedings of the National Academy of Sciences of the United States of America. 1999;96(25):14523-8. PubMed PMID: 10588738; PMCID: PMC24469.
176. Cappuccini F, Stribbling S, Pollock E, Hill AV, Redchenko I. Immunogenicity and efficacy of the novel cancer vaccine based on simian adenovirus and MVA vectors alone and in combination with PD-1 mAb in a mouse model of prostate cancer. Cancer immunology, immunotherapy : CII. 2016;65(6):701-13. doi: 10.1007/s00262-016-1831-8. PubMed PMID: 27052571; PMCID: PMC4880633.
177. Lubaroff DM, Konety BR, Link B, Gerstbrein J, Madsen T, Shannon M, Howard J, Paisley J, Boeglin D, Ratliff TL, Williams RD. Phase I clinical trial of an adenovirus/prostate-specific antigen vaccine for prostate cancer: safety and immunologic results. Clinical cancer research : an official journal of the American Association for Cancer Research. 2009;15(23):7375-80. doi: 10.1158/1078-0432.CCR-09-1910. PubMed PMID: 19920098; PMCID: PMC2787649.
178. Nesslinger NJ, Ng A, Tsang KY, Ferrara T, Schlom J, Gulley JL, Nelson BH. A viral vaccine encoding prostate-specific antigen induces antigen spreading to a common set of self-proteins in prostate cancer patients. Clinical cancer research : an official journal of the American Association for Cancer Research. 2010;16(15):4046-56. doi: 10.1158/1078-0432.CCR-10-0948. PubMed PMID: 20562209; PMCID: PMC2912964.
179. Ayala G, Satoh T, Li R, Shalev M, Gdor Y, Aguilar-Cordova E, Frolov A, Wheeler TM, Miles BJ, Rauen K, Teh BS, Butler EB, Thompson TC, Kadmon D. Biological response determinants in HSV-tk + ganciclovir gene therapy for prostate cancer. Mol Ther. 2006;13(4):716-28. doi: 10.1016/j.ymthe.2005.11.022. PubMed PMID: 16480930.
180. Teh BS, Ayala G, Aguilar L, Mai WY, Timme TL, Vlachaki MT, Miles B, Kadmon D, Wheeler T, Caillouet J, Davis M, Carpenter LS, Lu HH, Chiu JK, Woo SY, Thompson T, Aguilar-Cordova E, Butler EB. Phase I-II trial evaluating combined intensity-modulated radiotherapy and in situ gene therapy with or without hormonal therapy in treatment of prostate cancer-interim report on PSA response and biopsy data. International journal of radiation oncology, biology, physics. 2004;58(5):1520-9. doi: 10.1016/j.ijrobp.2003.09.083. PubMed PMID: 15050332.
181. Karan D. Formulation of the bivalent prostate cancer vaccine with surgifoam elicits antigen-specific effector T cells in PSA-transgenic mice. Vaccine.

2017;35(43):5794-8. doi: 10.1016/j.vaccine.2017.09.037. PubMed PMID: 28939158; PMCID: PMC5617798.
182. Lilleby W, Gaudernack G, Brunsvig PF, Vlatkovic L, Schulz M, Mills K, Hole KH, Inderberg EM. Phase I/IIa clinical trial of a novel hTERT peptide vaccine in men with metastatic hormone-naive prostate cancer. Cancer immunology, immunotherapy : CII. 2017;66(7):891-901. doi: 10.1007/s00262-017-1994-y. PubMed PMID: 28391357.
183. Huo W, Ye J, Liu R, Chen J, Li Q. Vaccination with a chaperone complex based on PSCA and GRP170 adjuvant enhances the CTL response and inhibits the tumor growth in mice. Vaccine. 2010;28(38):6333-7. doi: 10.1016/j.vaccine.2010.06.093. PubMed PMID: 20637304.
184. Nikitina EY, Desai SA, Zhao X, Song W, Luo AZ, Gangula RD, Slawin KM, Spencer DM. Versatile prostate cancer treatment with inducible caspase and interleukin-12. Cancer research. 2005;65(10):4309-19. doi: 10.1158/0008-5472.CAN-04-3119. PubMed PMID: 15899823.
185. Zhang S, Zeng G, Wilkes DS, Reed GE, McGarry RC, Eble JN, Cheng L. Dendritic cells transfected with interleukin-12 and pulsed with tumor extract inhibit growth of murine prostatic carcinoma in vivo. The Prostate. 2003;55(4):292-8. doi: 10.1002/pros.10246. PubMed PMID: 12712408.
186. Kramer G, Steiner GE, Sokol P, Handisurya A, Klingler HC, Maier U, Foldy M, Marberger M. Local intratumoral tumor necrosis factor-alpha and systemic IFN-alpha 2b in patients with locally advanced prostate cancer. J Interferon Cytokine Res. 2001;21(7):475-84. doi: 10.1089/10799900152434349. PubMed PMID: 11506741.
187. Noguchi M, Moriya F, Suekane S, Matsuoka K, Arai G, Matsueda S, Sasada T, Yamada A, Itoh K. Phase II study of personalized peptide vaccination for castration-resistant prostate cancer patients who failed in docetaxel-based chemotherapy. The Prostate. 2012;72(8):834-45. doi: 10.1002/pros.21485. PubMed PMID: 21932426.
188. Yoshimura K, Minami T, Nozawa M, Kimura T, Egawa S, Fujimoto H, Yamada A, Itoh K, Uemura H. A Phase 2 Randomized Controlled Trial of Personalized Peptide Vaccine Immunotherapy with Low-dose Dexamethasone Versus Dexamethasone Alone in Chemotherapy-naive Castration-resistant Prostate Cancer. European urology. 2016;70(1):35-41. doi: 10.1016/j.eururo.2015.12.050. PubMed PMID: 26782346.
189. Noguchi M, Moriya F, Koga N, Matsueda S, Sasada T, Yamada A, Kakuma T, Itoh K. A randomized phase II clinical trial of personalized peptide vaccination with metronomic low-dose cyclophosphamide in patients with metastatic castration-resistant prostate cancer. Cancer immunology, immunotherapy : CII. 2016;65(2):151-60. doi: 10.1007/s00262-015-1781-6. PubMed PMID: 26728480.
190. Becker JT, Olson BM, Johnson LE, Davies JG, Dunphy EJ, McNeel DG. DNA vaccine encoding prostatic acid phosphatase (PAP) elicits long-term T-cell responses in patients with recurrent prostate cancer. Journal of immunotherapy.

2010;33(6):639-47. doi: 10.1097/CJI.0b013e3181dda23e. PubMed PMID: 20551832; PMCID: PMC3045767.
191. McNeel DG, Dunphy EJ, Davies JG, Frye TP, Johnson LE, Staab MJ, Horvath DL, Straus J, Alberti D, Marnocha R, Liu G, Eickhoff JC, Wilding G. Safety and immunological efficacy of a DNA vaccine encoding prostatic acid phosphatase in patients with stage D0 prostate cancer. Journal of clinical oncology : official journal of the American Society of Clinical Oncology. 2009;27(25):4047-54. doi: 10.1200/JCO.2008.19.9968. PubMed PMID: 19636017; PMCID: PMC2734418.
192. McNeel DG, Becker JT, Eickhoff JC, Johnson LE, Bradley E, Pohlkamp I, Staab MJ, Liu G, Wilding G, Olson BM. Real-time immune monitoring to guide plasmid DNA vaccination schedule targeting prostatic acid phosphatase in patients with castration-resistant prostate cancer. Clinical cancer research : an official journal of the American Association for Cancer Research. 2014;20(14):3692-704. doi: 10.1158/1078-0432.CCR-14-0169. PubMed PMID: 24850844; PMCID: PMC4102643.
193. Pavlenko M, Roos AK, Lundqvist A, Palmborg A, Miller AM, Ozenci V, Bergman B, Egevad L, Hellstrom M, Kiessling R, Masucci G, Wersall P, Nilsson S, Pisa P. A phase I trial of DNA vaccination with a plasmid expressing prostate-specific antigen in patients with hormone-refractory prostate cancer. British journal of cancer. 2004;91(4):688-94. doi: 10.1038/sj.bjc.6602019. PubMed PMID: 15280930; PMCID: PMC2364780.
194. Muthumani K, Marnin L, Kudchodkar SB, Perales-Puchalt A, Choi H, Agarwal S, Scott VL, Reuschel EL, Zaidi FI, Duperret EK, Wise MC, Kraynyak KA, Ugen KE, Sardesai NY, Joseph Kim J, Weiner DB. Novel prostate cancer immunotherapy with a DNA-encoded anti-prostate-specific membrane antigen monoclonal antibody. Cancer immunology, immunotherapy : CII. 2017. doi: 10.1007/s00262-017-2042-7. PubMed PMID: 28819703.
195. Ahmad S, Casey G, Sweeney P, Tangney M, O'Sullivan GC. Prostate stem cell antigen DNA vaccination breaks tolerance to self-antigen and inhibits prostate cancer growth. Mol Ther. 2009;17(6):1101-8. doi: 10.1038/mt.2009.66. PubMed PMID: 19337234; PMCID: PMC2835175.
196. Garcia-Hernandez Mde L, Gray A, Hubby B, Klinger OJ, Kast WM. Prostate stem cell antigen vaccination induces a long-term protective immune response against prostate cancer in the absence of autoimmunity. Cancer research. 2008;68(3):861-9. doi: 10.1158/0008-5472.CAN-07-0445. PubMed PMID: 18245488.
197. Dong L, Zhang X, Ren J, Wu S, Yu T, Hou L, Fu L, Yi S, Yu C. Human prostate stem cell antigen and HSP70 fusion protein vaccine inhibits prostate stem cell antigen-expressing tumor growth in mice. Cancer biotherapy & radiopharmaceuticals. 2013;28(5):391-7. doi: 10.1089/cbr.2012.1357. PubMed PMID: 23701419.
198. Mai TJ, Ma R, Li Z, Bi SC. Construction of a fusion plasmid containing the PSCA gene and cytotoxic T-lymphocyte associated antigen-4 (CTLA-4) and its anti-tumor

effect in an animal model of prostate cancer. Braz J Med Biol Res. 2016;49(11):e5620. doi: 10.1590/1414-431X20165620. PubMed PMID: 27783810; PMCID: PMC5089234.
199. Ott PA, Hodi FS, Buchbinder EI. Inhibition of Immune Checkpoints and Vascular Endothelial Growth Factor as Combination Therapy for Metastatic Melanoma: An Overview of Rationale, Preclinical Evidence, and Initial Clinical Data. Frontiers in oncology. 2015;5:202. doi: 10.3389/fonc.2015.00202. PubMed PMID: 26442214; PMCID: PMC4585112.
200. Harper ME, Glynne-Jones E, Goddard L, Thurston VJ, Griffiths K. Vascular endothelial growth factor (VEGF) expression in prostatic tumours and its relationship to neuroendocrine cells. British journal of cancer. 1996;74(6):910-6. PubMed PMID: 8826857; PMCID: PMC2074752.
201. George DJ, Halabi S, Shepard TF, Vogelzang NJ, Hayes DF, Small EJ, Kantoff PW, Cancer, Leukemia Group B. Prognostic significance of plasma vascular endothelial growth factor levels in patients with hormone-refractory prostate cancer treated on Cancer and Leukemia Group B 9480. Clinical cancer research : an official journal of the American Association for Cancer Research. 2001;7(7):1932-6. PubMed PMID: 11448906.
202. Kelly WK, Halabi S, Carducci M, George D, Mahoney JF, Stadler WM, Morris M, Kantoff P, Monk JP, Kaplan E, Vogelzang NJ, Small EJ. Randomized, Double-Blind, Placebo-Controlled Phase III Trial Comparing Docetaxel and Prednisone With or Without Bevacizumab in Men With Metastatic Castration-Resistant Prostate Cancer: CALGB 90401. Journal of Clinical Oncology. 2012;30(13):1534-40. doi: 10.1200/jco.2011.39.4767. PubMed PMID: 22454414.
203. McKay RR, Zurita AJ, Werner L, Bruce JY, Carducci MA, Stein MN, Heath EI, Hussain A, Tran HT, Sweeney CJ, Ross RW, Kantoff PW, Slovin SF, Taplin ME. A Randomized Phase II Trial of Short-Course Androgen Deprivation Therapy With or Without Bevacizumab for Patients With Recurrent Prostate Cancer After Definitive Local Therapy. Journal of clinical oncology : official journal of the American Society of Clinical Oncology. 2016;34(16):1913-20. doi: 10.1200/JCO.2015.65.3154. PubMed PMID: 27044933; PMCID: PMC5321094.
204. Hwang C, Heath EI. Angiogenesis inhibitors in the treatment of prostate cancer. J Hematol Oncol. 2010;3:26. doi: 10.1186/1756-8722-3-26. PubMed PMID: 20678204; PMCID: PMC2922886.
205. Dahut WL, Madan RA, Karakunnel JJ, Adelberg D, Gulley JL, Turkbey IB, Chau CH, Spencer SD, Mulquin M, Wright J, Parnes HL, Steinberg SM, Choyke PL, Figg WD. Phase II clinical trial of cediranib in patients with metastatic castration-resistant prostate cancer. BJU international. 2013;111(8):1269-80. doi: 10.1111/j.1464-410X.2012.11667.x. PubMed PMID: 23419134; PMCID: PMC3660464.
206. Tannock IF, Fizazi K, Ivanov S, Karlsson CT, Flechon A, Skoneczna I, Orlandi F, Gravis G, Matveev V, Bavbek S, Gil T, Viana L, Aren O, Karyakin O, Elliott T, Birtle A, Magherini E, Hatteville L, Petrylak D, Tombal B, Rosenthal M, investigators V. Aflibercept versus placebo in combination with docetaxel and prednisone for

treatment of men with metastatic castration-resistant prostate cancer (VENICE): a phase 3, double-blind randomised trial. The Lancet Oncology. 2013;14(8):760-8. doi: 10.1016/S1470-2045(13)70184-0. PubMed PMID: 23742877.
207. Bjork P, Bjork A, Vogl T, Stenstrom M, Liberg D, Olsson A, Roth J, Ivars F, Leanderson T. Identification of human S100A9 as a novel target for treatment of autoimmune disease via binding to quinoline-3-carboxamides. PLoS biology. 2009;7(4):e97. doi: 10.1371/journal.pbio.1000097. PubMed PMID: 19402754; PMCID: PMC2671563 which is developing quinolines for commercial purposes. FI has a research grant from Active Biotech.
208. Hermani A, Hess J, De Servi B, Medunjanin S, Grobholz R, Trojan L, Angel P, Mayer D. Calcium-binding proteins S100A8 and S100A9 as novel diagnostic markers in human prostate cancer. Clinical cancer research : an official journal of the American Association for Cancer Research. 2005;11(14):5146-52. doi: 10.1158/1078-0432.CCR-05-0352. PubMed PMID: 16033829.
209. Cheng P, Corzo CA, Luetteke N, Yu B, Nagaraj S, Bui MM, Ortiz M, Nacken W, Sorg C, Vogl T, Roth J, Gabrilovich DI. Inhibition of dendritic cell differentiation and accumulation of myeloid-derived suppressor cells in cancer is regulated by S100A9 protein. The Journal of experimental medicine. 2008;205(10):2235-49. doi: 10.1084/jem.20080132. PubMed PMID: 18809714; PMCID: PMC2556797.
210. Sinha P, Okoro C, Foell D, Freeze HH, Ostrand-Rosenberg S, Srikrishna G. Proinflammatory S100 proteins regulate the accumulation of myeloid-derived suppressor cells. Journal of immunology. 2008;181(7):4666-75. PubMed PMID: 18802069; PMCID: PMC2810501.
211. Shen L, Sundstedt A, Ciesielski M, Miles KM, Celander M, Adelaiye R, Orillion A, Ciamporcero E, Ramakrishnan S, Ellis L, Fenstermaker R, Abrams SI, Eriksson H, Leanderson T, Olsson A, Pili R. Tasquinimod modulates suppressive myeloid cells and enhances cancer immunotherapies in murine models. Cancer immunology research. 2015;3(2):136-48. doi: 10.1158/2326-6066.CIR-14-0036. PubMed PMID: 25370534; PMCID: PMC4323929.
212. Bratt O, Haggman M, Ahlgren G, Nordle O, Bjork A, Damber JE. Open-label, clinical phase I studies of tasquinimod in patients with castration-resistant prostate cancer. British journal of cancer. 2009;101(8):1233-40. doi: 10.1038/sj.bjc.6605322. PubMed PMID: 19755981; PMCID: PMC2768463.
213. Pili R, Haggman M, Stadler WM, Gingrich JR, Assikis VJ, Bjork A, Nordle O, Forsberg G, Carducci MA, Armstrong AJ. Phase II randomized, double-blind, placebo-controlled study of tasquinimod in men with minimally symptomatic metastatic castrate-resistant prostate cancer. Journal of clinical oncology : official journal of the American Society of Clinical Oncology. 2011;29(30):4022-8. doi: 10.1200/JCO.2011.35.6295. PubMed PMID: 21931019.
214. Armstrong AJ, Haggman M, Stadler WM, Gingrich JR, Assikis V, Polikoff J, Damber JE, Belkoff L, Nordle O, Forsberg G, Carducci MA, Pili R. Long-term survival and biomarker correlates of tasquinimod efficacy in a multicenter randomized study of men with minimally symptomatic metastatic castration-resistant prostate cancer.

Clinical cancer research : an official journal of the American Association for Cancer Research. 2013;19(24):6891-901. doi: 10.1158/1078-0432.CCR-13-1581. PubMed PMID: 24255071; PMCID: PMC4251453.
215. Armstrong AJ, Kaboteh R, Carducci MA, Damber JE, Stadler WM, Hansen M, Edenbrandt L, Forsberg G, Nordle O, Pili R, Morris MJ. Assessment of the bone scan index in a randomized placebo-controlled trial of tasquinimod in men with metastatic castration-resistant prostate cancer (mCRPC). Urologic oncology. 2014;32(8):1308-16. doi: 10.1016/j.urolonc.2014.08.006. PubMed PMID: 25240761.
216. Mehta AR, Armstrong AJ. Tasquinimod in the treatment of castrate-resistant prostate cancer - current status and future prospects. Ther Adv Urol. 2016;8(1):9-18. doi: 10.1177/1756287215603558. PubMed PMID: 26834836; PMCID: PMC4707420.
217. Armstrong AJ, Humeniuk MS, Healy P, Szmulewitz R, Winters C, Kephart J, Harrison MR, Martinez E, Mundy K, Halabi S, George D. Phase Ib Trial of Cabazitaxel and Tasquinimod in Men With Heavily Pretreated Metastatic Castration Resistant Prostate Cancer (mCRPC): The CATCH Trial. The Prostate. 2017;77(4):385-95. doi: 10.1002/pros.23277. PubMed PMID: 27862097.
218. Jackson HJ, Rafiq S, Brentjens RJ. Driving CAR T-cells forward. Nat Rev Clin Oncol. 2016;13(6):370-83. doi: 10.1038/nrclinonc.2016.36. PubMed PMID: 27000958; PMCID: PMC5529102.
219. Gong MC, Latouche JB, Krause A, Heston WD, Bander NH, Sadelain M. Cancer patient T cells genetically targeted to prostate-specific membrane antigen specifically lyse prostate cancer cells and release cytokines in response to prostate-specific membrane antigen. Neoplasia. 1999;1(2):123-7. PubMed PMID: 10933046; PMCID: PMC1508130.
220. Ma Q, Safar M, Holmes E, Wang Y, Boynton AL, Junghans RP. Anti-prostate specific membrane antigen designer T cells for prostate cancer therapy. The Prostate. 2004;61(1):12-25. doi: 10.1002/pros.20073. PubMed PMID: 15287090.
221. Ma Q, Gomes EM, Lo AS, Junghans RP. Advanced generation anti-prostate specific membrane antigen designer T cells for prostate cancer immunotherapy. The Prostate. 2014;74(3):286-96. doi: 10.1002/pros.22749. PubMed PMID: 24174378.
222. Maher J, Brentjens RJ, Gunset G, Riviere I, Sadelain M. Human T-lymphocyte cytotoxicity and proliferation directed by a single chimeric TCRzeta /CD28 receptor. Nat Biotechnol. 2002;20(1):70-5. doi: 10.1038/nbt0102-70. PubMed PMID: 11753365.
223. Gade TP, Hassen W, Santos E, Gunset G, Saudemont A, Gong MC, Brentjens R, Zhong XS, Stephan M, Stefanski J, Lyddane C, Osborne JR, Buchanan IM, Hall SJ, Heston WD, Riviere I, Larson SM, Koutcher JA, Sadelain M. Targeted elimination of prostate cancer by genetically directed human T lymphocytes. Cancer research. 2005;65(19):9080-8. doi: 10.1158/0008-5472.CAN-05-0436. PubMed PMID: 16204083.

224. Zuccolotto G, Fracasso G, Merlo A, Montagner IM, Rondina M, Bobisse S, Figini M, Cingarlini S, Colombatti M, Zanovello P, Rosato A. PSMA-specific CAR-engineered T cells eradicate disseminated prostate cancer in preclinical models. PloS one. 2014;9(10):e109427. doi: 10.1371/journal.pone.0109427. PubMed PMID: 25279468; PMCID: PMC4184866.
225. Serganova I, Moroz E, Cohen I, Moroz M, Mane M, Zurita J, Shenker L, Ponomarev V, Blasberg R. Enhancement of PSMA-Directed CAR Adoptive Immunotherapy by PD-1/PD-L1 Blockade. Mol Ther Oncolytics. 2017;4:41-54. doi: 10.1016/j.omto.2016.11.005. PubMed PMID: 28345023; PMCID: PMC5363727.
226. Santoro SP, Kim S, Motz GT, Alatzoglou D, Li C, Irving M, Powell DJ, Jr., Coukos G. T cells bearing a chimeric antigen receptor against prostate-specific membrane antigen mediate vascular disruption and result in tumor regression. Cancer immunology research. 2015;3(1):68-84. doi: 10.1158/2326-6066.CIR-14-0192. PubMed PMID: 25358763; PMCID: PMC4289112.
227. Feldmann A, Arndt C, Bergmann R, Loff S, Cartellieri M, Bachmann D, Aliperta R, Hetzenecker M, Ludwig F, Albert S, Ziller-Walter P, Kegler A, Koristka S, Gartner S, Schmitz M, Ehninger A, Ehninger G, Pietzsch J, Steinbach J, Bachmann M. Retargeting of T lymphocytes to PSCA- or PSMA positive prostate cancer cells using the novel modular chimeric antigen receptor platform technology "UniCAR". Oncotarget. 2017;8(19):31368-85. doi: 10.18632/oncotarget.15572. PubMed PMID: 28404896; PMCID: PMC5458214.
228. Slovin SF, Wang X, Hullings M, Arauz G, Bartido S, Lewis JS, Schöder H, Zanzonico P, Scher HI, Sadelain M, Riviere I. Chimeric antigen receptor (CAR+) modified T cells targeting prostate-specific membrane antigen (PSMA) in patients (pts) with castrate metastatic prostate cancer (CMPC). Journal of Clinical Oncology. 2013;31(6_suppl):72-. doi: 10.1200/jco.2013.31.6_suppl.72. PubMed PMID: 28137105.
229. Slovin SF, Wang X, Borquez-Ojeda O, Stefanski J, Olszewska M, Taylor C, Bartido S, Scher HI, Sadelain M, Riviere I. Targeting castration resistant prostate cancer (CRPC) with autologous PSMA-directed CAR+ T cells. Journal of Clinical Oncology. 2012;30(15_suppl):TPS4700-TPS. doi: 10.1200/jco.2012.30.15_suppl.tps4700.
230. Junghans RP, Ma Q, Rathore R, Davies R, Bais A, Gomes E, Harvey R, Cohen SI. Abstract C13: Phase I trial of anti-PSMA designer T cells in advanced prostate cancer. Cancer research. 2012;72(4 Supplement):C13-C. doi: 10.1158/1538-7445.prca2012-c13.
231. Junghans RP, Ma Q, Rathore R, Gomes EM, Bais AJ, Lo AS, Abedi M, Davies RA, Cabral HJ, Al-Homsi AS, Cohen SI. Phase I Trial of Anti-PSMA Designer CAR-T Cells in Prostate Cancer: Possible Role for Interacting Interleukin 2-T Cell Pharmacodynamics as a Determinant of Clinical Response. The Prostate. 2016;76(14):1257-70. doi: 10.1002/pros.23214. PubMed PMID: 27324746.
232. Morgenroth A, Cartellieri M, Schmitz M, Gunes S, Weigle B, Bachmann M, Abken H, Rieber EP, Temme A. Targeting of tumor cells expressing the prostate stem

cell antigen (PSCA) using genetically engineered T-cells. The Prostate. 2007;67(10):1121-31. doi: 10.1002/pros.20608. PubMed PMID: 17492652.
233. Hillerdal V, Ramachandran M, Leja J, Essand M. Systemic treatment with CAR-engineered T cells against PSCA delays subcutaneous tumor growth and prolongs survival of mice. BMC cancer. 2014;14:30. doi: 10.1186/1471-2407-14-30. PubMed PMID: 24438073; PMCID: PMC3899402.
234. Abate-Daga D, Lagisetty KH, Tran E, Zheng Z, Gattinoni L, Yu Z, Burns WR, Miermont AM, Teper Y, Rudloff U, Restifo NP, Feldman SA, Rosenberg SA, Morgan RA. A novel chimeric antigen receptor against prostate stem cell antigen mediates tumor destruction in a humanized mouse model of pancreatic cancer. Hum Gene Ther. 2014;25(12):1003-12. doi: 10.1089/hum.2013.209. PubMed PMID: 24694017; PMCID: PMC4270113.
235. Kloss CC, Condomines M, Cartellieri M, Bachmann M, Sadelain M. Combinatorial antigen recognition with balanced signaling promotes selective tumor eradication by engineered T cells. Nat Biotechnol. 2013;31(1):71-5. doi: 10.1038/nbt.2459. PubMed PMID: 23242161; PMCID: PMC5505184.
236. Pinthus JH, Waks T, Kaufman-Francis K, Schindler DG, Harmelin A, Kanety H, Ramon J, Eshhar Z. Immuno-gene therapy of established prostate tumors using chimeric receptor-redirected human lymphocytes. Cancer research. 2003;63(10):2470-6. PubMed PMID: 12750268.
237. Pinthus JH, Waks T, Malina V, Kaufman-Francis K, Harmelin A, Aizenberg I, Kanety H, Ramon J, Eshhar Z. Adoptive immunotherapy of prostate cancer bone lesions using redirected effector lymphocytes. J Clin Invest. 2004;114(12):1774-81. doi: 10.1172/JCI22284. PubMed PMID: 15599402; PMCID: PMC535069.
238. Hillerdal V, Nilsson B, Carlsson B, Eriksson F, Essand M. T cells engineered with a T cell receptor against the prostate antigen TARP specifically kill HLA-A2+ prostate and breast cancer cells. Proceedings of the National Academy of Sciences of the United States of America. 2012;109(39):15877-81. doi: 10.1073/pnas.1209042109. PubMed PMID: 23019373; PMCID: PMC3465394.
239. Liu W, Han W, Zhou L, Guo Y. MP84-15 PREVENT METASTASIS BY DOUBLE CHIMERIC ANTIGEN RECEPTOR T CELLS TARGETING CIRCULATING CANCER CELLS FOR PROSTATE CANCER TREATMENT. The Journal of urology.195(4):e1095. doi: 10.1016/j.juro.2016.02.2239.
240. Buhler P, Wolf P, Gierschner D, Schaber I, Katzenwadel A, Schultze-Seemann W, Wetterauer U, Tacke M, Swamy M, Schamel WW, Elsasser-Beile U. A bispecific diabody directed against prostate-specific membrane antigen and CD3 induces T-cell mediated lysis of prostate cancer cells. Cancer immunology, immunotherapy : CII. 2008;57(1):43-52. doi: 10.1007/s00262-007-0348-6. PubMed PMID: 17579857; PMCID: PMC2755730.
241. Buhler P, Molnar E, Dopfer EP, Wolf P, Gierschner D, Wetterauer U, Schamel WW, Elsasser-Beile U. Target-dependent T-cell activation by coligation with a PSMA x CD3 diabody induces lysis of prostate cancer cells. Journal of immunotherapy.

2009;32(6):565-73. doi: 10.1097/CJI.0b013e3181a697eb. PubMed PMID: 19483653.
242. Fortmuller K, Alt K, Gierschner D, Wolf P, Baum V, Freudenberg N, Wetterauer U, Elsasser-Beile U, Buhler P. Effective targeting of prostate cancer by lymphocytes redirected by a PSMA x CD3 bispecific single-chain diabody. The Prostate. 2011;71(6):588-96. doi: 10.1002/pros.21274. PubMed PMID: 20945402.
243. Friedrich M, Raum T, Lutterbuese R, Voelkel M, Deegen P, Rau D, Kischel R, Hoffmann P, Brandl C, Schuhmacher J, Mueller P, Finnern R, Fuergut M, Zopf D, Slootstra JW, Baeuerle PA, Rattel B, Kufer P. Regression of human prostate cancer xenografts in mice by AMG 212/BAY2010112, a novel PSMA/CD3-Bispecific BiTE antibody cross-reactive with non-human primate antigens. Molecular cancer therapeutics. 2012;11(12):2664-73. doi: 10.1158/1535-7163.MCT-12-0042. PubMed PMID: 23041545.
244. Baum V, Buhler P, Gierschner D, Herchenbach D, Fiala GJ, Schamel WW, Wolf P, Elsasser-Beile U. Antitumor activities of PSMAxCD3 diabodies by redirected T-cell lysis of prostate cancer cells. Immunotherapy. 2013;5(1):27-38. doi: 10.2217/imt.12.136. PubMed PMID: 23256796.
245. Arndt C, Feldmann A, Koristka S, Cartellieri M, Dimmel M, Ehninger A, Ehninger G, Bachmann M. Simultaneous targeting of prostate stem cell antigen and prostate-specific membrane antigen improves the killing of prostate cancer cells using a novel modular T cell-retargeting system. The Prostate. 2014;74(13):1335-46. doi: 10.1002/pros.22850. PubMed PMID: 25053443.
246. Hernandez-Hoyos G, Sewell T, Bader R, Bannink J, Chenault RA, Daugherty M, Dasovich M, Fang H, Gottschalk R, Kumer J, Miller RE, Ravikumar P, Wiens J, Algate PA, Bienvenue D, McMahan CJ, Natarajan SK, Gross JA, Blankenship JW. MOR209/ES414, a Novel Bispecific Antibody Targeting PSMA for the Treatment of Metastatic Castration-Resistant Prostate Cancer. Molecular cancer therapeutics. 2016;15(9):2155-65. doi: 10.1158/1535-7163.MCT-15-0242. PubMed PMID: 27406985.
247. Feldmann A, Stamova S, Bippes CC, Bartsch H, Wehner R, Schmitz M, Temme A, Cartellieri M, Bachmann M. Retargeting of T cells to prostate stem cell antigen expressing tumor cells: comparison of different antibody formats. The Prostate. 2011;71(9):998-1011. doi: 10.1002/pros.21315. PubMed PMID: 21541976.
248. Feldmann A, Arndt C, Topfer K, Stamova S, Krone F, Cartellieri M, Koristka S, Michalk I, Lindemann D, Schmitz M, Temme A, Bornhauser M, Ehninger G, Bachmann M. Novel humanized and highly efficient bispecific antibodies mediate killing of prostate stem cell antigen-expressing tumor cells by CD8+ and CD4+ T cells. Journal of immunology. 2012;189(6):3249-59. doi: 10.4049/jimmunol.1200341. PubMed PMID: 22875801.
249. Arndt C, Feldmann A, Topfer K, Koristka S, Cartellieri M, Temme A, Ehninger A, Ehninger G, Bachmann M. Redirection of CD4+ and CD8+ T lymphocytes via a novel antibody-based modular targeting system triggers efficient killing of PSCA+

prostate tumor cells. The Prostate. 2014;74(13):1347-58. doi: 10.1002/pros.22851. PubMed PMID: 25053504.
250. Davol PA, Smith JA, Kouttab N, Elfenbein GJ, Lum LG. Anti-CD3 x anti-HER2 bispecific antibody effectively redirects armed T cells to inhibit tumor development and growth in hormone-refractory prostate cancer-bearing severe combined immunodeficient beige mice. Clin Prostate Cancer. 2004;3(2):112-21. PubMed PMID: 15479495.
251. Grabert RC, Cousens LP, Smith JA, Olson S, Gall J, Young WB, Davol PA, Lum LG. Human T cells armed with Her2/neu bispecific antibodies divide, are cytotoxic, and secrete cytokines with repeated stimulation. Clinical cancer research : an official journal of the American Association for Cancer Research. 2006;12(2):569-76. doi: 10.1158/1078-0432.CCR-05-2005. PubMed PMID: 16428502.
252. Lum HE, Miller M, Davol PA, Grabert RC, Davis JB, Lum LG. Preclinical studies comparing different bispecific antibodies for redirecting T cell cytotoxicity to extracellular antigens on prostate carcinomas. Anticancer research. 2005;25(1A):43-52. PubMed PMID: 15816517.
253. Vaishampayan U, Thakur A, Rathore R, Kouttab N, Lum LG. Phase I Study of Anti-CD3 x Anti-Her2 Bispecific Antibody in Metastatic Castrate Resistant Prostate Cancer Patients. Prostate Cancer. 2015;2015:285193. doi: 10.1155/2015/285193. PubMed PMID: 25802762; PMCID: PMC4352947.
254. Galluzzi L, Buque A, Kepp O, Zitvogel L, Kroemer G. Immunogenic cell death in cancer and infectious disease. Nature reviews Immunology. 2017;17(2):97-111. doi: 10.1038/nri.2016.107. PubMed PMID: 27748397.
255. Hodge JW, Garnett CT, Farsaci B, Palena C, Tsang KY, Ferrone S, Gameiro SR. Chemotherapy-induced immunogenic modulation of tumor cells enhances killing by cytotoxic T lymphocytes and is distinct from immunogenic cell death. International journal of cancer Journal international du cancer. 2013;133(3):624-36. doi: 10.1002/ijc.28070. PubMed PMID: 23364915; PMCID: PMC3663913.
256. Bezu L, Gomes-de-Silva LC, Dewitte H, Breckpot K, Fucikova J, Spisek R, Galluzzi L, Kepp O, Kroemer G. Combinatorial strategies for the induction of immunogenic cell death. Front Immunol. 2015;6:187. doi: 10.3389/fimmu.2015.00187. PubMed PMID: 25964783; PMCID: PMC4408862.
257. Kodumudi KN, Woan K, Gilvary DL, Sahakian E, Wei S, Djeu JY. A novel chemoimmunomodulating property of docetaxel: suppression of myeloid-derived suppressor cells in tumor bearers. Clinical cancer research : an official journal of the American Association for Cancer Research. 2010;16(18):4583-94. doi: 10.1158/1078-0432.CCR-10-0733. PubMed PMID: 20702612; PMCID: PMC3874864.
258. Qian DZ, Rademacher BL, Pittsenbarger J, Huang CY, Myrthue A, Higano CS, Garzotto M, Nelson PS, Beer TM. CCL2 is induced by chemotherapy and protects prostate cancer cells from docetaxel-induced cytotoxicity. The Prostate. 2010;70(4):433-42. doi: 10.1002/pros.21077. PubMed PMID: 19866475; PMCID: PMC2931415.

259. Gameiro SR, Jammeh ML, Wattenberg MM, Tsang KY, Ferrone S, Hodge JW. Radiation-induced immunogenic modulation of tumor enhances antigen processing and calreticulin exposure, resulting in enhanced T-cell killing. Oncotarget. 2014;5(2):403-16. doi: 10.18632/oncotarget.1719. PubMed PMID: 24480782; PMCID: PMC3964216.
260. Rozkova D, Tiserova H, Fucikova J, Last'ovicka J, Podrazil M, Ulcova H, Budinsky V, Prausova J, Linke Z, Minarik I, Sediva A, Spisek R, Bartunkova J. FOCUS on FOCIS: combined chemo-immunotherapy for the treatment of hormone-refractory metastatic prostate cancer. Clin Immunol. 2009;131(1):1-10. doi: 10.1016/j.clim.2009.01.001. PubMed PMID: 19201656.
261. Suzuki E, Kapoor V, Jassar AS, Kaiser LR, Albelda SM. Gemcitabine selectively eliminates splenic Gr-1+/CD11b+ myeloid suppressor cells in tumor-bearing animals and enhances antitumor immune activity. Clinical cancer research : an official journal of the American Association for Cancer Research. 2005;11(18):6713-21. doi: 10.1158/1078-0432.CCR-05-0883. PubMed PMID: 16166452.
262. Le HK, Graham L, Cha E, Morales JK, Manjili MH, Bear HD. Gemcitabine directly inhibits myeloid derived suppressor cells in BALB/c mice bearing 4T1 mammary carcinoma and augments expansion of T cells from tumor-bearing mice. Int Immunopharmacol. 2009;9(7-8):900-9. doi: 10.1016/j.intimp.2009.03.015. PubMed PMID: 19336265.
263. Buchbinder EI, Desai A. CTLA-4 and PD-1 Pathways: Similarities, Differences, and Implications of Their Inhibition. Am J Clin Oncol. 2016;39(1):98-106. doi: 10.1097/COC.0000000000000239. PubMed PMID: 26558876; PMCID: PMC4892769.
264. Kwon ED, Hurwitz AA, Foster BA, Madias C, Feldhaus AL, Greenberg NM, Burg MB, Allison JP. Manipulation of T cell costimulatory and inhibitory signals for immunotherapy of prostate cancer. Proceedings of the National Academy of Sciences of the United States of America. 1997;94(15):8099-103. PubMed PMID: 9223321; PMCID: PMC21563.
265. Small EJ, Tchekmedyian NS, Rini BI, Fong L, Lowy I, Allison JP. A pilot trial of CTLA-4 blockade with human anti-CTLA-4 in patients with hormone-refractory prostate cancer. Clinical cancer research : an official journal of the American Association for Cancer Research. 2007;13(6):1810-5. doi: 10.1158/1078-0432.CCR-06-2318. PubMed PMID: 17363537.
266. Fong L, Kwek SS, O'Brien S, Kavanagh B, McNeel DG, Weinberg V, Lin AM, Rosenberg J, Ryan CJ, Rini BI, Small EJ. Potentiating endogenous antitumor immunity to prostate cancer through combination immunotherapy with CTLA4 blockade and GM-CSF. Cancer research. 2009;69(2):609-15. doi: 10.1158/0008-5472.CAN-08-3529. PubMed PMID: 19147575.
267. Kwek SS, Dao V, Roy R, Hou Y, Alajajian D, Simko JP, Small EJ, Fong L. Diversity of antigen-specific responses induced in vivo with CTLA-4 blockade in prostate cancer patients. Journal of immunology. 2012;189(7):3759-66. doi: 10.4049/jimmunol.1201529. PubMed PMID: 22956585; PMCID: PMC3448828.

268. Cha E, Klinger M, Hou Y, Cummings C, Ribas A, Faham M, Fong L. Improved survival with T cell clonotype stability after anti-CTLA-4 treatment in cancer patients. Sci Transl Med. 2014;6(238):238ra70. doi: 10.1126/scitranslmed.3008211. PubMed PMID: 24871131; PMCID: PMC4558099.
269. Slovin SF, Higano CS, Hamid O, Tejwani S, Harzstark A, Alumkal JJ, Scher HI, Chin K, Gagnier P, McHenry MB, Beer TM. Ipilimumab alone or in combination with radiotherapy in metastatic castration-resistant prostate cancer: results from an open-label, multicenter phase I/II study. Annals of oncology : official journal of the European Society for Medical Oncology / ESMO. 2013;24(7):1813-21. doi: 10.1093/annonc/mdt107. PubMed PMID: 23535954; PMCID: PMC3707423.
270. Kwon ED, Drake CG, Scher HI, Fizazi K, Bossi A, van den Eertwegh AJ, Krainer M, Houede N, Santos R, Mahammedi H, Ng S, Maio M, Franke FA, Sundar S, Agarwal N, Bergman AM, Ciuleanu TE, Korbenfeld E, Sengelov L, Hansen S, Logothetis C, Beer TM, McHenry MB, Gagnier P, Liu D, Gerritsen WR, Investigators CA. Ipilimumab versus placebo after radiotherapy in patients with metastatic castration-resistant prostate cancer that had progressed after docetaxel chemotherapy (CA184-043): a multicentre, randomised, double-blind, phase 3 trial. The Lancet Oncology. 2014;15(7):700-12. doi: 10.1016/S1470-2045(14)70189-5. PubMed PMID: 24831977; PMCID: PMC4418935.
271. Beer TM, Kwon ED, Drake CG, Fizazi K, Logothetis C, Gravis G, Ganju V, Polikoff J, Saad F, Humanski P, Piulats JM, Gonzalez Mella P, Ng SS, Jaeger D, Parnis FX, Franke FA, Puente J, Carvajal R, Sengelov L, McHenry MB, Varma A, van den Eertwegh AJ, Gerritsen W. Randomized, Double-Blind, Phase III Trial of Ipilimumab Versus Placebo in Asymptomatic or Minimally Symptomatic Patients With Metastatic Chemotherapy-Naive Castration-Resistant Prostate Cancer. Journal of clinical oncology : official journal of the American Society of Clinical Oncology. 2017;35(1):40-7. doi: 10.1200/JCO.2016.69.1584. PubMed PMID: 28034081.
272. Graff JN, Puri S, Bifulco CB, Fox BA, Beer TM. Sustained complete response to CTLA-4 blockade in a patient with metastatic, castration-resistant prostate cancer. Cancer immunology research. 2014;2(5):399-403. doi: 10.1158/2326-6066.CIR-13-0193. PubMed PMID: 24795352; PMCID: PMC4418943.
273. Cabel L, Loir E, Gravis G, Lavaud P, Massard C, Albiges L, Baciarello G, Loriot Y, Fizazi K. Long-term complete remission with Ipilimumab in metastatic castrate-resistant prostate cancer: case report of two patients. Journal for immunotherapy of cancer. 2017;5:31. doi: 10.1186/s40425-017-0232-7. PubMed PMID: 28428880; PMCID: PMC5394619.
274. Hurwitz AA, Foster BA, Kwon ED, Truong T, Choi EM, Greenberg NM, Burg MB, Allison JP. Combination immunotherapy of primary prostate cancer in a transgenic mouse model using CTLA-4 blockade. Cancer research. 2000;60(9):2444-8. PubMed PMID: 10811122.
275. de Gruijl T, Santegoets S, Stam A, Lougheed S, Jooss K, Sacks N, Harding T, Hege K, Gerritsen W, van den Eertwegh A. S48. Biomarker development for ipilimumab and prostate GVAX treatment. Journal for immunotherapy of cancer.

2014;2(Suppl 2):I11-I. doi: 10.1186/2051-1426-2-S2-I11. PubMed PMID: PMC4072253.
276. McNeel DG, Smith HA, Eickhoff JC, Lang JM, Staab MJ, Wilding G, Liu G. Phase I trial of tremelimumab in combination with short-term androgen deprivation in patients with PSA-recurrent prostate cancer. Cancer immunology, immunotherapy : CII. 2012;61(7):1137-47. doi: 10.1007/s00262-011-1193-1. PubMed PMID: 22210552; PMCID: PMC3349783.
277. Autio KA, Eastham JA, Danila DC, Slovin SF, Morris MJ, Abida W, Laudone VP, Touijer KA, Gopalan A, Wong P, Curley T, Dayan ES, Bellomo LP, Scardino PT, Scher HI. A phase II study combining ipilimumab and degarelix with or without radical prostatectomy (RP) in men with newly diagnosed metastatic noncastration prostate cancer (mNCPC) or biochemically recurrent (BR) NCPC. Journal of Clinical Oncology. 2017;35(6_suppl):203-. doi: 10.1200/JCO.2017.35.6_suppl.203.
278. Aparicio A, Sun J, Tang DN, Arap W, Araujo J, Corn P, Tannir N, Wang X, Siefker-Radtke A, Sharma P. Abstract 5368: A phase II study of ipilumimab plus androgen deprivation therapy in castration-sensitive prostate carcinoma. Cancer research. 2012;72(8 Supplement):5368-. doi: 10.1158/1538-7445.am2012-5368.
279. Kavanagh B, O'Brien S, Lee D, Hou Y, Weinberg V, Rini B, Allison JP, Small EJ, Fong L. CTLA4 blockade expands FoxP3+ regulatory and activated effector CD4+ T cells in a dose-dependent fashion. Blood. 2008;112(4):1175-83. doi: 10.1182/blood-2007-11-125435. PubMed PMID: 18523152; PMCID: PMC2515138.
280. Hirschhorn-Cymerman D, Rizzuto GA, Merghoub T, Cohen AD, Avogadri F, Lesokhin AM, Weinberg AD, Wolchok JD, Houghton AN. OX40 engagement and chemotherapy combination provides potent antitumor immunity with concomitant regulatory T cell apoptosis. The Journal of experimental medicine. 2009;206(5):1103-16. doi: 10.1084/jem.20082205. PubMed PMID: 19414558; PMCID: PMC2715041.
281. Gevensleben H, Dietrich D, Golletz C, Steiner S, Jung M, Thiesler T, Majores M, Stein J, Uhl B, Muller S, Ellinger J, Stephan C, Jung K, Brossart P, Kristiansen G. The Immune Checkpoint Regulator PD-L1 Is Highly Expressed in Aggressive Primary Prostate Cancer. Clinical cancer research : an official journal of the American Association for Cancer Research. 2016;22(8):1969-77. doi: 10.1158/1078-0432.CCR-15-2042. PubMed PMID: 26573597.
282. Brahmer JR, Drake CG, Wollner I, Powderly JD, Picus J, Sharfman WH, Stankevich E, Pons A, Salay TM, McMiller TL, Gilson MM, Wang C, Selby M, Taube JM, Anders R, Chen L, Korman AJ, Pardoll DM, Lowy I, Topalian SL. Phase I study of single-agent anti-programmed death-1 (MDX-1106) in refractory solid tumors: safety, clinical activity, pharmacodynamics, and immunologic correlates. Journal of clinical oncology : official journal of the American Society of Clinical Oncology. 2010;28(19):3167-75. doi: 10.1200/JCO.2009.26.7609. PubMed PMID: 20516446; PMCID: PMC4834717.
283. Topalian SL, Hodi FS, Brahmer JR, Gettinger SN, Smith DC, McDermott DF, Powderly JD, Carvajal RD, Sosman JA, Atkins MB, Leming PD, Spigel DR, Antonia SJ,

Horn L, Drake CG, Pardoll DM, Chen L, Sharfman WH, Anders RA, Taube JM, McMiller TL, Xu H, Korman AJ, Jure-Kunkel M, Agrawal S, McDonald D, Kollia GD, Gupta A, Wigginton JM, Sznol M. Safety, activity, and immune correlates of anti-PD-1 antibody in cancer. The New England journal of medicine. 2012;366(26):2443-54. doi: 10.1056/NEJMoa1200690. PubMed PMID: 22658127; PMCID: PMC3544539.
284. Taube JM, Klein A, Brahmer JR, Xu H, Pan X, Kim JH, Chen L, Pardoll DM, Topalian SL, Anders RA. Association of PD-1, PD-1 ligands, and other features of the tumor immune microenvironment with response to anti-PD-1 therapy. Clinical cancer research : an official journal of the American Association for Cancer Research. 2014;20(19):5064-74. doi: 10.1158/1078-0432.CCR-13-3271. PubMed PMID: 24714771; PMCID: PMC4185001.
285. Bishop JL, Sio A, Angeles A, Roberts ME, Azad AA, Chi KN, Zoubeidi A. PD-L1 is highly expressed in Enzalutamide resistant prostate cancer. Oncotarget. 2015;6(1):234-42. doi: 10.18632/oncotarget.2703. PubMed PMID: 25428917; PMCID: PMC4381591.
286. Graff JN, Alumkal JJ, Drake CG, Thomas GV, Redmond WL, Farhad M, Cetnar JP, Ey FS, Bergan RC, Slottke R, Beer TM. Early evidence of anti-PD-1 activity in enzalutamide-resistant prostate cancer. Oncotarget. 2016;7(33):52810-7. doi: 10.18632/oncotarget.10547. PubMed PMID: 27429197; PMCID: PMC5288150.
287. Basnet A, Khullar G, Mehta R, Chittoria N. A Case of Locally Advanced Castration-resistant Prostate Cancer With Remarkable Response to Nivolumab. Clin Genitourin Cancer. 2017;15(5):e881-e4. doi: 10.1016/j.clgc.2017.05.005. PubMed PMID: 28625691.
288. Li L, Karanika S, Yang G, Wang J, Park S, Broom BM, Manyam GC, Wu W, Luo Y, Basourakos S, Song JH, Gallick GE, Karantanos T, Korentzelos D, Azad AK, Kim J, Corn PG, Aparicio AM, Logothetis CJ, Troncoso P, Heffernan T, Toniatti C, Lee HS, Lee JS, Zuo X, Chang W, Yin J, Thompson TC. Androgen receptor inhibitor-induced "BRCAness" and PARP inhibition are synthetically lethal for castration-resistant prostate cancer. Science signaling. 2017;10(480). doi: 10.1126/scisignal.aam7479. PubMed PMID: 28536297.
289. Gao J, Ward JF, Pettaway CA, Shi LZ, Subudhi SK, Vence LM, Zhao H, Chen J, Chen H, Efstathiou E, Troncoso P, Allison JP, Logothetis CJ, Wistuba, II, Sepulveda MA, Sun J, Wargo J, Blando J, Sharma P. VISTA is an inhibitory immune checkpoint that is increased after ipilimumab therapy in patients with prostate cancer. Nature medicine. 2017;23(5):551-5. doi: 10.1038/nm.4308. PubMed PMID: 28346412; PMCID: PMC5466900.
290. Grosso JF, Kelleher CC, Harris TJ, Maris CH, Hipkiss EL, De Marzo A, Anders R, Netto G, Getnet D, Bruno TC, Goldberg MV, Pardoll DM, Drake CG. LAG-3 regulates CD8+ T cell accumulation and effector function in murine self- and tumor-tolerance systems. J Clin Invest. 2007;117(11):3383-92. doi: 10.1172/JCI31184. PubMed PMID: 17932562; PMCID: PMC2000807.

291. Piao Y, Jin X. Analysis of Tim-3 as a therapeutic target in prostate cancer. Tumour Biol. 2017;39(7):1010428317716628. doi: 10.1177/1010428317716628. PubMed PMID: 28681697.
292. Piao YR, Piao LZ, Zhu LH, Jin ZH, Dong XZ. Prognostic value of T cell immunoglobulin mucin-3 in prostate cancer. Asian Pac J Cancer Prev. 2013;14(6):3897-901. PubMed PMID: 23886204.
293. Zang X, Thompson RH, Al-Ahmadie HA, Serio AM, Reuter VE, Eastham JA, Scardino PT, Sharma P, Allison JP. B7-H3 and B7x are highly expressed in human prostate cancer and associated with disease spread and poor outcome. Proceedings of the National Academy of Sciences of the United States of America. 2007;104(49):19458-63. doi: 10.1073/pnas.0709802104. PubMed PMID: 18042703; PMCID: PMC2148311.
294. Qian Y, Yao HP, Shen L, Cheng LF, Zhang LH. [Expression of B7-H4 in prostate cancer and its clinical significance]. Zhejiang Da Xue Xue Bao Yi Xue Ban. 2010;39(4):345-9. PubMed PMID: 20731031.
295. Roth TJ, Sheinin Y, Lohse CM, Kuntz SM, Frigola X, Inman BA, Krambeck AE, McKenney ME, Karnes RJ, Blute ML, Cheville JC, Sebo TJ, Kwon ED. B7-H3 ligand expression by prostate cancer: a novel marker of prognosis and potential target for therapy. Cancer research. 2007;67(16):7893-900. doi: 10.1158/0008-5472.CAN-07-1068. PubMed PMID: 17686830.
296. Yuan H, Wei X, Zhang G, Li C, Zhang X, Hou J. B7-H3 over expression in prostate cancer promotes tumor cell progression. The Journal of urology. 2011;186(3):1093-9. doi: 10.1016/j.juro.2011.04.103. PubMed PMID: 21784485.
297. Liu Y, Vlatkovic L, Saeter T, Servoll E, Waaler G, Nesland JM, Giercksky KE, Axcrona K. Is the clinical malignant phenotype of prostate cancer a result of a highly proliferative immune-evasive B7-H3-expressing cell population? Int J Urol. 2012;19(8):749-56. doi: 10.1111/j.1442-2042.2012.03017.x. PubMed PMID: 22487487.
298. Parker AS, Heckman MG, Sheinin Y, Wu KJ, Hilton TW, Diehl NN, Pisansky TM, Schild SE, Kwon ED, Buskirk SJ. Evaluation of B7-H3 expression as a biomarker of biochemical recurrence after salvage radiation therapy for recurrent prostate cancer. International journal of radiation oncology, biology, physics. 2011;79(5):1343-9. doi: 10.1016/j.ijrobp.2010.01.061. PubMed PMID: 20598810.
299. Chavin G, Sheinin Y, Crispen PL, Boorjian SA, Roth TJ, Rangel L, Blute ML, Sebo TJ, Tindall DJ, Kwon ED, Karnes RJ. Expression of immunosuppresive B7-H3 ligand by hormone-treated prostate cancer tumors and metastases. Clinical cancer research : an official journal of the American Association for Cancer Research. 2009;15(6):2174-80. doi: 10.1158/1078-0432.CCR-08-2262. PubMed PMID: 19276267; PMCID: PMC2676580.
300. Kreymborg K, Haak S, Murali R, Wei J, Waitz R, Gasteiger G, Savage PA, van den Brink MR, Allison JP. Ablation of B7-H3 but Not B7-H4 Results in Highly Increased Tumor Burden in a Murine Model of Spontaneous Prostate Cancer. Cancer

immunology research. 2015;3(8):849-54. doi: 10.1158/2326-6066.CIR-15-0100. PubMed PMID: 26122284.
301. Curti BD, Kovacsovics-Bankowski M, Morris N, Walker E, Chisholm L, Floyd K, Walker J, Gonzalez I, Meeuwsen T, Fox BA, Moudgil T, Miller W, Haley D, Coffey T, Fisher B, Delanty-Miller L, Rymarchyk N, Kelly T, Crocenzi T, Bernstein E, Sanborn R, Urba WJ, Weinberg AD. OX40 is a potent immune-stimulating target in late-stage cancer patients. Cancer research. 2013;73(24):7189-98. doi: 10.1158/0008-5472.CAN-12-4174. PubMed PMID: 24177180; PMCID: PMC3922072.
302. Forbes NS. Engineering the perfect (bacterial) cancer therapy. Nature reviews Cancer. 2010;10(11):785-94. doi: 10.1038/nrc2934. PubMed PMID: 20944664; PMCID: PMC3756932.
303. Felgner S, Pawar V, Kocijancic D, Erhardt M, Weiss S. Tumour-targeting bacteria-based cancer therapies for increased specificity and improved outcome. Microb Biotechnol. 2017;10(5):1074-8. doi: 10.1111/1751-7915.12787. PubMed PMID: 28771926; PMCID: PMC5609243.
304. Zheng JH, Min JJ. Targeted Cancer Therapy Using Engineered Salmonella typhimurium. Chonnam Med J. 2016;52(3):173-84. doi: 10.4068/cmj.2016.52.3.173. PubMed PMID: 27689027; PMCID: PMC5040766.
305. Wood LM, Paterson Y. Attenuated Listeria monocytogenes: a powerful and versatile vector for the future of tumor immunotherapy. Front Cell Infect Microbiol. 2014;4:51. doi: 10.3389/fcimb.2014.00051. PubMed PMID: 24860789; PMCID: PMC4026700.
306. Staedtke V, Roberts NJ, Bai R-Y, Zhou S. Clostridium novyi-NT in cancer therapy. Genes & Diseases. 2016;3(2):144-52. doi: https://doi.org/10.1016/j.gendis.2016.01.003.
307. Zhao M, Yang M, Li XM, Jiang P, Baranov E, Li S, Xu M, Penman S, Hoffman RM. Tumor-targeting bacterial therapy with amino acid auxotrophs of GFP-expressing Salmonella typhimurium. Proceedings of the National Academy of Sciences of the United States of America. 2005;102(3):755-60. doi: 10.1073/pnas.0408422102. PubMed PMID: 15644448; PMCID: PMC545558.
308. Zhao M, Geller J, Ma H, Yang M, Penman S, Hoffman RM. Monotherapy with a tumor-targeting mutant of Salmonella typhimurium cures orthotopic metastatic mouse models of human prostate cancer. Proceedings of the National Academy of Sciences of the United States of America. 2007;104(24):10170-4. doi: 10.1073/pnas.0703867104. PubMed PMID: 17548809; PMCID: PMC1891231.
309. Zhong Z, Kazmierczak RA, Dino A, Khreis R, Eisenstark A, Schatten H. Salmonella-host cell interactions, changes in host cell architecture, and destruction of prostate tumor cells with genetically altered Salmonella. Microsc Microanal. 2007;13(5):372-83. doi: 10.1017/S1431927607070833. PubMed PMID: 17900389.
310. Ahmad S, Casey G, Cronin M, Rajendran S, Sweeney P, Tangney M, O'Sullivan GC. Induction of effective antitumor response after mucosal bacterial vector mediated DNA vaccination with endogenous prostate cancer specific antigen. The

Journal of urology. 2011;186(2):687-93. doi: 10.1016/j.juro.2011.03.139. PubMed PMID: 21683415.
311. Fensterle J, Bergmann B, Yone CL, Hotz C, Meyer SR, Spreng S, Goebel W, Rapp UR, Gentschev I. Cancer immunotherapy based on recombinant Salmonella enterica serovar Typhimurium aroA strains secreting prostate-specific antigen and cholera toxin subunit B. Cancer gene therapy. 2008;15(2):85-93. doi: 10.1038/sj.cgt.7701109. PubMed PMID: 18084243.
312. Jiang T, Zhou C, Gu J, Liu Y, Zhao L, Li W, Wang G, Li Y, Cai L. Enhanced therapeutic effect of cisplatin on the prostate cancer in tumor-bearing mice by transfecting the attenuated Salmonella carrying a plasmid co-expressing p53 gene and mdm2 siRNA. Cancer letters. 2013;337(1):133-42. doi: 10.1016/j.canlet.2013.05.028. PubMed PMID: 23726840.
313. Li X, Li Y, Wang B, Ji K, Liang Z, Guo B, Hu J, Yin D, Du Y, Kopecko DJ, Kalvakolanu DV, Zhao X, Xu D, Zhang L. Delivery of the co-expression plasmid pEndo-Si-Stat3 by attenuated Salmonella serovar typhimurium for prostate cancer treatment. Journal of cancer research and clinical oncology. 2013;139(6):971-80. doi: 10.1007/s00432-013-1398-0. PubMed PMID: 23463096; PMCID: PMC3874139.
314. Shahabi V, Reyes-Reyes M, Wallecha A, Rivera S, Paterson Y, Maciag P. Development of a Listeria monocytogenes based vaccine against prostate cancer. Cancer immunology, immunotherapy : CII. 2008;57(9):1301-13. doi: 10.1007/s00262-008-0463-z. PubMed PMID: 18273616.
315. Wallecha A, Maciag PC, Rivera S, Paterson Y, Shahabi V. Construction and characterization of an attenuated Listeria monocytogenes strain for clinical use in cancer immunotherapy. Clin Vaccine Immunol. 2009;16(1):96-103. doi: 10.1128/CVI.00274-08. PubMed PMID: 19020110; PMCID: PMC2620657.
316. Hannan R, Zhang H, Wallecha A, Singh R, Liu L, Cohen P, Alfieri A, Rothman J, Guha C. Combined immunotherapy with Listeria monocytogenes-based PSA vaccine and radiation therapy leads to a therapeutic response in a murine model of prostate cancer. Cancer immunology, immunotherapy : CII. 2012;61(12):2227-38. doi: 10.1007/s00262-012-1257-x. PubMed PMID: 22644735.
317. Melero I, Berman DM, Aznar MA, Korman AJ, Perez Gracia JL, Haanen J. Evolving synergistic combinations of targeted immunotherapies to combat cancer. Nature reviews Cancer. 2015;15(8):457-72. doi: 10.1038/nrc3973. PubMed PMID: 26205340.
318. Galluzzi L, Senovilla L, Zitvogel L, Kroemer G. The secret ally: immunostimulation by anticancer drugs. Nat Rev Drug Discov. 2012;11(3):215-33. doi: 10.1038/nrd3626. PubMed PMID: 22301798.
319. Gameiro SR, Malamas AS, Tsang KY, Ferrone S, Hodge JW. Inhibitors of histone deacetylase 1 reverse the immune evasion phenotype to enhance T-cell mediated lysis of prostate and breast carcinoma cells. Oncotarget. 2016;7(7):7390-402. doi: 10.18632/oncotarget.7180. PubMed PMID: 26862729; PMCID: PMC4884926.

320. Eikawa S, Nishida M, Mizukami S, Yamazaki C, Nakayama E, Udono H. Immune-mediated antitumor effect by type 2 diabetes drug, metformin. Proceedings of the National Academy of Sciences of the United States of America. 2015;112(6):1809-14. doi: 10.1073/pnas.1417636112. PubMed PMID: 25624476; PMCID: PMC4330733.
321. Scharping NE, Menk AV, Whetstone RD, Zeng X, Delgoffe GM. Efficacy of PD-1 Blockade Is Potentiated by Metformin-Induced Reduction of Tumor Hypoxia. Cancer immunology research. 2017;5(1):9-16. doi: 10.1158/2326-6066.CIR-16-0103. PubMed PMID: 27941003; PMCID: PMC5340074.
322. Quick ML, Wong L, Mukherjee S, Done JD, Schaeffer AJ, Thumbikat P. Th1-Th17 cells contribute to the development of uropathogenic Escherichia coli-induced chronic pelvic pain. PloS one. 2013;8(4):e60987. Epub 2013/04/12. doi: 10.1371/journal.pone.0060987. PubMed PMID: 23577183; PMCID: 3618515.
323. Rudick CN, Berry RE, Johnson JR, Johnston B, Klumpp DJ, Schaeffer AJ, Thumbikat P. Uropathogenic Escherichia coli induces chronic pelvic pain. Infect Immun. 2011;79(2):628-35. doi: 10.1128/IAI.00910-10. PubMed PMID: 21078846; PMCID: PMC3028831.
324. Simons BW, Durham NM, Bruno TC, Grosso JF, Schaeffer AJ, Ross AE, Hurley PJ, Berman DM, Drake CG, Thumbikat P, Schaeffer EM. A human prostatic bacterial isolate alters the prostatic microenvironment and accelerates prostate cancer progression. The Journal of pathology. 2015;235(3):478-89. Epub 2014/10/29. doi: 10.1002/path.4472. PubMed PMID: 25348195; PMCID: 4352321.
325. Anker JF, Naseem AF, Mok H, Schaeffer AJ, Abdulkadir SA, Thumbikat P. Multi-faceted immunomodulatory and tissue-tropic clinical bacterial isolate potentiates prostate cancer immunotherapy. Nat Commun. 2018;9(1):1591. doi: 10.1038/s41467-018-03900-x. PubMed PMID: 29686284; PMCID: PMC5913311.
326. Barbosa-Cesnik C, Schwartz K, Foxman B. Lactation mastitis. JAMA. 2003;289(13):1609-12. doi: 10.1001/jama.289.13.1609. PubMed PMID: 12672715.
327. Garcia-Rodriguez JA, Fresnadillo Martinez MJ. Dynamics of nasopharyngeal colonization by potential respiratory pathogens. J Antimicrob Chemother. 2002;50 Suppl S2:59-73. PubMed PMID: 12556435.
328. Flores-Mireles AL, Walker JN, Caparon M, Hultgren SJ. Urinary tract infections: epidemiology, mechanisms of infection and treatment options. Nat Rev Microbiol. 2015;13(5):269-84. doi: 10.1038/nrmicro3432. PubMed PMID: 25853778; PMCID: PMC4457377.
329. Ling Z, Liu X, Chen X, Zhu H, Nelson KE, Xia Y, Li L, Xiang C. Diversity of cervicovaginal microbiota associated with female lower genital tract infections. Microb Ecol. 2011;61(3):704-14. doi: 10.1007/s00248-011-9813-z. PubMed PMID: 21287345.
330. Quick ML, Done JD, Thumbikat P. Measurement of tactile allodynia in a murine model of bacterial prostatitis. J Vis Exp. 2013(71):e50158. doi: 10.3791/50158. PubMed PMID: 23353558; PMCID: PMC3582676.

331. Nurk S, Bankevich A, Antipov D, Gurevich A, Korobeynikov A, Lapidus A, Prjibelsky A, Pyshkin A, Sirotkin A, Sirotkin Y, Stepanauskas R, McLean J, Lasken R, Clingenpeel SR, Woyke T, Tesler G, Alekseyev MA, Pevzner PA. Assembling Genomes and Mini-metagenomes from Highly Chimeric Reads. In: Deng M, Jiang R, Sun F, Zhang X, editors. Research in Computational Molecular Biology: 17th Annual International Conference, RECOMB 2013, Beijing, China, April 7-10, 2013 Proceedings. Berlin, Heidelberg: Springer Berlin Heidelberg; 2013. p. 158-70.
332. Wick RR, Schultz MB, Zobel J, Holt KE. Bandage: interactive visualization of de novo genome assemblies. Bioinformatics. 2015;31(20):3350-2. doi: 10.1093/bioinformatics/btv383. PubMed PMID: 26099265; PMCID: PMC4595904.
333. Aziz RK, Bartels D, Best AA, DeJongh M, Disz T, Edwards RA, Formsma K, Gerdes S, Glass EM, Kubal M, Meyer F, Olsen GJ, Olson R, Osterman AL, Overbeek RA, McNeil LK, Paarmann D, Paczian T, Parrello B, Pusch GD, Reich C, Stevens R, Vassieva O, Vonstein V, Wilke A, Zagnitko O. The RAST Server: rapid annotations using subsystems technology. BMC Genomics. 2008;9:75. doi: 10.1186/1471-2164-9-75. PubMed PMID: 18261238; PMCID: PMC2265698.
334. Rutherford K, Parkhill J, Crook J, Horsnell T, Rice P, Rajandream MA, Barrell B. Artemis: sequence visualization and annotation. Bioinformatics. 2000;16(10):944-5. PubMed PMID: 11120685.
335. Clermont O, Bonacorsi S, Bingen E. Rapid and simple determination of the Escherichia coli phylogenetic group. Appl Environ Microbiol. 2000;66(10):4555-8. PubMed PMID: 11010916; PMCID: PMC92342.
336. Wirth T, Falush D, Lan R, Colles F, Mensa P, Wieler LH, Karch H, Reeves PR, Maiden MC, Ochman H, Achtman M. Sex and virulence in Escherichia coli: an evolutionary perspective. Mol Microbiol. 2006;60(5):1136-51. doi: 10.1111/j.1365-2958.2006.05172.x. PubMed PMID: 16689791; PMCID: PMC1557465.
337. Kumar S, Stecher G, Tamura K. MEGA7: Molecular Evolutionary Genetics Analysis Version 7.0 for Bigger Datasets. Mol Biol Evol. 2016;33(7):1870-4. doi: 10.1093/molbev/msw054. PubMed PMID: 27004904.
338. Anker JF, Mok H, Naseem AF, Thumbikat P, Abdulkadir SA. A Bioluminescent and Fluorescent Orthotopic Syngeneic Murine Model of Androgen-dependent and Castration-resistant Prostate Cancer. J Vis Exp. 2018(133). doi: 10.3791/57301. PubMed PMID: 29578515.
339. Ellis L, Lehet K, Ku S, Azabdaftari G, Pili R. Generation of a syngeneic orthotopic transplant model of prostate cancer metastasis. Oncoscience. 2014;1(10):609-13. doi: 10.18632/oncoscience.88. PubMed PMID: 25485289; PMCID: PMC4254774.
340. Wallace J. Humane endpoints and cancer research. ILAR J. 2000;41(2):87-93. PubMed PMID: 11417496.
341. Field SB, Needham S, Burney IA, Maxwell RJ, Coggle JE, Griffiths JR. Differences in vascular response between primary and transplanted tumours. Br J Cancer. 1991;63(5):723-6. PubMed PMID: 1645562; PMCID: PMC1972409.

342. Cowen SE, Bibby MC, Double JA. Characterisation of the vasculature within a murine adenocarcinoma growing in different sites to evaluate the potential of vascular therapies. Acta Oncol. 1995;34(3):357-60. PubMed PMID: 7779423.
343. Kuo TH, Kubota T, Watanabe M, Furukawa T, Kase S, Tanino H, Saikawa Y, Ishibiki K, Kitajima M, Hoffman RM. Site-specific chemosensitivity of human small-cell lung carcinoma growing orthotopically compared to subcutaneously in SCID mice: the importance of orthotopic models to obtain relevant drug evaluation data. Anticancer Res. 1993;13(3):627-30. PubMed PMID: 8391244.
344. Fidler IJ, Wilmanns C, Staroselsky A, Radinsky R, Dong Z, Fan D. Modulation of tumor cell response to chemotherapy by the organ environment. Cancer Metastasis Rev. 1994;13(2):209-22. PubMed PMID: 7923551.
345. Wilmanns C, Fan D, Obrian C, Radinsky R, Bucana C, Tsan R, Fidler I. Modulation of Doxorubicin sensitivity and level of p-glycoprotein expression in human colon-carcinoma cells by ectopic and orthotopic environments in nude-mice. Int J Oncol. 1993;3(3):413-22. PubMed PMID: 21573380.
346. Fidler IJ. Orthotopic implantation of human colon carcinomas into nude mice provides a valuable model for the biology and therapy of metastasis. Cancer Metastasis Rev. 1991;10(3):229-43. PubMed PMID: 1764766.
347. Pasqualini R, Ruoslahti E. Organ targeting in vivo using phage display peptide libraries. Nature. 1996;380(6572):364-6. doi: 10.1038/380364a0. PubMed PMID: 8598934.
348. Conway EM, Carmeliet P. The diversity of endothelial cells: a challenge for therapeutic angiogenesis. Genome Biol. 2004;5(2):207. doi: 10.1186/gb-2004-5-2-207. PubMed PMID: 14759250; PMCID: PMC395741.
349. Loi M, Di Paolo D, Becherini P, Zorzoli A, Perri P, Carosio R, Cilli M, Ribatti D, Brignole C, Pagnan G, Ponzoni M, Pastorino F. The use of the orthotopic model to validate antivascular therapies for cancer. Int J Dev Biol. 2011;55(4-5):547-55. doi: 10.1387/ijdb.103230ml. PubMed PMID: 21858775.
350. Bianchi-Frias D, Hernandez SA, Coleman R, Wu H, Nelson PS. The landscape of somatic chromosomal copy number aberrations in GEM models of prostate carcinoma. Mol Cancer Res. 2015;13(2):339-47. doi: 10.1158/1541-7786.MCR-14-0262. PubMed PMID: 25298407; PMCID: PMC4527302.
351. Pan Y, Kytola S, Farnebo F, Wang N, Lui WO, Nupponen N, Isola J, Visakorpi T, Bergerheim US, Larsson C. Characterization of chromosomal abnormalities in prostate cancer cell lines by spectral karyotyping. Cytogenetics and cell genetics. 1999;87(3-4):225-32. Epub 2000/03/07. doi: 15432. PubMed PMID: 10702678.
352. Fujiwara M, Anstadt EJ, Clark RB. Cbl-b Deficiency Mediates Resistance to Programmed Death-Ligand 1/Programmed Death-1 Regulation. Front Immunol. 2017;8:42. doi: 10.3389/fimmu.2017.00042. PubMed PMID: 28184224; PMCID: PMC5266705.
353. Tang H, Wang Y, Chlewicki LK, Zhang Y, Guo J, Liang W, Wang J, Wang X, Fu YX. Facilitating T Cell Infiltration in Tumor Microenvironment Overcomes

Resistance to PD-L1 Blockade. Cancer cell. 2016;30(3):500. doi: 10.1016/j.ccell.2016.08.011. PubMed PMID: 27622338.
354. Berry RE, Klumpp DJ, Schaeffer AJ. Urothelial cultures support intracellular bacterial community formation by uropathogenic Escherichia coli. Infect Immun. 2009;77(7):2762-72. doi: 10.1128/IAI.00323-09. PubMed PMID: 19451249; PMCID: PMC2708588.
355. Schneck K, Washington M, Holder D, Lodge K, Motzel S. Hematologic and serum biochemical reference values in nontransgenic FVB mice. Comp Med. 2000;50(1):32-5. PubMed PMID: 10987664.
356. Zufferey R, Dull T, Mandel RJ, Bukovsky A, Quiroz D, Naldini L, Trono D. Self-inactivating lentivirus vector for safe and efficient in vivo gene delivery. J Virol. 1998;72(12):9873-80. PubMed PMID: 9811723; PMCID: PMC110499.
357. Daugherty RL, Serebryannyy L, Yemelyanov A, Flozak AS, Yu HJ, Kosak ST, deLanerolle P, Gottardi CJ. alpha-Catenin is an inhibitor of transcription. Proc Natl Acad Sci U S A. 2014;111(14):5260-5. doi: 10.1073/pnas.1308663111. PubMed PMID: 24706864; PMCID: PMC3986139.
358. Sanjana NE, Shalem O, Zhang F. Improved vectors and genome-wide libraries for CRISPR screening. Nat Methods. 2014;11(8):783-4. doi: 10.1038/nmeth.3047. PubMed PMID: 25075903; PMCID: PMC4486245.
359. Hsu PD, Scott DA, Weinstein JA, Ran FA, Konermann S, Agarwala V, Li Y, Fine EJ, Wu X, Shalem O, Cradick TJ, Marraffini LA, Bao G, Zhang F. DNA targeting specificity of RNA-guided Cas9 nucleases. Nat Biotechnol. 2013;31(9):827-32. doi: 10.1038/nbt.2647. PubMed PMID: 23873081; PMCID: PMC3969858.
360. Cerami E, Gao J, Dogrusoz U, Gross BE, Sumer SO, Aksoy BA, Jacobsen A, Byrne CJ, Heuer ML, Larsson E, Antipin Y, Reva B, Goldberg AP, Sander C, Schultz N. The cBio cancer genomics portal: an open platform for exploring multidimensional cancer genomics data. Cancer discovery. 2012;2(5):401-4. doi: 10.1158/2159-8290.CD-12-0095. PubMed PMID: 22588877; PMCID: PMC3956037.
361. Cancer Genome Atlas Research N. The Molecular Taxonomy of Primary Prostate Cancer. Cell. 2015;163(4):1011-25. doi: 10.1016/j.cell.2015.10.025. PubMed PMID: 26544944; PMCID: PMC4695400.
362. Robinson D, Van Allen EM, Wu YM, Schultz N, Lonigro RJ, Mosquera JM, Montgomery B, Taplin ME, Pritchard CC, Attard G, Beltran H, Abida W, Bradley RK, Vinson J, Cao X, Vats P, Kunju LP, Hussain M, Feng FY, Tomlins SA, Cooney KA, Smith DC, Brennan C, Siddiqui J, Mehra R, Chen Y, Rathkopf DE, Morris MJ, Solomon SB, Durack JC, Reuter VE, Gopalan A, Gao J, Loda M, Lis RT, Bowden M, Balk SP, Gaviola G, Sougnez C, Gupta M, Yu EY, Mostaghel EA, Cheng HH, Mulcahy H, True LD, Plymate SR, Dvinge H, Ferraldeschi R, Flohr P, Miranda S, Zafeiriou Z, Tunariu N, Mateo J, Perez-Lopez R, Demichelis F, Robinson BD, Schiffman M, Nanus DM, Tagawa ST, Sigaras A, Eng KW, Elemento O, Sboner A, Heath EI, Scher HI, Pienta KJ, Kantoff P, de Bono JS, Rubin MA, Nelson PS, Garraway LA, Sawyers CL, Chinnaiyan AM. Integrative clinical genomics of advanced prostate cancer. Cell. 2015;161(5):1215-28. doi: 10.1016/j.cell.2015.05.001. PubMed PMID: 26000489; PMCID: PMC4484602.

363. Roh M, Gary B, Song C, Said-Al-Naief N, Tousson A, Kraft A, Eltoum IE, Abdulkadir SA. Overexpression of the oncogenic kinase Pim-1 leads to genomic instability. Cancer Res. 2003;63(23):8079-84. PubMed PMID: 14678956.
364. Olesen B, Hansen DS, Nilsson F, Frimodt-Moller J, Leihof RF, Struve C, Scheutz F, Johnston B, Krogfelt KA, Johnson JR. Prevalence and characteristics of the epidemic multiresistant Escherichia coli ST131 clonal group among extended-spectrum beta-lactamase-producing E. coli isolates in Copenhagen, Denmark. J Clin Microbiol. 2013;51(6):1779-85. doi: 10.1128/JCM.00346-13. PubMed PMID: 23554186; PMCID: PMC3716056.
365. Bien J, Sokolova O, Bozko P. Role of Uropathogenic Escherichia coli Virulence Factors in Development of Urinary Tract Infection and Kidney Damage. Int J Nephrol. 2012;2012:681473. doi: 10.1155/2012/681473. PubMed PMID: 22506110; PMCID: PMC3312279.
366. Watson PA, Ellwood-Yen K, King JC, Wongvipat J, Lebeau MM, Sawyers CL. Context-dependent hormone-refractory progression revealed through characterization of a novel murine prostate cancer cell line. Cancer research. 2005;65(24):11565-71. doi: 10.1158/0008-5472.CAN-05-3441. PubMed PMID: 16357166.
367. Blattner FR, Plunkett G, 3rd, Bloch CA, Perna NT, Burland V, Riley M, Collado-Vides J, Glasner JD, Rode CK, Mayhew GF, Gregor J, Davis NW, Kirkpatrick HA, Goeden MA, Rose DJ, Mau B, Shao Y. The complete genome sequence of Escherichia coli K-12. Science. 1997;277(5331):1453-62. PubMed PMID: 9278503.
368. Kepp O, Senovilla L, Vitale I, Vacchelli E, Adjemian S, Agostinis P, Apetoh L, Aranda F, Barnaba V, Bloy N, Bracci L, Breckpot K, Brough D, Buque A, Castro MG, Cirone M, Colombo MI, Cremer I, Demaria S, Dini L, Eliopoulos AG, Faggioni A, Formenti SC, Fucikova J, Gabriele L, Gaipl US, Galon J, Garg A, Ghiringhelli F, Giese NA, Guo ZS, Hemminki A, Herrmann M, Hodge JW, Holdenrieder S, Honeychurch J, Hu HM, Huang X, Illidge TM, Kono K, Korbelik M, Krysko DV, Loi S, Lowenstein PR, Lugli E, Ma Y, Madeo F, Manfredi AA, Martins I, Mavilio D, Menger L, Merendino N, Michaud M, Mignot G, Mossman KL, Multhoff G, Oehler R, Palombo F, Panaretakis T, Pol J, Proietti E, Ricci JE, Riganti C, Rovere-Querini P, Rubartelli A, Sistigu A, Smyth MJ, Sonnemann J, Spisek R, Stagg J, Sukkurwala AQ, Tartour E, Thorburn A, Thorne SH, Vandenabeele P, Velotti F, Workenhe ST, Yang H, Zong WX, Zitvogel L, Kroemer G, Galluzzi L. Consensus guidelines for the detection of immunogenic cell death. Oncoimmunology. 2014;3(9):e955691. doi: 10.4161/21624011.2014.955691. PubMed PMID: 25941621; PMCID: PMC4292729.
369. Yang H, Ma Y, Chen G, Zhou H, Yamazaki T, Klein C, Pietrocola F, Vacchelli E, Souquere S, Sauvat A, Zitvogel L, Kepp O, Kroemer G. Contribution of RIP3 and MLKL to immunogenic cell death signaling in cancer chemotherapy. Oncoimmunology. 2016;5(6):e1149673. doi: 10.1080/2162402X.2016.1149673. PubMed PMID: 27471616; PMCID: PMC4938314.
370. Crane CA, Panner A, Murray JC, Wilson SP, Xu H, Chen L, Simko JP, Waldman FM, Pieper RO, Parsa AT. PI(3) kinase is associated with a mechanism of

immunoresistance in breast and prostate cancer. Oncogene. 2009;28(2):306-12. doi: 10.1038/onc.2008.384. PubMed PMID: 18850006; PMCID: PMC3786571.
371. Peng W, Chen JQ, Liu C, Malu S, Creasy C, Tetzlaff MT, Xu C, McKenzie JA, Zhang C, Liang X, Williams LJ, Deng W, Chen G, Mbofung R, Lazar AJ, Torres-Cabala CA, Cooper ZA, Chen PL, Tieu TN, Spranger S, Yu X, Bernatchez C, Forget MA, Haymaker C, Amaria R, McQuade JL, Glitza IC, Cascone T, Li HS, Kwong LN, Heffernan TP, Hu J, Bassett RL, Jr., Bosenberg MW, Woodman SE, Overwijk WW, Lizee G, Roszik J, Gajewski TF, Wargo JA, Gershenwald JE, Radvanyi L, Davies MA, Hwu P. Loss of PTEN Promotes Resistance to T Cell-Mediated Immunotherapy. Cancer discovery. 2016;6(2):202-16. doi: 10.1158/2159-8290.CD-15-0283. PubMed PMID: 26645196; PMCID: PMC4744499.
372. Liu W, Xie CC, Thomas CY, Kim ST, Lindberg J, Egevad L, Wang Z, Zhang Z, Sun J, Sun J, Koty PP, Kader AK, Cramer SD, Bova GS, Zheng SL, Gronberg H, Isaacs WB, Xu J. Genetic markers associated with early cancer-specific mortality following prostatectomy. Cancer. 2013;119(13):2405-12. doi: 10.1002/cncr.27954. PubMed PMID: 23609948; PMCID: PMC3863778.
373. Wolchok JD, Hoos A, O'Day S, Weber JS, Hamid O, Lebbe C, Maio M, Binder M, Bohnsack O, Nichol G, Humphrey R, Hodi FS. Guidelines for the evaluation of immune therapy activity in solid tumors: immune-related response criteria. Clinical cancer research : an official journal of the American Association for Cancer Research. 2009;15(23):7412-20. doi: 10.1158/1078-0432.CCR-09-1624. PubMed PMID: 19934295.
374. Brinkmann V, Cyster JG, Hla T. FTY720: sphingosine 1-phosphate receptor-1 in the control of lymphocyte egress and endothelial barrier function. Am J Transplant. 2004;4(7):1019-25. doi: 10.1111/j.1600-6143.2004.00476.x. PubMed PMID: 15196057.
375. Trapani JA, Smyth MJ. Functional significance of the perforin/granzyme cell death pathway. Nature reviews Immunology. 2002;2(10):735-47. doi: 10.1038/nri911. PubMed PMID: 12360212.
376. Ye J, Livergood RS, Peng G. The role and regulation of human Th17 cells in tumor immunity. The American journal of pathology. 2013;182(1):10-20. doi: 10.1016/j.ajpath.2012.08.041. PubMed PMID: 23159950; PMCID: PMC3532708.
377. Olesch C, Sha W, Angioni C, Sha LK, Acaf E, Patrignani P, Jakobsson PJ, Radeke HH, Grosch S, Geisslinger G, von Knethen A, Weigert A, Brune B. MPGES-1-derived PGE2 suppresses CD80 expression on tumor-associated phagocytes to inhibit anti-tumor immune responses in breast cancer. Oncotarget. 2015;6(12):10284-96. doi: 10.18632/oncotarget.3581. PubMed PMID: 25871398; PMCID: PMC4496355.
378. Guillerey C, Huntington ND, Smyth MJ. Targeting natural killer cells in cancer immunotherapy. Nat Immunol. 2016;17(9):1025-36. doi: 10.1038/ni.3518. PubMed PMID: 27540992.
379. Aggarwal NR, King LS, D'Alessio FR. Diverse macrophage populations mediate acute lung inflammation and resolution. Am J Physiol Lung Cell Mol Physiol.

2014;306(8):L709-25. doi: 10.1152/ajplung.00341.2013. PubMed PMID: 24508730; PMCID: PMC3989724.
380. Shariat SF, Andrews B, Kattan MW, Kim J, Wheeler TM, Slawin KM. Plasma levels of interleukin-6 and its soluble receptor are associated with prostate cancer progression and metastasis. Urology. 2001;58(6):1008-15. PubMed PMID: 11744478.
381. Wu CT, Chen MF, Chen WC, Hsieh CC. The role of IL-6 in the radiation response of prostate cancer. Radiat Oncol. 2013;8:159. doi: 10.1186/1748-717X-8-159. PubMed PMID: 23806095; PMCID: PMC3717100.
382. Lu H. TLR Agonists for Cancer Immunotherapy: Tipping the Balance between the Immune Stimulatory and Inhibitory Effects. Front Immunol. 2014;5:83. doi: 10.3389/fimmu.2014.00083. PubMed PMID: 24624132; PMCID: PMC3939428.
383. Zheng JH, Nguyen VH, Jiang SN, Park SH, Tan W, Hong SH, Shin MG, Chung IJ, Hong Y, Bom HS, Choy HE, Lee SE, Rhee JH, Min JJ. Two-step enhanced cancer immunotherapy with engineered Salmonella typhimurium secreting heterologous flagellin. Sci Transl Med. 2017;9(376). doi: 10.1126/scitranslmed.aak9537. PubMed PMID: 28179508.
384. Maciag PC, Radulovic S, Rothman J. The first clinical use of a live-attenuated Listeria monocytogenes vaccine: a Phase I safety study of Lm-LLO-E7 in patients with advanced carcinoma of the cervix. Vaccine. 2009;27(30):3975-83. doi: 10.1016/j.vaccine.2009.04.041. PubMed PMID: 19389451.
385. Koh CM, Bieberich CJ, Dang CV, Nelson WG, Yegnasubramanian S, De Marzo AM. MYC and Prostate Cancer. Genes Cancer. 2010;1(6):617-28. doi: 10.1177/1947601910379132. PubMed PMID: 21779461; PMCID: PMC3092219.
386. Shappell SB, Thomas GV, Roberts RL, Herbert R, Ittmann MM, Rubin MA, Humphrey PA, Sundberg JP, Rozengurt N, Barrios R, Ward JM, Cardiff RD. Prostate pathology of genetically engineered mice: definitions and classification. The consensus report from the Bar Harbor meeting of the Mouse Models of Human Cancer Consortium Prostate Pathology Committee. Cancer research. 2004;64(6):2270-305. PubMed PMID: 15026373.
387. McNeal JE, Redwine EA, Freiha FS, Stamey TA. Zonal distribution of prostatic adenocarcinoma. Correlation with histologic pattern and direction of spread. Am J Surg Pathol. 1988;12(12):897-906. PubMed PMID: 3202246.
388. Price D. Comparative Aspects of Development and Structure in the Prostate. Natl Cancer Inst Monogr. 1963;12:1-27. PubMed PMID: 14072991.
389. Roy-Burman P, Wu H, Powell WC, Hagenkord J, Cohen MB. Genetically defined mouse models that mimic natural aspects of human prostate cancer development. Endocr Relat Cancer. 2004;11(2):225-54. PubMed PMID: 15163300.
390. Berquin IM, Min Y, Wu R, Wu H, Chen YQ. Expression signature of the mouse prostate. The Journal of biological chemistry. 2005;280(43):36442-51. doi: 10.1074/jbc.M504945200. PubMed PMID: 16055444.
391. Bartee MY, Dunlap KM, Bartee E. Tumor-Localized Secretion of Soluble PD1 Enhances Oncolytic Virotherapy. Cancer research. 2017;77(11):2952-63. doi:

10.1158/0008-5472.CAN-16-1638. PubMed PMID: 28314785; PMCID: PMC5457316.
392. Bartee E, Li Z. In vivo and in situ programming of tumor immunity by combining oncolytics and PD-1 immune checkpoint blockade. Exp Hematol Oncol. 2017;6:15. doi: 10.1186/s40164-017-0075-4. PubMed PMID: 28546884; PMCID: PMC5443360.
393. Ahmadi T, Flies A, Efebera Y, Sherr DH. CD40 Ligand-activated, antigen-specific B cells are comparable to mature dendritic cells in presenting protein antigens and major histocompatibility complex class I- and class II-binding peptides. Immunology. 2008;124(1):129-40. doi: 10.1111/j.1365-2567.2007.02749.x. PubMed PMID: 18067555; PMCID: PMC2434387.
394. Germain C, Gnjatic S, Tamzalit F, Knockaert S, Remark R, Goc J, Lepelley A, Becht E, Katsahian S, Bizouard G, Validire P, Damotte D, Alifano M, Magdeleinat P, Cremer I, Teillaud JL, Fridman WH, Sautes-Fridman C, Dieu-Nosjean MC. Presence of B cells in tertiary lymphoid structures is associated with a protective immunity in patients with lung cancer. Am J Respir Crit Care Med. 2014;189(7):832-44. doi: 10.1164/rccm.201309-1611OC. PubMed PMID: 24484236.
395. Alexandrov LB, Nik-Zainal S, Wedge DC, Aparicio SA, Behjati S, Biankin AV, Bignell GR, Bolli N, Borg A, Borresen-Dale AL, Boyault S, Burkhardt B, Butler AP, Caldas C, Davies HR, Desmedt C, Eils R, Eyfjord JE, Foekens JA, Greaves M, Hosoda F, Hutter B, Ilicic T, Imbeaud S, Imielinski M, Jager N, Jones DT, Jones D, Knappskog S, Kool M, Lakhani SR, Lopez-Otin C, Martin S, Munshi NC, Nakamura H, Northcott PA, Pajic M, Papaemmanuil E, Paradiso A, Pearson JV, Puente XS, Raine K, Ramakrishna M, Richardson AL, Richter J, Rosenstiel P, Schlesner M, Schumacher TN, Span PN, Teague JW, Totoki Y, Tutt AN, Valdes-Mas R, van Buuren MM, van 't Veer L, Vincent-Salomon A, Waddell N, Yates LR, Australian Pancreatic Cancer Genome I, Consortium IBC, Consortium IM-S, PedBrain I, Zucman-Rossi J, Futreal PA, McDermott U, Lichter P, Meyerson M, Grimmond SM, Siebert R, Campo E, Shibata T, Pfister SM, Campbell PJ, Stratton MR. Signatures of mutational processes in human cancer. Nature. 2013;500(7463):415-21. Epub 2013/08/16. doi: 10.1038/nature12477. PubMed PMID: 23945592; PMCID: 3776390.
396. Grasso CS, Wu YM, Robinson DR, Cao X, Dhanasekaran SM, Khan AP, Quist MJ, Jing X, Lonigro RJ, Brenner JC, Asangani IA, Ateeq B, Chun SY, Siddiqui J, Sam L, Anstett M, Mehra R, Prensner JR, Palanisamy N, Ryslik GA, Vandin F, Raphael BJ, Kunju LP, Rhodes DR, Pienta KJ, Chinnaiyan AM, Tomlins SA. The mutational landscape of lethal castration-resistant prostate cancer. Nature. 2012;487(7406):239-43. doi: 10.1038/nature11125. PubMed PMID: 22722839; PMCID: PMC3396711.
397. Chen YP, Zhang Y, Lv JW, Li YQ, Wang YQ, He QM, Yang XJ, Sun Y, Mao YP, Yun JP, Liu N, Ma J. Genomic Analysis of Tumor Microenvironment Immune Types across 14 Solid Cancer Types: Immunotherapeutic Implications. Theranostics. 2017;7(14):3585-94. doi: 10.7150/thno.21471. PubMed PMID: 28912897; PMCID: PMC5596445.

398. Brown SD, Warren RL, Gibb EA, Martin SD, Spinelli JJ, Nelson BH, Holt RA. Neo-antigens predicted by tumor genome meta-analysis correlate with increased patient survival. Genome research. 2014;24(5):743-50. Epub 2014/05/02. doi: 10.1101/gr.165985.113. PubMed PMID: 24782321; PMCID: 4009604.
399. Rizvi NA, Hellmann MD, Snyder A, Kvistborg P, Makarov V, Havel JJ, Lee W, Yuan J, Wong P, Ho TS, Miller ML, Rekhtman N, Moreira AL, Ibrahim F, Bruggeman C, Gasmi B, Zappasodi R, Maeda Y, Sander C, Garon EB, Merghoub T, Wolchok JD, Schumacher TN, Chan TA. Cancer immunology. Mutational landscape determines sensitivity to PD-1 blockade in non-small cell lung cancer. Science. 2015;348(6230):124-8. Epub 2015/03/15. doi: 10.1126/science.aaa1348. PubMed PMID: 25765070.
400. Van Allen EM, Miao D, Schilling B, Shukla SA, Blank C, Zimmer L, Sucker A, Hillen U, Foppen MHG, Goldinger SM, Utikal J, Hassel JC, Weide B, Kaehler KC, Loquai C, Mohr P, Gutzmer R, Dummer R, Gabriel S, Wu CJ, Schadendorf D, Garraway LA. Genomic correlates of response to CTLA-4 blockade in metastatic melanoma. Science. 2015;350(6257):207-11. doi: 10.1126/science.aad0095. PubMed PMID: 26359337; PMCID: PMC5054517.
401. Le DT, Uram JN, Wang H, Bartlett BR, Kemberling H, Eyring AD, Skora AD, Luber BS, Azad NS, Laheru D, Biedrzycki B, Donehower RC, Zaheer A, Fisher GA, Crocenzi TS, Lee JJ, Duffy SM, Goldberg RM, de la Chapelle A, Koshiji M, Bhaijee F, Huebner T, Hruban RH, Wood LD, Cuka N, Pardoll DM, Papadopoulos N, Kinzler KW, Zhou S, Cornish TC, Taube JM, Anders RA, Eshleman JR, Vogelstein B, Diaz LA, Jr. PD-1 Blockade in Tumors with Mismatch-Repair Deficiency. The New England journal of medicine. 2015;372(26):2509-20. Epub 2015/06/02. doi: 10.1056/NEJMoa1500596. PubMed PMID: 26028255.
402. Overman MJ, McDermott R, Leach JL, Lonardi S, Lenz HJ, Morse MA, Desai J, Hill A, Axelson M, Moss RA, Goldberg MV, Cao ZA, Ledeine JM, Maglinte GA, Kopetz S, Andre T. Nivolumab in patients with metastatic DNA mismatch repair-deficient or microsatellite instability-high colorectal cancer (CheckMate 142): an open-label, multicentre, phase 2 study. Lancet Oncol. 2017. doi: 10.1016/S1470-2045(17)30422-9. PubMed PMID: 28734759.
403. Le DT, Durham JN, Smith KN, Wang H, Bartlett BR, Aulakh LK, Lu S, Kemberling H, Wilt C, Luber BS, Wong F, Azad NS, Rucki AA, Laheru D, Donehower R, Zaheer A, Fisher GA, Crocenzi TS, Lee JJ, Greten TF, Duffy AG, Ciombor KK, Eyring AD, Lam BH, Joe A, Kang SP, Holdhoff M, Danilova L, Cope L, Meyer C, Zhou S, Goldberg RM, Armstrong DK, Bever KM, Fader AN, Taube J, Housseau F, Spetzler D, Xiao N, Pardoll DM, Papadopoulos N, Kinzler KW, Eshleman JR, Vogelstein B, Anders RA, Diaz LA, Jr. Mismatch repair deficiency predicts response of solid tumors to PD-1 blockade. Science. 2017;357(6349):409-13. doi: 10.1126/science.aan6733. PubMed PMID: 28596308.
404. Clarke B, Tinker AV, Lee CH, Subramanian S, van de Rijn M, Turbin D, Kalloger S, Han G, Ceballos K, Cadungog MG, Huntsman DG, Coukos G, Gilks CB. Intraepithelial T cells and prognosis in ovarian carcinoma: novel associations with

stage, tumor type, and BRCA1 loss. Mod Pathol. 2009;22(3):393-402. doi: 10.1038/modpathol.2008.191. PubMed PMID: 19060844.
405. Strickland KC, Howitt BE, Shukla SA, Rodig S, Ritterhouse LL, Liu JF, Garber JE, Chowdhury D, Wu CJ, D'Andrea AD, Matulonis UA, Konstantinopoulos PA. Association and prognostic significance of BRCA1/2-mutation status with neoantigen load, number of tumor-infiltrating lymphocytes and expression of PD-1/PD-L1 in high grade serous ovarian cancer. Oncotarget. 2016. doi: 10.18632/oncotarget.7277. PubMed PMID: 26871470.
406. Howitt BE, Shukla SA, Sholl LM, Ritterhouse LL, Watkins JC, Rodig S, Stover E, Strickland KC, D'Andrea AD, Wu CJ, Matulonis UA, Konstantinopoulos PA. Association of Polymerase e-Mutated and Microsatellite-Instable Endometrial Cancers With Neoantigen Load, Number of Tumor-Infiltrating Lymphocytes, and Expression of PD-1 and PD-L1. JAMA Oncol. 2015;1(9):1319-23. doi: 10.1001/jamaoncol.2015.2151. PubMed PMID: 26181000.
407. Guedes LB, Antonarakis ES, Schweizer MT, Mirkheshti N, Almutairi F, Park JC, Glavaris S, Hicks J, Eisenberger MA, De Marzo AM, Epstein JI, Isaacs WB, Eshleman JR, Pritchard CC, Lotan TL. MSH2 Loss in Primary Prostate Cancer. Clinical cancer research : an official journal of the American Association for Cancer Research. 2017. doi: 10.1158/1078-0432.CCR-17-0955. PubMed PMID: 28790115.
408. Robinson D, Van Allen EM, Wu YM, Schultz N, Lonigro RJ, Mosquera JM, Montgomery B, Taplin ME, Pritchard CC, Attard G, Beltran H, Abida W, Bradley RK, Vinson J, Cao X, Vats P, Kunju LP, Hussain M, Feng FY, Tomlins SA, Cooney KA, Smith DC, Brennan C, Siddiqui J, Mehra R, Chen Y, Rathkopf DE, Morris MJ, Solomon SB, Durack JC, Reuter VE, Gopalan A, Gao J, Loda M, Lis RT, Bowden M, Balk SP, Gaviola G, Sougnez C, Gupta M, Yu EY, Mostaghel EA, Cheng HH, Mulcahy H, True LD, Plymate SR, Dvinge H, Ferraldeschi R, Flohr P, Miranda S, Zafeiriou Z, Tunariu N, Mateo J, Perez-Lopez R, Demichelis F, Robinson BD, Sboner A, Schiffman M, Nanus DM, Tagawa ST, Sigaras A, Eng KW, Elemento O, Sboner A, Heath EI, Scher HI, Pienta KJ, Kantoff P, de Bono JS, Rubin MA, Nelson PS, Garraway LA, Sawyers CL, Chinnaiyan AM. Integrative Clinical Genomics of Advanced Prostate Cancer. Cell. 2015;162(2):454. doi: 10.1016/j.cell.2015.06.053. PubMed PMID: 28843286.
409. Pritchard CC, Morrissey C, Kumar A, Zhang X, Smith C, Coleman I, Salipante SJ, Milbank J, Yu M, Grady WM, Tait JF, Corey E, Vessella RL, Walsh T, Shendure J, Nelson PS. Complex MSH2 and MSH6 mutations in hypermutated microsatellite unstable advanced prostate cancer. Nat Commun. 2014;5:4988. doi: 10.1038/ncomms5988. PubMed PMID: 25255306; PMCID: PMC4176888.
410. Decker B, Karyadi DM, Davis BW, Karlins E, Tillmans LS, Stanford JL, Thibodeau SN, Ostrander EA. Biallelic BRCA2 Mutations Shape the Somatic Mutational Landscape of Aggressive Prostate Tumors. American journal of human genetics. 2016;98(5):818-29. doi: 10.1016/j.ajhg.2016.03.003. PubMed PMID: 27087322; PMCID: PMC4863563.
411. Pritchard CC, Mateo J, Walsh MF, De Sarkar N, Abida W, Beltran H, Garofalo A, Gulati R, Carreira S, Eeles R, Elemento O, Rubin MA, Robinson D, Lonigro R, Hussain

M, Chinnaiyan A, Vinson J, Filipenko J, Garraway L, Taplin ME, AlDubayan S, Han GC, Beightol M, Morrissey C, Nghiem B, Cheng HH, Montgomery B, Walsh T, Casadei S, Berger M, Zhang L, Zehir A, Vijai J, Scher HI, Sawyers C, Schultz N, Kantoff PW, Solit D, Robson M, Van Allen EM, Offit K, de Bono J, Nelson PS. Inherited DNA-Repair Gene Mutations in Men with Metastatic Prostate Cancer. The New England journal of medicine. 2016;375(5):443-53. doi: 10.1056/NEJMoa1603144. PubMed PMID: 27433846; PMCID: PMC4986616.

412. Leongamornlert D, Saunders E, Dadaev T, Tymrakiewicz M, Goh C, Jugurnauth-Little S, Kozarewa I, Fenwick K, Assiotis I, Barrowdale D, Govindasami K, Guy M, Sawyer E, Wilkinson R, Collaborators U, Antoniou AC, Eeles R, Kote-Jarai Z. Frequent germline deleterious mutations in DNA repair genes in familial prostate cancer cases are associated with advanced disease. British journal of cancer. 2014;110(6):1663-72. doi: 10.1038/bjc.2014.30. PubMed PMID: 24556621; PMCID: PMC3960610.

413. Hart SN, Ellingson MS, Schahl K, Vedell PT, Carlson RE, Sinnwell JP, Barman P, Sicotte H, Eckel-Passow JE, Wang L, Kalari KR, Qin R, Kruisselbrink TM, Jimenez RE, Bryce AH, Tan W, Weinshilboum R, Wang L, Kohli M. Determining the frequency of pathogenic germline variants from exome sequencing in patients with castrate-resistant prostate cancer. BMJ Open. 2016;6(4):e010332. doi: 10.1136/bmjopen-2015-010332. PubMed PMID: 27084275; PMCID: PMC4838679.

414. Banks P, Xu W, Murphy D, James P, Sandhu S. Relevance of DNA damage repair in the management of prostate cancer. Curr Probl Cancer. 2017;41(4):287-301. doi: 10.1016/j.currproblcancer.2017.06.001. PubMed PMID: 28712484.

415. Beltran H, Yelensky R, Frampton GM, Park K, Downing SR, MacDonald TY, Jarosz M, Lipson D, Tagawa ST, Nanus DM, Stephens PJ, Mosquera JM, Cronin MT, Rubin MA. Targeted next-generation sequencing of advanced prostate cancer identifies potential therapeutic targets and disease heterogeneity. European urology. 2013;63(5):920-6. doi: 10.1016/j.eururo.2012.08.053. PubMed PMID: 22981675; PMCID: PMC3615043.

416. Spranger S, Bao R, Gajewski TF. Melanoma-intrinsic beta-catenin signalling prevents anti-tumour immunity. Nature. 2015;523(7559):231-5. doi: 10.1038/nature14404. PubMed PMID: 25970248.

417. Sfanos KS, Sauvageot J, Fedor HL, Dick JD, De Marzo AM, Isaacs WB. A molecular analysis of prokaryotic and viral DNA sequences in prostate tissue from patients with prostate cancer indicates the presence of multiple and diverse microorganisms. The Prostate. 2008;68(3):306-20. doi: 10.1002/pros.20680. PubMed PMID: 18163428.

418. Cavarretta I, Ferrarese R, Cazzaniga W, Saita D, Luciano R, Ceresola ER, Locatelli I, Visconti L, Lavorgna G, Briganti A, Nebuloni M, Doglioni C, Clementi M, Montorsi F, Canducci F, Salonia A. The Microbiome of the Prostate Tumor Microenvironment. European urology. 2017;72(4):625-31. doi: 10.1016/j.eururo.2017.03.029. PubMed PMID: 28434677.

419. Sfanos KS, Yegnasubramanian S, Nelson WG, De Marzo AM. The inflammatory microenvironment and microbiome in prostate cancer development. Nat Rev Urol. 2017. doi: 10.1038/nrurol.2017.167. PubMed PMID: 29089606.
420. Viaud S, Saccheri F, Mignot G, Yamazaki T, Daillere R, Hannani D, Enot DP, Pfirschke C, Engblom C, Pittet MJ, Schlitzer A, Ginhoux F, Apetoh L, Chachaty E, Woerther PL, Eberl G, Berard M, Ecobichon C, Clermont D, Bizet C, Gaboriau-Routhiau V, Cerf-Bensussan N, Opolon P, Yessaad N, Vivier E, Ryffel B, Elson CO, Dore J, Kroemer G, Lepage P, Boneca IG, Ghiringhelli F, Zitvogel L. The intestinal microbiota modulates the anticancer immune effects of cyclophosphamide. Science. 2013;342(6161):971-6. doi: 10.1126/science.1240537. PubMed PMID: 24264990; PMCID: PMC4048947.
421. Iida N, Dzutsev A, Stewart CA, Smith L, Bouladoux N, Weingarten RA, Molina DA, Salcedo R, Back T, Cramer S, Dai RM, Kiu H, Cardone M, Naik S, Patri AK, Wang E, Marincola FM, Frank KM, Belkaid Y, Trinchieri G, Goldszmid RS. Commensal bacteria control cancer response to therapy by modulating the tumor microenvironment. Science. 2013;342(6161):967-70. doi: 10.1126/science.1240527. PubMed PMID: 24264989.
422. Vetizou M, Pitt JM, Daillere R, Lepage P, Waldschmitt N, Flament C, Rusakiewicz S, Routy B, Roberti MP, Duong CP, Poirier-Colame V, Roux A, Becharef S, Formenti S, Golden E, Cording S, Eberl G, Schlitzer A, Ginhoux F, Mani S, Yamazaki T, Jacquelot N, Enot DP, Berard M, Nigou J, Opolon P, Eggermont A, Woerther PL, Chachaty E, Chaput N, Robert C, Mateus C, Kroemer G, Raoult D, Boneca IG, Carbonnel F, Chamaillard M, Zitvogel L. Anticancer immunotherapy by CTLA-4 blockade relies on the gut microbiota. Science. 2015;350(6264):1079-84. doi: 10.1126/science.aad1329. PubMed PMID: 26541610; PMCID: PMC4721659.
423. Sivan A, Corrales L, Hubert N, Williams JB, Aquino-Michaels K, Earley ZM, Benyamin FW, Lei YM, Jabri B, Alegre ML, Chang EB, Gajewski TF. Commensal Bifidobacterium promotes antitumor immunity and facilitates anti-PD-L1 efficacy. Science. 2015;350(6264):1084-9. doi: 10.1126/science.aac4255. PubMed PMID: 26541606; PMCID: PMC4873287.
424. Routy B, Le Chatelier E, Derosa L, Duong CPM, Alou MT, Daillere R, Fluckiger A, Messaoudene M, Rauber C, Roberti MP, Fidelle M, Flament C, Poirier-Colame V, Opolon P, Klein C, Iribarren K, Mondragon L, Jacquelot N, Qu B, Ferrere G, Clemenson C, Mezquita L, Masip JR, Naltet C, Brosseau S, Kaderbhai C, Richard C, Rizvi H, Levenez F, Galleron N, Quinquis B, Pons N, Ryffel B, Minard-Colin V, Gonin P, Soria JC, Deutsch E, Loriot Y, Ghiringhelli F, Zalcman G, Goldwasser F, Escudier B, Hellmann MD, Eggermont A, Raoult D, Albiges L, Kroemer G, Zitvogel L. Gut microbiome influences efficacy of PD-1-based immunotherapy against epithelial tumors. Science. 2017. doi: 10.1126/science.aan3706. PubMed PMID: 29097494.
425. Gopalakrishnan V, Spencer CN, Nezi L, Reuben A, Andrews MC, Karpinets TV, Prieto PA, Vicente D, Hoffman K, Wei SC, Cogdill AP, Zhao L, Hudgens CW, Hutchinson DS, Manzo T, Petaccia de Macedo M, Cotechini T, Kumar T, Chen WS, Reddy SM, Szczepaniak Sloane R, Galloway-Pena J, Jiang H, Chen PL, Shpall EJ,

Rezvani K, Alousi AM, Chemaly RF, Shelburne S, Vence LM, Okhuysen PC, Jensen VB, Swennes AG, McAllister F, Marcelo Riquelme Sanchez E, Zhang Y, Le Chatelier E, Zitvogel L, Pons N, Austin-Breneman JL, Haydu LE, Burton EM, Gardner JM, Sirmans E, Hu J, Lazar AJ, Tsujikawa T, Diab A, Tawbi H, Glitza IC, Hwu WJ, Patel SP, Woodman SE, Amaria RN, Davies MA, Gershenwald JE, Hwu P, Lee JE, Zhang J, Coussens LM, Cooper ZA, Futreal PA, Daniel CR, Ajami NJ, Petrosino JF, Tetzlaff MT, Sharma P, Allison JP, Jenq RR, Wargo JA. Gut microbiome modulates response to anti-PD-1 immunotherapy in melanoma patients. Science. 2018;359(6371):97-103. doi: 10.1126/science.aan4236. PubMed PMID: 29097493; PMCID: PMC5827966.